

INFORMATION TO USERS

This manuscript has been reproduced from the microfilm master. UMI films the text directly from the original or copy submitted. Thus, some thesis and dissertation copies are in typewriter face, while others may be from any type of computer printer.

The quality of this reproduction is dependent upon the quality of the copy submitted. Broken or indistinct print, colored or poor quality illustrations and photographs, print bleedthrough, substandard margins, and improper alignment can adversely affect reproduction.

In the unlikely event that the author did not send UMI a complete manuscript and there are missing pages, these will be noted. Also, if unauthorized copyright material had to be removed, a note will indicate the deletion.

Oversize materials (e.g., maps, drawings, charts) are reproduced by sectioning the original, beginning at the upper left-hand corner and continuing from left to right in equal sections with small overlaps. Each original is also photographed in one exposure and is included in reduced form at the back of the book.

Photographs included in the original manuscript have been reproduced xerographically in this copy. Higher quality 6" x 9" black and white photographic prints are available for any photographs or illustrations appearing in this copy for an additional charge. Contact UMI directly to order.

UMI

A Bell & Howell Information Company
300 North Zeeb Road, Ann Arbor MI 48106-1346 USA
313/761-4700 800/521-0600



Université d'Ottawa • University of Ottawa

**The Antioxidant and Photophysical Properties of Melatonin:
A Radical Perspective**

Mary Catherine King

A thesis presented to the
School of Graduate Studies and Research

In partial fulfillment of the requirements for the degree of
Master of Science
(Specialization in Chemical and Environmental Toxicology)



Université d'Ottawa • University of Ottawa

In the Ottawa-Carleton Chemistry Institute,
Department of Chemistry, University of Ottawa, Canada

© Mary Catherine King, Ottawa, Ontario, Canada, August 1997



National Library
of Canada

Bibliothèque nationale
du Canada

Acquisitions and
Bibliographic Services

Acquisitions et
services bibliographiques

395 Wellington Street
Ottawa ON K1A 0N4
Canada

395, rue Wellington
Ottawa ON K1A 0N4
Canada

Your file *Votre référence*

Our file *Notre référence*

The author has granted a non-exclusive licence allowing the National Library of Canada to reproduce, loan, distribute or sell copies of this thesis in microform, paper or electronic formats.

L'auteur a accordé une licence non exclusive permettant à la Bibliothèque nationale du Canada de reproduire, prêter, distribuer ou vendre des copies de cette thèse sous la forme de microfiche/film, de reproduction sur papier ou sur format électronique.

The author retains ownership of the copyright in this thesis. Neither the thesis nor substantial extracts from it may be printed or otherwise reproduced without the author's permission.

L'auteur conserve la propriété du droit d'auteur qui protège cette thèse. Ni la thèse ni des extraits substantiels de celle-ci ne doivent être imprimés ou autrement reproduits sans son autorisation.

0-612-26336-3

Canada

Abstract

Melatonin, or N-acetyl-5-methoxytryptamine, is an interesting neurohormone that governs the body's circadian rhythm, and is synthesized predominantly in the retina and the pineal gland, a small pea-sized gland in the centre of the brain. Since melatonin is found in low concentrations in almost all tissue, many have speculated that its biological function may include detoxification protection, but little is actually known. In the United States and other countries, such speculation has led to a growing interest and popularity in melatonin as an over-the-counter nutritional supplement, but the lack of research and clinical trials has led to a federal ban on the sale of this neurohormone in Canada. In this thesis, our research goal was to investigate some molecular properties of melatonin to further the knowledge of this popular and controversial indoleamine. Examination of the photophysical and photochemical properties of melatonin have shed some light on its role in the retina, while oxygen uptake experiments have exposed some of the misconceptions regarding its antioxidant activity.

The eye is predisposed to many photochemical processes, but it is unlikely that melatonin participates as an ocular photosensitizer since it is transparent to the light that is admitted by the eye. We characterized the photophysical properties of melatonin in solution, including quantum yields, lifetimes and kinetics of fluorescence and phosphorescence. In doing so, we have established that the excited states of melatonin are much like its precursor tryptophan, such that any photochemical involvement of melatonin *in vivo* would arise directly from sensitization of its triplet state, or indirectly by ground state reaction with proximal excited species.

Almost every article written about melatonin, scientific and otherwise, makes some reference to its antioxidant capabilities, yet there is no really conclusive evidence to support this claim. There are many inconsistencies and conflicting reports in the literature regarding the radical scavenging behaviour and antioxidant activity of melatonin. Many researchers believe

that the apparent antioxidant action associated with melatonin *in vivo* is due to its ability to trap peroxy and hydroxyl radicals in much the same way as vitamin E. In fact, melatonin has been attributed antioxidant properties that are superior to that of vitamin E.

Since melatonin is structurally different from vitamin E, our research goal was to establish the validity of these claims. By measuring the rate of oxygen uptake of temperature controlled, initiated lipid peroxidation reactions, we were able to determine that melatonin does not behave like a typical chain-breaking antioxidant, such as vitamin E and related tocopherols. The results presented in this thesis prove that melatonin is, at best, a mild retarder of lipid peroxidations. Using fluorescence techniques, we showed that melatonin may act as a preventive antioxidant by chelating such peroxidation catalysts as Fe^{2+} and Cu^{2+} ions. Although all of our experiments were conducted *in vitro*, at the molecular level, the results may have biological significance in determining the extent to which melatonin is capable of providing detoxification protection *in vivo*.

Acknowledgements

I am sincerely grateful for the opportunity to have studied under Tito Scaiano who is a veritable wealth of inspiration and innovation, a truly outstanding scientist and great supervisor. I would like to express my gratitude to Keith Ingold not only for the use of his laboratory but also for his time, wisdom, and patience which he so generously shared with me. I would also like to thank Lydia Martinez for stimulating discussions about melatonin, phototoxicity and solvated electrons. Andre Simard has been instrumental in his assistance with the laser system and deserves heartfelt thanks. Thanks are also due to Nadereh Mohtat for her assistance with the picosecond laser work. I would like to acknowledge Dupont and Paprican for financial support.

I am deeply indebted to my family for their love, support and perseverance, always.

for Madeleine, Alana, Alexander, Malcolm

and Ian

In every passionate pursuit, the pursuit counts more than the object pursued.

—Bruce Lee

Table of Contents

Abstract	ii
Acknowledgements	iv
Table of Contents	vi
Abbreviations	ix
List of Schemes	xi
List of Figures	xii
List of Tables	xiii
Chapter 1	1
— Introduction —	1
1.1.0 Introduction	1
1.1.1 Physiological Synthesis and Activity	1
1.1.2 Metabolism of Melatonin	3
1.2.0 Research Objectives	4
1.2.1 Characterization of Excited States	4
1.2.2 Antioxidant Activity in Lipid Peroxidations	5
Chapter 2	6
— Experimental Techniques —	6
2.1.0 Introduction	6
2.1.1 Laser Flash Photolysis	6
2.1.2 Sample Preparation	8
2.1.3 Steady State Optical Measurements	8
2.1.4 Time-Resolved Fluorescence Measurements	9
2.1.5 Singlet Oxygen Detection	9
2.2.1 Oxygen Uptake	11

— Photophysical Properties of Melatonin — **13**

3.1.0 Introduction	13
3.1.1 Absorption of Visible and Ultraviolet Radiation	13
3.1.2 Energy Transfer	15
3.1.3 Singlet Oxygen Quenching	18
3.2.0 Materials and Methods	20
3.3.0 Results	20
3.3.1 Absorption and Fluorescence Spectra	20
3.3.2 Fluorescence Quantum Yield	23
3.3.3 Fluorescence Lifetimes	24
3.3.4 Phosphorescence	26
3.3.5 Singlet Oxygen Emission	27
3.3.6 Laser Flash Photolysis Studies	28
3.3.7 Triplet State Involvement	30
3.3.8 Intersystem Crossing Quantum Yield	35
3.4.0 Discussion	37
3.4.1 Absorption Characteristics and Electronic Transitions	37
3.4.2 Fluorescence Decay Mechanisms	38
3.4.3 Triplet Energy Transfer Efficiency	39

— Antioxidant Properties of Melatonin — **41**

4.1.0 Introduction	41
4.1.1 Reactive Oxygen Species	42
4.1.2 Protective Defenses Against Oxidative Attack	44
4.1.3 Melatonin vs. Vitamin E	44
4.1.4 Antioxidant Measurement - Methods and Techniques	47
4.1.5 Oxygen Uptake Kinetic Measurements	51
4.2.0 Materials and Methods	56
4.2.1 Autoxidation of Styrene and Tetralin	57
4.2.2 Autoxidation of Styrene and Linoleic Acid in Micelles	58
4.2.3 Fluorescence Studies	60
4.3.0 Results	61
4.3.1 Oxygen Uptake: Tetralin and Styrene Substrates	61

4.3.2 Oxygen Uptake: Styrene in SDS	62
4.3.3 Oxygen Uptake: Linoleic Acid in SDS - Effect of Metal Ions	64
4.3.4 Fluorescence Studies	70
4.4.0 Discussion	73
4.4.1 Product Studies in Mimetic Bilayer Systems	76
4.4.2 A Proposed Radical Trapping Mechanism	77
4.4.3 Melatonin is a Preventive Antioxidant	80
4.4.4 Melatonin as a Ligand and Fenton Chemistry	81
4.4.5 Interpretations in the Literature Revisited	84
Chapter 5	88
— Conclusions —	88
5.1.0 Conclusions	88
5.1.1 Spectroscopy and The Role of Retinal Melatonin	88
5.1.2 The Antioxidant Role of Melatonin	91
5.2.1 Final Comments	93
Claims to Original Research	94
Appendix 1	95
A.1.0 A Computational Approach	95
A.2.1 Locating the Lowest Energy Conformation	95
A.2.2 Methods for Geometry Optimization	96
A.3.1 Computational Results	97
References	102

Abbreviations

AFMK	N-acetyl-N-formyl-5-methoxykynuramine
LFP	laser flash photolysis
UV	ultraviolet
Δ OD	change in optical density
PMT	photomultiplier tube
Hz	Hertz (cycles per second)
I_0	intensity of light source
UV-VIS	ultraviolet-visible
YAG	Yttrium aluminum garnet
IR	infrared
$^1\Delta$	delta singlet electronic state
mJ	millijoules
kcal/mol	kilocalories per mole
PEEK	polyethylene ethyl ketone
h ν	energy
ic	internal conversion
isc	intersystem crossing
VR	vibrational relaxation
τ	lifetime in Chapter 2/ induction period in Chapter 3
ET	energy transfer
Φ	quantum yield
k	rate constant
LOOH/ROOH	lipid hydroperoxide
LH/RH	lipid with abstractable hydrogen atom

PBD	2-(4-biphenyl)-5-phenyl-1,3,4-oxadiazole
OD	optical density or absorbance
IRF	instrument response function
RF	radiofrequency
T_1	lowest excited triplet state
S_1	lowest excited singlet state
TOD	top or highest optical density
ORAC	Oxygen-radical absorbing capacity
ABAP	2,2'-azobis(2-amidinopropane)dihydrochloride
SDS	sodium dodecyl sulfate
e	fraction radicals that escape from reaction cage
R_i	rate of chain initiation
n	stoichiometric factor
AIBN	2,2'-bis(isobutyronitrile)
DTPA	diethylenetriaminepentaacetic acid
HPLC	high pressure liquid chromatography
PLPC	1-palmitoyl-2-linoleoylphosphatidylcholine
EDTA	ethylenediaminetetraacetic acid
DMPO	5,5-dimethylpyrroline-N-oxide
ESR	electron spin resonance
DABCO	1,4-diazabicyclooctane

List of Schemes

Scheme 1.1:	Synthesis of melatonin from tryptophan	2
Scheme 3.1:	Unimolecular and bimolecular energy conversion mechanisms	16
Scheme 3.2:	Type II photooxidation mechanism	19
Scheme 3.3:	Energy transfer from triplet melatonin to triplet biphenyl	39
Scheme 4.1:	Successive univalent one electron reduction of oxygen to water	42
Scheme 4.2:	Hydroxyl radical generation via Haber-Weiss and Fenton reactions	43
Scheme 4.3:	Decomposition of lipid hydroperoxides by iron(II)	43
Scheme 4.4:	Resonance stabilization of the phenoxyl radical by the chroman ring	46
Scheme 4.5:	Mechanism of lipid peroxidation	48
Scheme 4.6:	Reaction of melatonin with peroxy radicals generated <i>in situ</i>	49
Scheme 4.7:	Thermal decomposition of an azo-initiator	52
Scheme 4.8:	Mechanism of azo-initiated autoxidation	53
Scheme 4.9:	Reverse peroxidation inhibition reaction	54
Scheme 4.10:	Mechanism of back reaction of hydroperoxides with Fe ³⁺	70
Scheme 4.11:	Mechanism for retarded autoxidation	75
Scheme 4.12:	Proposed mechanism for reaction of melatonin with oxidizing radicals	80
Scheme 5.1:	Reaction of superoxide anion with melatonin in the retina	90
Scheme 5.2:	Proposed mechanism for peroxy radical trapping and peroxidation retardation by melatonin	92

List of Figures

Figure 2.1:	Schematics of the laser flash photolysis set-up	7
Figure 2.2:	Schematics of the singlet oxygen detection photolysis set-up	10
Figure 2.3:	Schematic of the pressure transducer	12
Figure 3.1:	Jablonski diagram of unimolecular decay processes	14
Figure 3.2:	Absorption spectrum of melatonin in acetonitrile	21
Figure 3.3:	Solvent effect on melatonin fluorescence spectrum	22
Figure 3.4:	Melatonin fluorescence decay in pH 7 phosphate buffer	25
Figure 3.5:	Excitation, emission, and phosphorescence spectra of melatonin	26
Figure 3.6:	Singlet oxygen sensitization by melatonin and benzophenone	27
Figure 3.7:	LFP transient spectra of melatonin in acetonitrile and water	29
Figure 3.8:	LFP transient spectra of melatonin in methanol	30
Figure 3.9:	Quenching of LFP melatonin transients by O ₂ and diene	31
Figure 3.10:	Jablonski diagram depicting triplet state energy transfer	32
Figure 3.11:	LFP transient spectra of melatonin and biphenyl - effect of diffuser	33
Figure 3.12:	Plot of transient growth rate constant vs. quencher concentration	34
Figure 3.13:	Decay of biphenyl triplet sensitized by melatonin and acetophenone	36
Figure 4.1:	Plot of reciprocal [melatonin] vs. % initial rate of O ₂ uptake	62
Figure 4.2:	Effect of melatonin and trolox on O ₂ uptake by styrene	63
Figure 4.3:	Fe ²⁺ catalyzed rate of O ₂ uptake by linoleic acid (Chelex) with melatonin	64
Figure 4.4:	Fe ²⁺ catalyzed rate of O ₂ uptake by linoleic acid with melatonin	65
Figure 4.5:	Fe ²⁺ catalyzed rate of O ₂ uptake by linoleic acid with DTPA	66
Figure 4.6:	Melatonin and Fe ²⁺ catalyzed rate of O ₂ uptake by linoleic acid	67
Figure 4.7:	DTPA and Fe ²⁺ catalyzed rate of O ₂ uptake by linoleic acid	68
Figure 4.8:	Fe ³⁺ and Cu ²⁺ - catalyzed rate of O ₂ uptake by linoleic acid with melatonin	69
Figure 4.9:	Effect of [Fe ²⁺] on absorption and fluorescence spectra of melatonin	71

Figure 4.10:	Stern-Volmer plot of fluorescence intensity ratio vs. $[\text{Fe}^{2+}]$	72
Figure 4.13:	Kinetic and thermodynamic peroxidation products of PLPC	77
Figure A.1:	Radical structures following hydrogen atom and electron abstraction	98
Figure A.2:	Numbering scheme for heavy atoms of melatonin	101

List of Tables

Table 3.1:	Fluorescence lifetimes and quantum yields in different solvents	24
Table A.1:	ΔH_{F} calculations for melatonin radicals using PM3	99
Table A.2:	Calculated atomic charges for melatonin radicals	100

Chapter 1

— Introduction —

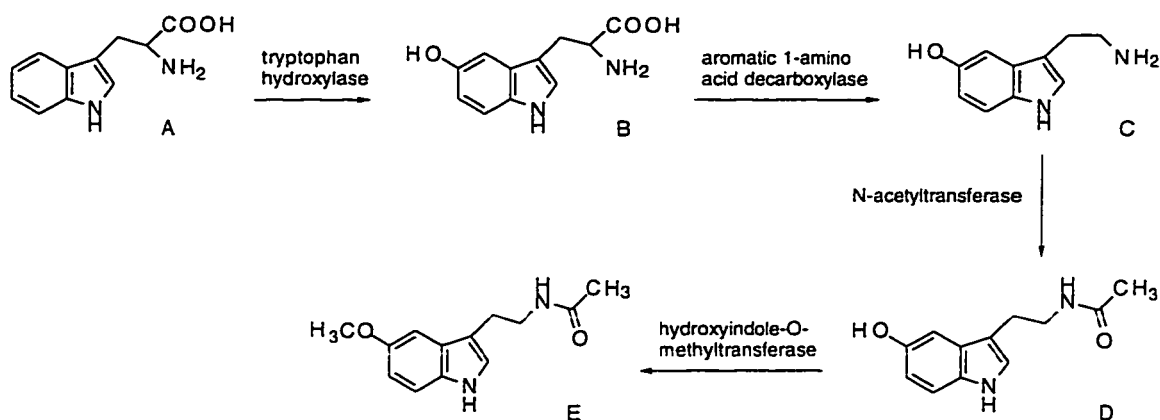
1.1.0 Introduction

Early in the century, it was discovered that the skin of tadpoles became transparent upon exposure to the ground up pineal glands of cows; they lost their pigmentation to the extent that their internal organs and skeleton became visible. In 1958 Lerner identified the main constituent of the pineal gland as N-acetyl-5-methoxytryptamine, or melatonin.¹ Melatonin is ubiquitous in nature; it is present in vertebrates, invertebrates, plants and even unicellular organisms. In vertebrates, melatonin is synthesized from tryptophan in the pineal gland via the multistep process depicted in Scheme 1.1, a synthesis that is photoperiodic and is triggered in response to light impinging upon the retina. The production and secretion of melatonin follow a circadian rhythm where nocturnal pineal levels are two to twelve times higher than diurnal levels; the pattern and magnitude of the nocturnal rise is dependent on the species but independent of their locomotor activity.² Both nuclear and high affinity membrane receptors have been identified for which melatonin is a ligand.⁸⁵ While the photoperiodic roles of pineal melatonin are well established, its presence in the unicellular dinoflagellate, *Gonyaulax polyedra*, has led to the hypothesis that the functions of melatonin have evolved from its initial role as a free radical scavenger and antioxidant.³

1.1.1 Physiological Synthesis and Activity

The synthesis of melatonin also occurs to a lesser extent in nonpineal tissues of most vertebrates - the gut, the Harderian gland, leukocytes and the retina. Pineal melatonin is secreted into the bloodstream and readily penetrates cell membranes due to its high

lipophilicity. Circulating melatonin mediates such photoperiodic functions as circadian rhythm and seasonal reproduction in some mammal species, whereas the role of retinal melatonin seems to be confined locally, to functions within the retina. It is believed that retinal melatonin is responsible for photoreceptor disc shedding via a light mediated process in which pineal melatonin plays little or no role.^{4,5} Retinal melatonin also functions as a neuromodulator effecting the release of the neurotransmitter dopamine at a specific concentration of approximately 10^{-9} M.⁶ Pigment migration, the movement of rods and cones, as well as microtubule separation within the eye, appear to be other local functions of retinally synthesized melatonin.^{5,7,8} Menaker has suggested that the role of melatonin may have evolved to incorporate these light-mediated retinomoter tasks within the eye in addition to its original role as neuromodulator.⁶



Scheme 1.1: Metabolism of tryptophan to melatonin. A - tryptophan; B - 5-hydroxytryptophan; C - serotonin; D - N-acetylserotonin; E - melatonin. The rate-limiting step in the synthesis of melatonin involves the enzyme N-acetyltransferase which is deactivated by light, causing a decrease in the diurnal levels of melatonin.²

1.1.2 Metabolism of Melatonin

Although melatonin is marginally photostable, it becomes extremely photolabile in the presence of oxygen and cellular photocatalysts in biological environments. Hardeland *et al.* reported that the main metabolite, caused by the protoporphyrin catalyzed photooxidation of melatonin, is N-acetyl-N-formyl-5-methoxykynuramine (AFMK).³ Protoporphyrin, which is present in the circulating blood that directly feeds the retina, absorbs light at wavelengths that pass through the lens, and then efficiently sensitizes singlet oxygen. Based on their results, Hardeland *et al.* concluded that while AFMK production does involve singlet oxygen scavenging by melatonin to some extent, the major reaction pathway involves electron transfer from the excited triplet state of protoporphyrin to molecular oxygen resulting in the production of superoxide anion. The protoporphyrin radical cation thus generated then abstracts an electron from melatonin to form the radical cation of melatonin which in turn reacts with the superoxide anion, thus forming AFMK. In the absence of light, reaction between superoxide anion and melatonin is catalyzed by hemin, the ferric iron-bound porphyrin component of blood. AFMK represents twelve percent of the metabolites of melatonin that are excreted in urine. All but one percent of melatonin produced and secreted by the pineal gland is metabolized, and about seventy-five percent is converted to 6-hydroxymelatonin which is further glucuronidated or sulfonated by microsomal enzymes in the liver prior to excretion.³

Reaction of free radicals with other molecules occurs via three possible pathways: addition, hydrogen atom abstraction or electron abstraction. In an earlier paper Hardeland *et al.* utilized the electron transfer mechanism to explain the reported ability of melatonin to terminate radical reaction chains and thus act as an antioxidant.⁹ This mechanism is widely accepted and appears in many reviews to describe the apparent antioxidant action of melatonin *in vitro*.^{3,10-14} However, it seems unlikely that only about twelve percent of melatonin produced would be metabolized to AFMK, particularly if it functions as a radical trap as well as a hormone *in vivo* - a popular idea expounded by others in the literature. Roles other than that of a hormone, such as free radical scavenger, would require much higher levels of melatonin than the physiological

picomolar concentration, unless this indoleamine is somehow regenerated and concentrated in tissue.

1.2.0 Research Objectives

Based on the many detoxification and preventive functions that it has been attributed, melatonin would appear to be the 'wonder drug of the nineties'. It has been promoted as a therapeutic agent and nutritional supplement to, among others, prevent cancer and Alzheimer's disease, treat Parkinson's disease, slow the effects of aging and provide antioxidant protection by free radical scavenging.^{12,14-18} However, there are many inconsistencies and conflicting reports in the literature concerning the radical scavenging behaviour and antioxidant activity of melatonin. The goal of the work comprised in this thesis was to examine the spectroscopy and the free radical chemistry of melatonin to evaluate the validity at the molecular level for such claims.

1.2.1 Characterization of Excited States

It is possible that retinal melatonin, if substantially concentrated in relation to blood levels,¹⁹ may also assume a custodial, protective role in the retina by actively participating in specific photochemical processes such as scavenging photoinduced radicals or quenching singlet oxygen.²⁰ By virtue of its capacity as the body's light receptor, the eye is predisposed to many photochemical effects including photooxidative processes. The photochemical and photooxidative processes of light absorbers within the eye such as rhodopsin, retinal, melanin, cytochrome-*c* and lipofuscin have been well documented,^{21,22} but little is known about the photochemistry of melatonin. One of the research goals of this thesis included an investigation into the behavior of the excited states of melatonin in solution. Fluorescence and phosphorescence properties of melatonin, including quantum yields, lifetimes and kinetics,

have been characterized in an attempt to further the knowledge about this popular and controversial indoleamine.

1.2.2 Antioxidant Activity in Lipid Peroxidations

An alternative radical trapping mechanism that includes a regeneration step and does not involve the oxidation of melatonin leading to the formation of the metabolite AFMK may provide a better explanation for the higher proportion of 6-hydroxymelatonin metabolite generated in the liver. This thesis describes one such alternative mechanism involving hydrogen atom abstraction to account for possible radical trapping and antioxidant roles of melatonin. It is based on the results of *in vitro* experiments involving the oxygen uptake of lipids undergoing peroxidation in biphasic, heterogeneous and homogeneous microenvironments. Our results do not support the conclusions drawn by others concerning the antioxidant potency and activity of melatonin; contrary to many reports in the literature, melatonin did not manifest itself as a chain breaking antioxidant to rival vitamin E. The *in vitro* work reported in this thesis indicates that melatonin acts a mild retarder of lipid peroxidations and there is also some evidence to suggest that it may also function as a preventive antioxidant by metal ion deactivation.

Chapter 2

— Experimental Techniques —

2.1.0 Introduction

The experimental methods described in this chapter include time-resolved and steady state spectroscopic methods to measure the photophysical and photochemical properties of melatonin, and an oxygen uptake system to measure the antioxidant properties of melatonin. Descriptions of sample preparation, chemicals and solvents, including purification details, are given in a 'Materials and Methods' section of the chapter appropriate to their use. All experiments reported in this thesis were performed in duplicate, except for the tetralin experiment in Section 4.2.1.

2.1.1 Laser Flash Photolysis

Laser flash photolysis (LFP) is a powerful spectroscopic technique by which fast processes and reactions can be observed. Laser excitation gives rise to a transient intermediate species whose absorption of a selected wavelength of light from a pulsed 150 W Xenon lamp causes a change in the optical density of the sample. By using fast, pulsed lasers this change in optical density or ΔOD can be measured as a function of time, thereby providing kinetic information about the transient. The duration of the laser pulse must not exceed the duration of the process being investigated and must also be of sufficient intensity to produce a measurable quantity of transient. Excitation for the LFP experiments reported in this thesis were provided by a Molectron UV-24 nitrogen laser (337 nm) and a Lumonics EX-530 XeCl₂ excimer laser (308 nm) capable of delivering ~6 mJ pulses, 6 ns in duration and ~50 - 60 mJ pulses, 10 ns in duration, respectively. Both lasers produced large rectangular beams which were focussed on

the sample by an arrangement of quartz lenses and prisms such that the laser excitation beam was orthogonal to the monitoring beam. The lasers were preset with an operating frequency of 1 Hz, and computer-controlled shutters directed the sample exposure to either the laser or monitoring beams. The transmitted light following each excitation 'event' was directed at a monochromator by a series of lenses, whereupon only light of the selected wavelength of the monochromator impinged upon a 6-dynode photomultiplier tube (PMT) detector. The resulting amplified signal from the PMT was terminated into a 93 ohm resistor, captured by a Tektronix 2440 digitizer and transferred to a PowerMacintosh computer equipped with software developed in the LabVIEW 3.1.1 environment from National Instruments. The laser flash photolysis set-up is depicted in Figure 2.1.

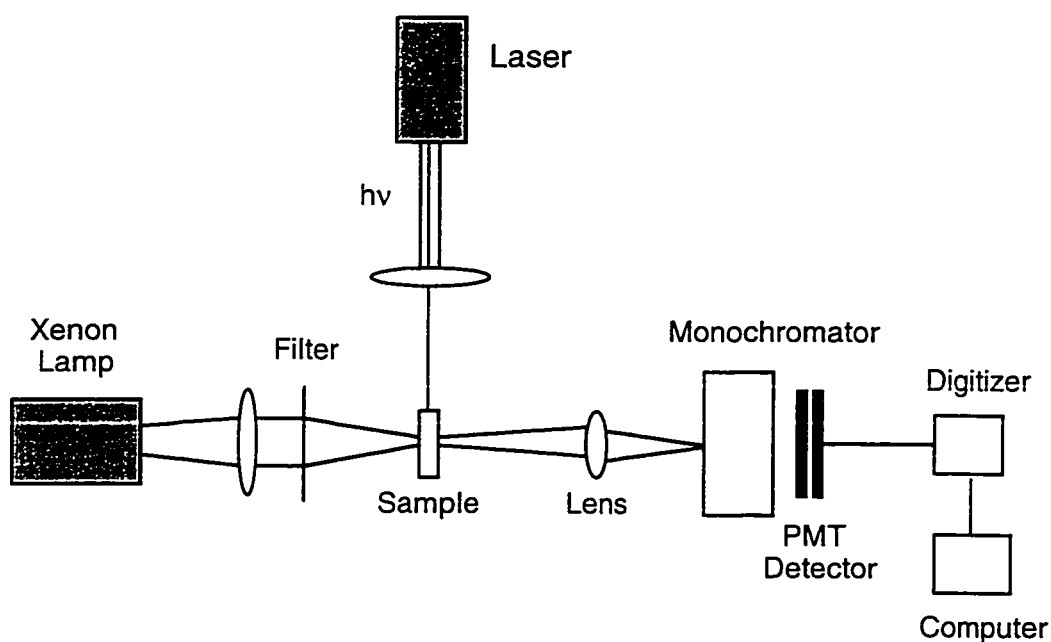


Figure 2.1: Schematics of the laser flash photolysis set-up.

Conversion of the PMT voltage signals to the more meaningful expression ΔOD , was achieved via equation 2.1 in the LabVIEW software:

$$\Delta OD = -\log\left(1 - \frac{\text{Signal}}{I_0}\right) \quad 2.1$$

To facilitate the acquisition of transient absorption spectra, a programmable power supply maintained a constant I_0 (ca. 280 mV) from the PMT output over the wavelength range of interest. Kinetic traces of the transient absorption at different wavelengths were plotted against wavelength, thereby constructing the transient spectrum.

2.1.2 Sample Preparation

Samples for laser flash photolysis were prepared at concentrations such that the optical density measured between 0.2 and 0.5; absorbances outside this range may produce inadequate signals at the low end and shock waves at the high end. Two types of 7 x 7 mm² sample cells, specially prepared from Suprasil quartz tubing with a volume of ~4 - 5 mL, were used: one was designed for static measurements and the other for flow conditions. All static samples were deaerated with high purity nitrogen for a minimum of 20 minutes (unless stated otherwise), and were shaken between laser shots to avoid possible accumulation of photoproducts. Flow samples were deaerated with nitrogen from a compressed nitrogen cylinder connected to the flow cell with teflon tubing, throughout the duration of the LFP experiment.

2.1.3 Steady State Optical Measurements

Phosphorescence and fluorescence (emission and excitation) spectra were recorded on a Perkin Elmer LS-50 spectrofluorimeter and absorption measurements were conducted using a Varian Cary-1 UV-VIS spectrophotometer for experiments requiring optically matched samples (i.e. singlet oxygen and intersystem crossing quantum yields) and a Hewlett Packard HP-

8451A diode array UV-VIS spectrophotometer for measuring optical densities of LFP and fluorescence lifetime samples.

2.1.4 Time-Resolved Fluorescence Measurements

Time-resolved fluorescence measurements in the picosecond time regime were conducted using a Hamamatsu streak scope C4334 system set in emission mode. The set-up consisted of a Continuum PY61 mode-locked Nd³⁺:YAG laser with a fundamental beam of 1064 nm that was frequency quadrupled to deliver pulses of 266 nm, ~2 - 3 mJ/pulse. The streak camera is capable of producing a two dimensional image of the emission which provides spectral information as well as temporal resolution. Instrument operation and data acquisition was controlled by Hamamatsu software.

2.1.5 Singlet Oxygen Detection

The energy of the ¹Δ excited state of molecular oxygen is low at 22.5 kcal/mol (94 kJ/mol), and energy transfer is readily attainable from the excited triplet state of most molecules - very few have triplet energies below this. Although sensitized singlet oxygen decays back down to the ground state predominantly by a radiationless pathway, there is a small component (less than 1%) of infrared (IR) emission at 1269 nm that can be measured with the aid of an extremely sensitive detector. Time-resolved measurement of this weak luminescence can be achieved with a germanium photodiode to provide kinetic information for the relaxation of singlet oxygen in solution.

The instrumental set-up used in our experiments is represented in Figure 2.2 and involved the use of a Lumonics EX-530 XeCl₂ excimer laser (308 nm) capable of delivering ~50 - 60 mJ pulses, 10 ns in duration. The laser beam was collected by means of a lens and collimated using an iris prior to impinging upon the sample. The luminescence from subsequent singlet oxygen sensitization was detected orthogonally by a EG&G Judson J16

8SP ROM5 (5mm) germanium photodiode which was mounted on a modified BNC connector. A 3 mm silicon filter was positioned between the sample cell and the detector to remove any lower wavelength infrared interference generated by non-linear optical effects, such as frequency dividing of the laser beam. Detection of the weak signal required amplification by a Stanford Research Systems low noise preamplifier equipped with short and long bandpass filters to facilitate the suppression of interfering signals which are common at this detection level. The gain of the preamplifier was typically set at $2 - 5 \times 10^3$ and the low pass filter settings were 10/30 KHz and 12 dB/octave; the signals were captured by a Tektronix 2400 digitizer. The laser, shutters, and PMT, as well as data acquisition were controlled by a similar system described for Laser Flash Photolysis in 2.1.1, with the exception of the absence of a monitoring beam.

Singlet oxygen quantum yield measurements involved the preparation of optically matched sample and reference standard, for which the quantum yield is accurately known in the solvent used, and the use of optical quality quartz sample cuvettes.

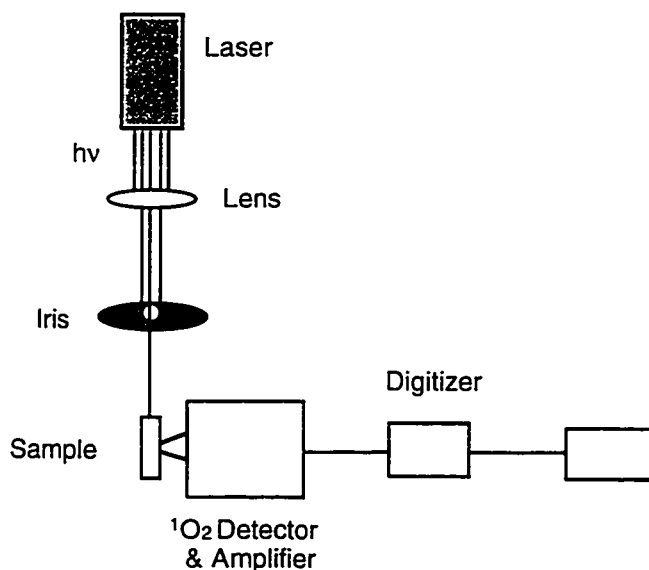


Figure 2.2: Schematics of the singlet oxygen detection set-up.

2.2.1 Oxygen Uptake

All autoxidations were conducted at 30°C and 101.3 kPa (760 Torr) of O₂ using a Validyne DP15 variable reluctance differential pressure transducer connected to a chart recorder. The transducer is constructed of a flat magnetically permeable stainless steel diaphragm which is clamped between two blocks of stainless steel, separated by small gaps on either side. Contained within the blocks are inductance coils that, as the pressure changes, sense deflection of the diaphragm by changes in the surrounding induced magnetic field.

A reaction cell and a reference cell were connected to the transducer, as shown in Figure 2.3, so that the pressure differential between the reference and the sample could be measured as voltage. Both cells were connected to each other by a stopcock that was closed during the oxygen uptake experiments in order to isolate them from each other. The transducer and cells were submerged in a constant temperature water bath (30 ± 0.5°C) and both sample and reference cells were constantly stirred by a common arm that was connected to an external stirring device. All autoxidation experiments were conducted in the dark to prevent photoinduced contributions to the rate of initiation. The oxygen uptake apparatus was pumped down and conditioned prior to changing solvents, and as required throughout the duration of the antioxidant study.

The assembly was vented to the atmosphere while the reaction cell containing substrate/initiator/solvent solution and the reference solution achieved temperature stabilization. After isolating the cells from the atmosphere and from each other, the pressure change generated by the uninhibited substrate (either linoleic acid, styrene, or tetralin) peroxidation was recorded for about 90 minutes prior to adding inhibitor or metal ion, depending on the experiment. The whole assembly is depicted in Figure 2.3 below.

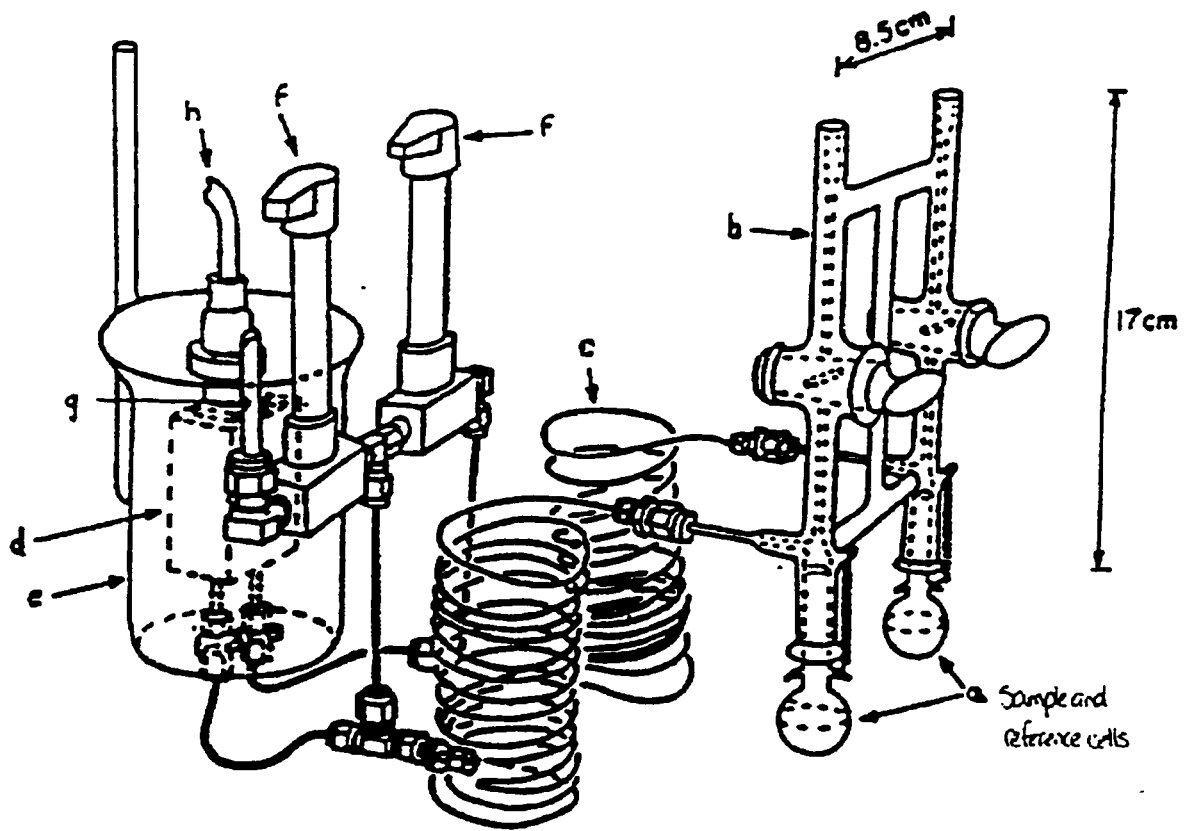


Figure 2.3: Schematic diagram of the pressure transducer assembly designed and built by Mr. Roger Smith of Mount Allison University, Sackville, New Brunswick. a - sample and reference cells; b - cell injection port ; c - PEEK tubing coil; d - pressure transducer; e - black casing; f - main valves connecting to transducer and atmosphere; g - vent to atmosphere; h - connection to vacuum line.

Chapter 3

— Photophysical Properties of Melatonin —

3.1.0 Introduction

While the excited state properties of tryptophan and other related indoles have been extensively studied,^{27-31, 33-37} little is known about the photophysics and photochemistry of melatonin. Melatonin is resident in the retina, which is exposed to light in the visible range of the electromagnetic spectrum, and although this indoleamine itself does not absorb visible light, it is proximal to ocular compounds that do. Using state-of-the-art lasers and flash photolysis instrumentation (described in detail in Chapter 2), we explored the steady state and time-resolved spectroscopic properties of melatonin to characterize its overall photochemistry, and in so doing, we determined whether this ocular component could be sensitized via triplet-triplet energy transfer. In this chapter we report the absorption and emission characteristics of ground state and excited state melatonin, including lifetimes, kinetics, and quantum yields for fluorescence and phosphorescence. Since the excited states of melatonin had never been examined in any depth before, the results of one experiment determined the direction of the next one. The experiments in this chapter are documented in the order that they were performed to recapitulate an investigative procedure for determining the photophysical properties of new or uncharacterized molecules.

3.1.1 Absorption of Visible and Ultraviolet Radiation

In order to explore the photochemical and photophysical properties of molecules in solution, it is necessary to employ techniques that are capable of monitoring processes that occur on the nanosecond and picosecond timescales. Absorption of light of an appropriate

wavelength involves the promotion of an electron to an excited singlet state which relaxes back down to the ground state via radiative or nonradiative pathways. The unimolecular photophysical processes that can occur to deactivate the excited state of a molecule are depicted by the simplified Jablonski Diagram in Figure 3.1:

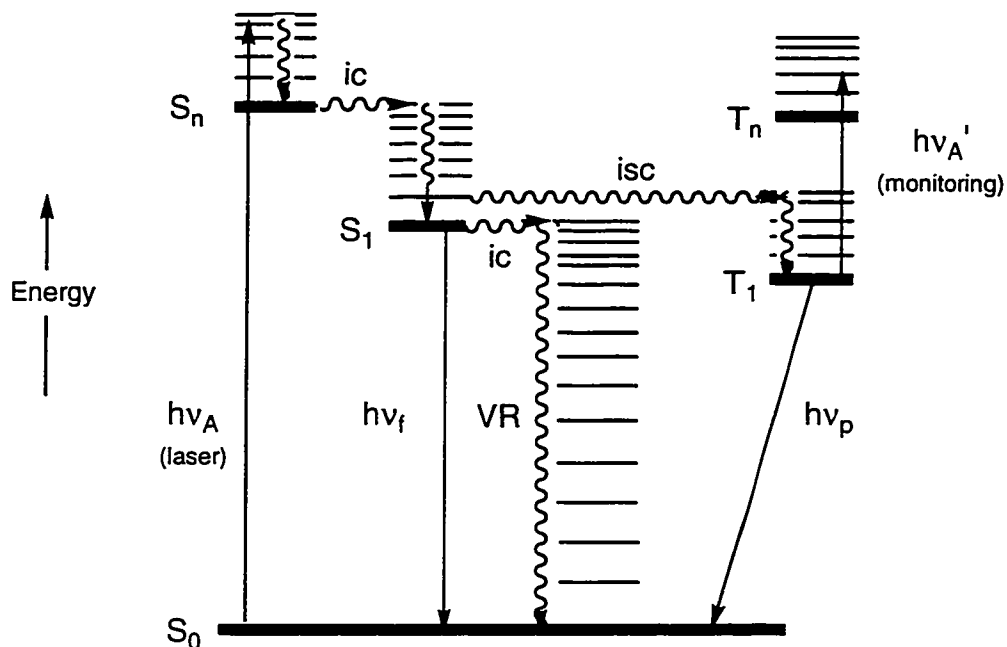


Figure 3.1: Jablonski diagram showing the absorption of laser light ($h\nu_A$ (laser)) and subsequent unimolecular deactivation processes. Radiative pathways are fluorescence ($h\nu_f$) and phosphorescence ($h\nu_p$); nonradiative pathways are internal conversion (ic), intersystem crossing (isc) and vibrational relaxation (VR). Absorption of photons from a monitoring beam ($h\nu_A'$ (monitoring)) by the triplet formed through intersystem crossing can be measured using the technique of laser flash photolysis (described in 2.1.1).

Fluorescence and internal conversion are spin allowed transitions while phosphorescence and intersystem crossing are spin forbidden. The kinetics of unimolecular decay processes follow a first order rate law according to equation 3.1:

$$I = I_0 e^{-k_E t} \quad 3.1$$

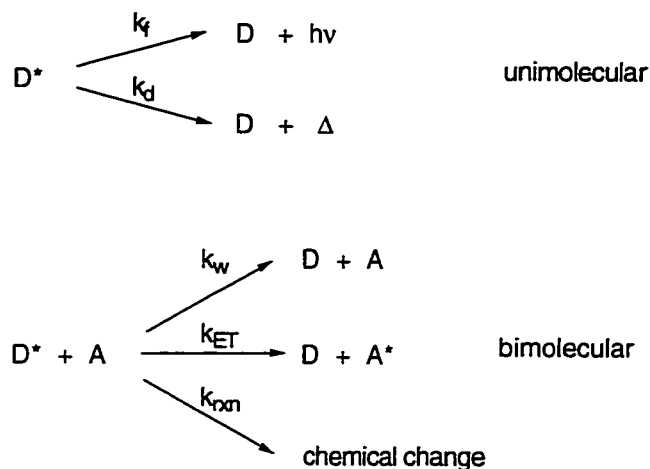
where I_0 is the intensity of light emitted which is measured immediately after excitation and I is that which is measured after time interval, t . The rate constant of emission, k_E , is inversely related to the lifetime of emission (τ_E) expressed in equation 3.2 which is the average time that a molecule spends in the excited state (emission can be either fluorescence or phosphorescence depending on the excited state).

$$\tau_E = \frac{1}{k_E} \quad 3.2$$

Rate constants for spin allowed transitions are relatively fast: fluorescence k_f are $\sim 10^6$ - 10^9 s^{-1} and internal conversion k_{ic} are $\sim 10^{12}$ - 10^{14} s^{-1} while phosphorescence k_p are usually $\sim 10^{-2}$ - 10^4 s^{-1} and intersystem crossing k_{isc} are 10^6 - 10^{11} s^{-1} .

3.1.2 Energy Transfer

Deactivation of the excited state can occur by emission, radiationless decay or by via energy transfer as depicted by Scheme 3.1. Bimolecular energy transfer occurs upon an encounter between the donor and the acceptor by diffusion through the solvent, whereas unimolecular energy transfer occurs via emission or radiationless decay. The kinetics of quenching in bimolecular encounters includes all of the possible forms of deactivation of the donor by the acceptor and can be mathematically expressed by equation 3.3.



Scheme 3.1: Unimolecular and bimolecular mechanisms for energy conversion from an excited state.

where D^* is the excited donor, A is the acceptor, k_f and k_d are the rate constants for fluorescence and radiationless decay, respectively; k_{ET} is the rate constant for energy transfer, k_w is the rate constant for 'wasted' energy loss through radiationless mechanisms, and k_{rxn} is the rate constant for chemical reaction between the excited donor and acceptor.

$$k_q = k_{ET} + k_w + k_{rxn} \quad 3.3$$

The quantum yield of energy transfer by quenching can be expressed by equation 3.4:

$$\Phi_q = \frac{k_q[A]}{k_f + k_d + k_q[A]} \quad 3.4$$

provided D^* is formed with $\Phi = 1$.

In characterizing the photophysical properties of melatonin, quantum yields for fluorescence and intersystem crossing for melatonin were determined utilizing this expression; experiments

were conducted under conditions whereby some of the terms could be eliminated for simplification. For example, the quantum yield for fluorescence in the absence of quencher is expressed by equation 3.5:

$$\Phi_f = \frac{k_f}{k_f + k_d} \quad 3.5$$

The ratio of the fluorescence quantum yields in the presence and absence of quencher leads to an important relationship, called the Stern-Volmer relationship (equation 3.6), that can be used to determine quenching rate constants (*vide infra*), provided the fluorescence lifetime is known.

$$\frac{\Phi_f}{\Phi_{f/A}} = 1 + \tau_f k_q [A] \quad 3.6$$

In determining the feasibility of a photobiological role for melatonin *in vivo*, only bimolecular ground state interactions with excited molecules need be considered, where melatonin is the ground state acceptor and potential excited state donors may be singlet oxygen and/or ocular chromophores capable of absorbing visible light. Usually energy transfer takes place from the longer-lived triplet state, and, due to spin conservation rules, would result in the generation of the excited triplet state of melatonin, providing the triplet energy of the donor exceeds that of melatonin. In addition to quenching via energy transfer, indole derivatives are also known to participate in charge transfer reactions from excited triplets by various mechanisms including photoaddition to the double bond in the pyrrole ring, hydrogen abstraction, and/or physical deactivation.²³ A review of the literature indicates that melatonin has been found to quench the triplet state of benzophenone by donating a hydrogen atom²⁴ and physically deactivate excited singlet oxygen,²⁵ but there seems to be a paucity of information regarding other deactivation mechanisms.

Hardeland *et al.* found that melatonin undergoes electron abstraction by the cation of protoporphyrin which is generated as a result of electron abstraction by ground state molecular oxygen from the triplet state of excited protoporphyrin.² Porphyrins are known to generate

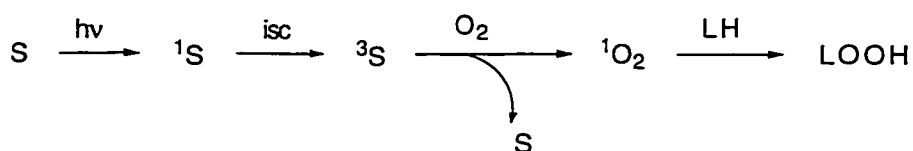
singlet oxygen with great efficiency and melatonin has been found to deactivate singlet oxygen efficiently. Since Reszka *et al.* found that melatonin did not undergo chemical alteration in the process of deactivating singlet oxygen,²⁵ it is likely that melatonin quenches singlet oxygen by the mechanism shown in Scheme 3.1, whereby energy transfer results in radiationless 'wasting' of energy. In the literature, the only report of an encounter between melatonin and an oxygen species that results in chemical reaction, occurs with superoxide anion to generate the N-acetyl-N-formyl-5-methoxykynuramine (AFMK) metabolite of melatonin.^{3,9} Both superoxide anion and singlet oxygen are products of excited protoporphyrins by way of charge transfer and energy transfer mechanisms, respectively. Since melatonin has been found to be an efficient scavenger of both oxygen species, it is highly probable that the role of retinal melatonin includes scavenging the singlet oxygen and superoxide anion arising from excited ocular protoporphyrin.

3.1.3 Singlet Oxygen Quenching

The electron configuration of the ground state of molecular oxygen is such that according to Hund's rule, two unpaired electrons occupy separate degenerate π orbitals with parallel spins. Thus, the lowest energy state of molecular oxygen is a triplet and the electronic distribution of these two electrons gives rise to three singlet states of varying energies. The four possible orbital configurations can be represented as triplet: $(\pi_x^* \uparrow)(\pi_y \uparrow)$ known as $^3\Sigma$ - ground state configuration; singlet: $(\pi_x^* \downarrow)(\pi_y^* \uparrow)$ known as $^1\Sigma$ with an energy that lies 37.5 kcal/mol above the triplet ground state; singlet $(\pi_x^* \uparrow \downarrow)^2$ known as $^1\Delta_x$; and singlet $(\pi_y^* \uparrow \downarrow)^2$ known as $^1\Delta_y$; the singlet $^1\Delta$ states are degenerate with an energy that lies 22.5 kcal/mol (94 kJ/mol) above the triplet ground state, and are the states that are referred to in this thesis as singlet oxygen. Due to the spin forbidden conversion of $^1\Delta$ to $^3\Sigma$, singlet oxygen lifetimes are generally long in solution, but because of its low lying energy, inefficient luminescence occurs in the infrared at 1269 nm, and measurement requires the use of sensitive infrared detectors.

Singlet oxygen sensitization occurs via the formation of an encounter complex with the triplet state of a substrate.

Due to long lifetimes and its relative selectivity in condensed phases, singlet oxygen can diffuse long distances, thereby reacting with molecules at sites far from its inception. The biological consequences of singlet oxygen reactivity include phototoxicity and photocarcinogenesis; singlet oxygen involvement in photosensitized polyunsaturated fatty acid/lipid peroxidation by the Type II photooxidation reaction^a depicted in Scheme 3.2, causes membrane damage and photohemolysis.²⁶



Scheme 3.2: Type II photoperoxidation mechanism, where S is a photosensitizer, LH is a membrane lipid substrate, and LOOH is the lipid hydroperoxide formed by the addition of singlet oxygen.

Certain amino acids, such as tryptophan and histidine and the nucleotides adenosine and guanine are particularly sensitive to oxidative damage by singlet oxygen attack. Unlike superoxide anion and hydrogen peroxide, there are no known enzymatic defenses to scavenge singlet oxygen *in vivo*. The low physiological levels of melatonin may be sufficient to contribute to ocular protection since melatonin efficiently scavenges singlet oxygen without chemical modification.

^a Photooxidation reactions are classed as either Type I or Type II. A Type I photooxidation involves the generation of free radicals that initiate peroxidation chain reactions while a Type II photooxidation involves the production of singlet oxygen through sensitization.

3.2.0 Materials and Methods

Melatonin, biphenyl, and 2-(4-biphenyl)-5-phenyl-1,3,4-oxadiazole (PBD) were used as received from Aldrich (Milwaukee, Wisconsin), benzophenone (Aldrich) was recrystallized from ethanol, and 1,3-cyclohexadiene and acetophenone were cold-trap distilled. The purity of melatonin was ascertained by GC-MS; only one major peak with a mass spectrum characteristic of melatonin was apparent. Cyclohexane, benzene, methanol, ethanol, and acetonitrile were Omnisolv grade and were used as received.

Phosphorescence was measured in a 4:1 ethanol/methanol glass at 77K. Fluorescence spectra and quantum yield measurements were performed on samples deaerated with N₂. Singlet oxygen generation was measured using a 308 nm excimer laser as the excitation source (described in Chapter 2), and a germanium diode was used to detect the infrared emission of ¹O₂. Kinetic measurements for the excited states of melatonin were conducted on a laser flash photolysis system also described in detail in Chapter 2.

Fluorescence lifetimes were measured using the fourth harmonic (266 nm) of a YAG pulsed picosecond Continuum laser system with a Hamamatsu Streakscope detector controlled by a Macintosh computer. Static and flow-through cells were used to obtain spectral information. All samples were prepared such that the optical density measured between 0.2 and 0.5 prior to LFP to avoid the occurrence of shock waves during laser experiments.

3.3.0 Results

3.3.1 Absorption and Fluorescence Spectra

Figure 3.2 shows that melatonin absorbs light only in the ultraviolet region with a maximum absorption at ~278 nm. Little or no shift in the absorption maxima was apparent with any of the solvents used. Solvent effects are induced by solvent-solute interactions, such as dispersion, polarization, electrostatic forces or charge transfer, which change upon

excitation. Usually, the excitation process occurs on such a fast timescale that the Franck-Condon principle holds; the Franck-Condon principle states that an electronic transition from the ground state to the excited state occurs much faster than vibrational motion such that the vibrational wavefunction of the nuclei is the same in both the ground and excited states. Even if melatonin did interact with the solvent to induce a change in the dipole moment, the solvent would not reorganize itself to accommodate the change in sufficient time to affect the electronic transition and cause a shift in the spectrum maximum. Minimal interaction between the melatonin and solute is reflected by a lack of shift in the absorption maximum of melatonin as a function of solvent.

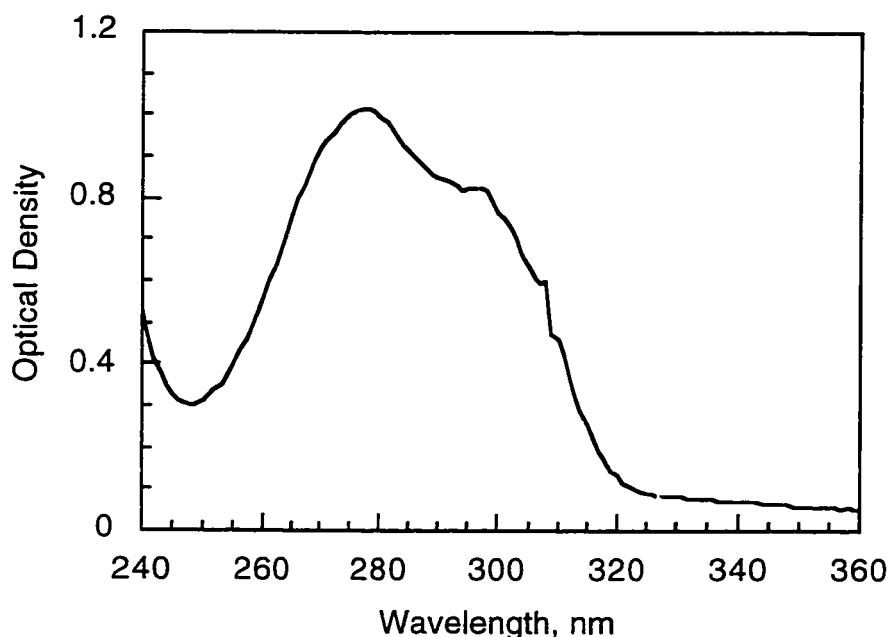


Figure 3.2: Absorption spectrum of 0.1 mM melatonin in acetonitrile at ambient temperature; optical path is 1.0 cm.

The fluorescence spectrum of melatonin is strong in the near UV with a maximum at ~340 nm, showing minimal overlap between the excitation and fluorescence spectrum and a (0,0) band of fluorescence at 295 nm representing a singlet energy of ~97 kcal/mol (406 kJ/mol) (Figure 3.5). Although the (0,0) band in Figure 3.5 is not resolved, it can be extracted

from the intersection between the excitation and emission spectra since this is the energy level at which lowest energy absorption and highest energy emission occurs. The absorption characteristics of melatonin appear to be unaffected by solvent except in water where the fluorescence spectrum shows a bathochromic shift (Figure 3.3). If a solute-solvent interaction causes a change in the polarization of the solute molecule, the time period between emission and absorption is sufficiently long for solvent reorientation to occur, and subsequent changes in the vibrational wavefunctions of the excited nuclei relative to the ground state manifest themselves as a Stokes shift in the emission spectrum. This Stokes shift in water appears to be characteristic of other indoles^{27,28} and is most likely due to the stabilizing effect of strong hydrogen bonding between the indolic N-H and water.

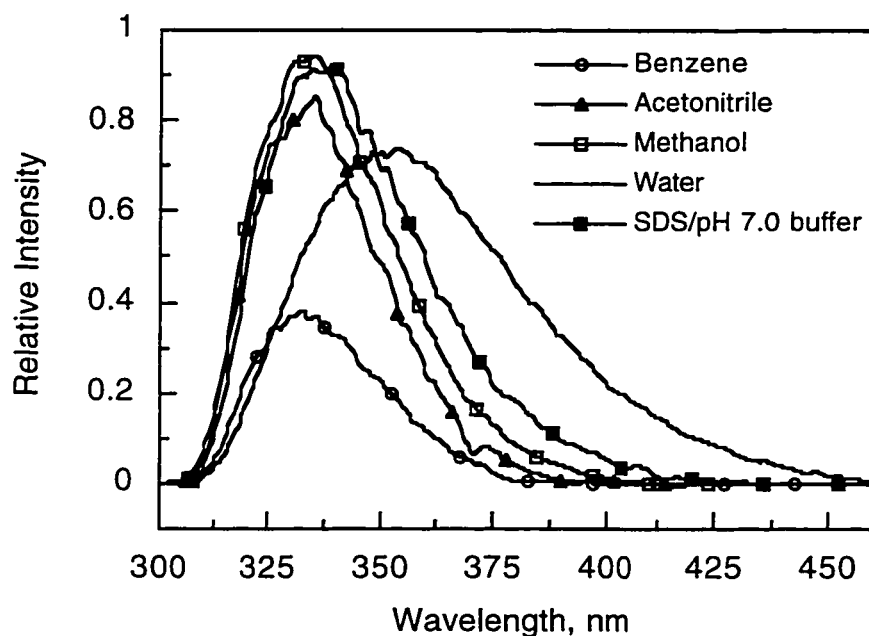


Figure 3.3: Effect of solvent on steady state fluorescence spectra of melatonin at ambient temperature (excitation wavelength 290 nm); optical path is 1.0 cm.

3.3.2 Fluorescence Quantum Yield

In order to measure the quantum yield of fluorescence accurately, a reference standard that fluoresces with a known quantum yield and has particular spectral characteristics must be employed. Ideally, the absorption and emission spectra of the reference compound should not overlap and should be similar to melatonin so that any wavelength-dependent fluctuations in the excitation source and/or detector will not affect the results. The compound 2-(4-biphenyl)-5-phenyl-1,3,4-oxadiazole (PBD) in cyclohexane was used as a reference to measure the fluorescence quantum yields for melatonin in various solvents. PBD was selected because its absorption and fluorescence spectral characteristics are very similar to those of melatonin, and PBD has a fairly high fluorescence quantum yield (0.69) in cyclohexane.²⁹

Fluorescence quantum yields were calculated using equation 3.7:

$$\Phi^M = \Phi_A \times \frac{I^M}{I^A} \times \frac{(n^2)^M}{(n^2)^A} \times \frac{1 - 10^{-OD(A)}}{1 - 10^{-OD(M)}} \quad 3.7$$

where Φ is quantum yield, n is the refractive index of solvent, OD is absorbance, I is the integrated area under the fluorescence spectrum, M is melatonin and A is the reference PBD. The quantum yields obtained are given in Table 3.1. Neutral density filters were used as required to bring the strong fluorescence into the instrumental range of detection.

SOLVENT	Φ_F	τ , ns
Acetonitrile	0.60	6.1
Methanol	0.52	5.6
Water (buffer at pH 7.0)	0.20	3.6
Benzene	0.54	- ^b
1:1 Acetonitrile/Water	-	5.4

Table 3.1: Fluorescence lifetimes and quantum yields ($\pm 10\%$) for melatonin in both protic and aprotic polar solvents and a non-polar solvent.

3.3.3 Fluorescence Lifetimes

The fluorescence lifetimes of melatonin in various solvents listed in Table 3.1 range from 4.7 ns in dioxane to 6.1 ns in acetonitrile, with an uncertainty in measurement of about $\pm 10\%$. Fluorescence decay was approximately monoexponential regardless of solvent, except in unbuffered water where a biexponential fit provided for an improved fitting. A typical fluorescence decay trace is illustrated in Figure 3.4.

^b The 266 nm laser employed in these studies cannot be used with benzene as solvent.

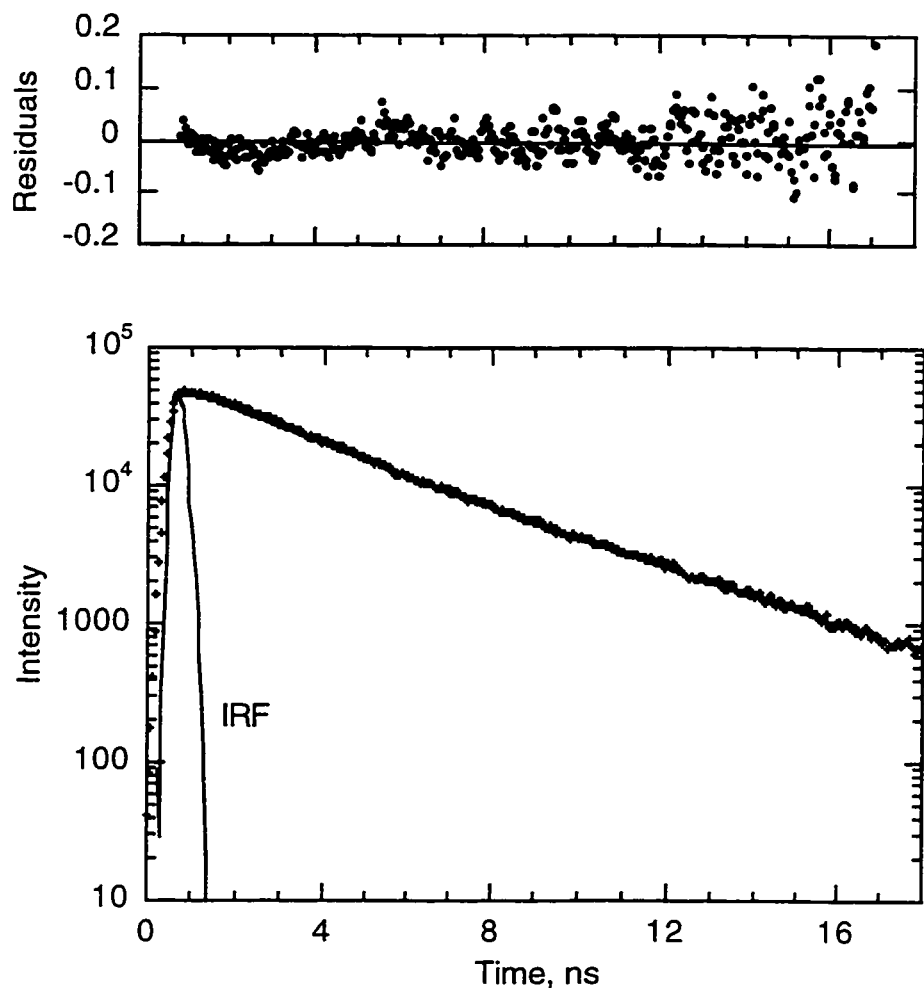


Figure 3.4: Fluorescence decay for melatonin in buffer at pH 7 following 266 nm picosecond excitation. *Top*: plot of residuals; *Bottom*: Fluorescence decay with monoexponential fit and instrument response function (IRF).

The similarities to the photophysics of tryptophan are once again evident with respect to fluorescence decay kinetics; Szabo and Rayner have reported biexponential decay of tryptophan in aqueous solutions of pH 7.0 with lifetimes of 3.14 ns and 5.1 ns.³⁰ The values in Table 3.1 provide our initial determinations of these lifetimes.

3.3.4 Phosphorescence

The triplet energy can be obtained by calculating the energy gap corresponding to the highest energy vibrational band in the phosphorescence spectrum, which represents the (0,0) transition. Figure 3.5 shows the (0,0) band for melatonin phosphorescence to be at 409 nm, representing a triplet energy of ~ 70 kcal/mol (293 kJ/mol). The phosphorescence spectrum of melatonin is similar to that of tryptophan in the same wavelength range; the (0,0) band of tryptophan emission is around 410 nm.³¹

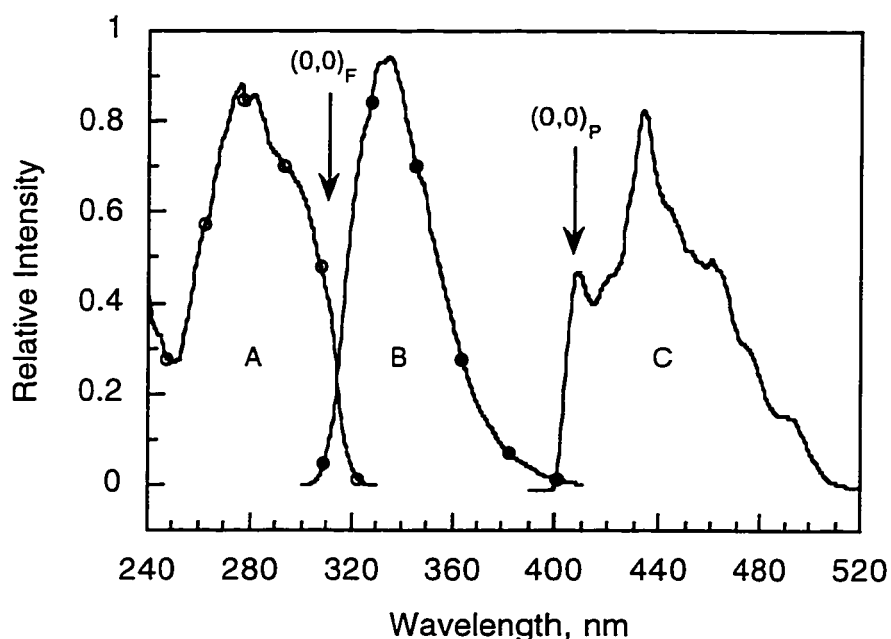


Figure 3.5: A - Excitation spectrum of melatonin in methanol at ambient temperature (emission $\lambda = 340$ nm). B - Fluorescence spectrum of melatonin in methanol at ambient temperature (excitation at 290 nm). C - Phosphorescence of melatonin in 4:1 ethanol/methanol glass at 77K; $(0,0)_F$ and $(0,0)_P$ indicates the (0,0) bands for fluorescence and phosphorescence, respectively.

3.3.5 Singlet Oxygen Emission

Generation of singlet oxygen is commonly used to confirm the existence of a triplet state and thus provide some evidence for the occurrence of intersystem crossing. Benzophenone was used as a reference standard since it is known to generate singlet oxygen with a quantum yield of 0.36 in acetonitrile and absorbs light at the selected excitation wavelength (i.e., 308 nm).³² All samples were deaerated with N₂ for 30 minutes after the singlet oxygen emission determination, and were then measured again to verify that the observed signals originated from the emission of electronically excited oxygen. Since the nitrogen saturated samples showed a significant, interfering spike where the maximum signal is usually measured (see Figure 3.6), the maximum signal on both the sample and the reference standard were measured after the spike at about 65 μ s. This interference was unavoidable at the time of the measurements and was later confirmed to be due to RF interference from other instruments in the laser room.

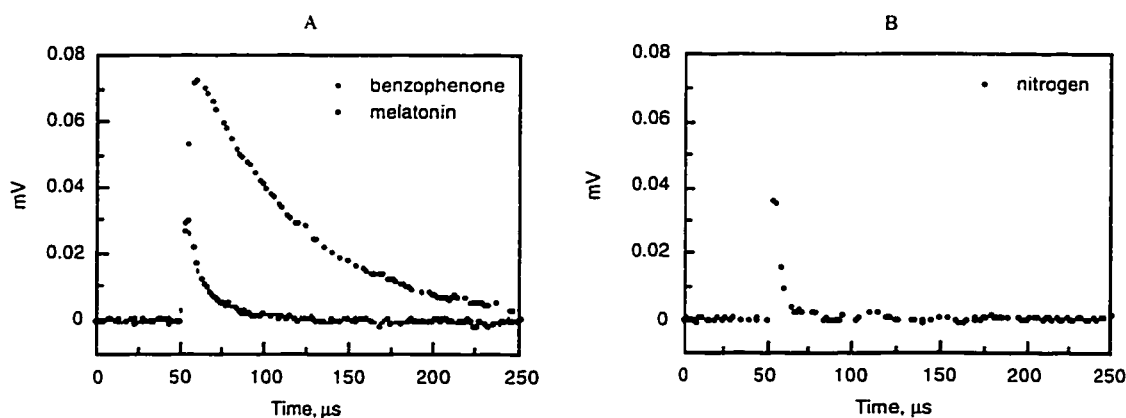


Figure 3.6: A - Comparison of the singlet oxygen emission resulting from sensitization by benzophenone and melatonin at ambient temperature. Both benzophenone (OD = 0.272) and melatonin (OD = 0.278) were optically matched in acetonitrile and saturated with oxygen prior to laser excitation at 308 nm. B - Signal generated by nitrogen-purged melatonin sample used in A.

Melatonin produced singlet oxygen with an efficiency of about 3% (Figure 3.6) in duplicate measurements, suggesting that intersystem crossing from the singlet manifold into the triplet, albeit inefficient, does occur. Benzophenone was selected as a reference standard for the determination of singlet oxygen quantum yield for melatonin because of its low quantum yield relative to commonly used reference standards such as phenazine ($\Phi_{\Delta} = 0.83$) or Rose Bengal ($\Phi_{\Delta} = \sim 0.80$).

3.3.6 Laser Flash Photolysis Studies

In order to determine the triplet absorption characteristics of melatonin, the technique of laser flash photolysis was employed. However, the resulting transient spectra of melatonin in various solvents were complex and difficult to interpret (see Figure 3.7). Transient spectra of several substituted indolyl radical species are available in the literature,³³ and characteristic absorptions at 320 and 520 nm for the neutral radicals and 330 and 580 nm for radical cations, with hypsochromic shifts of about 30 nm for electron attracting substituted groups, appear to be typical.^{33,34} Absorption by the neutral radical of melatonin occurs at 490 nm in acetonitrile.²⁴ Examination of the spectra of Figure 3.7 clearly shows absorptions in the 400-480 nm region that cannot be due to radical species.

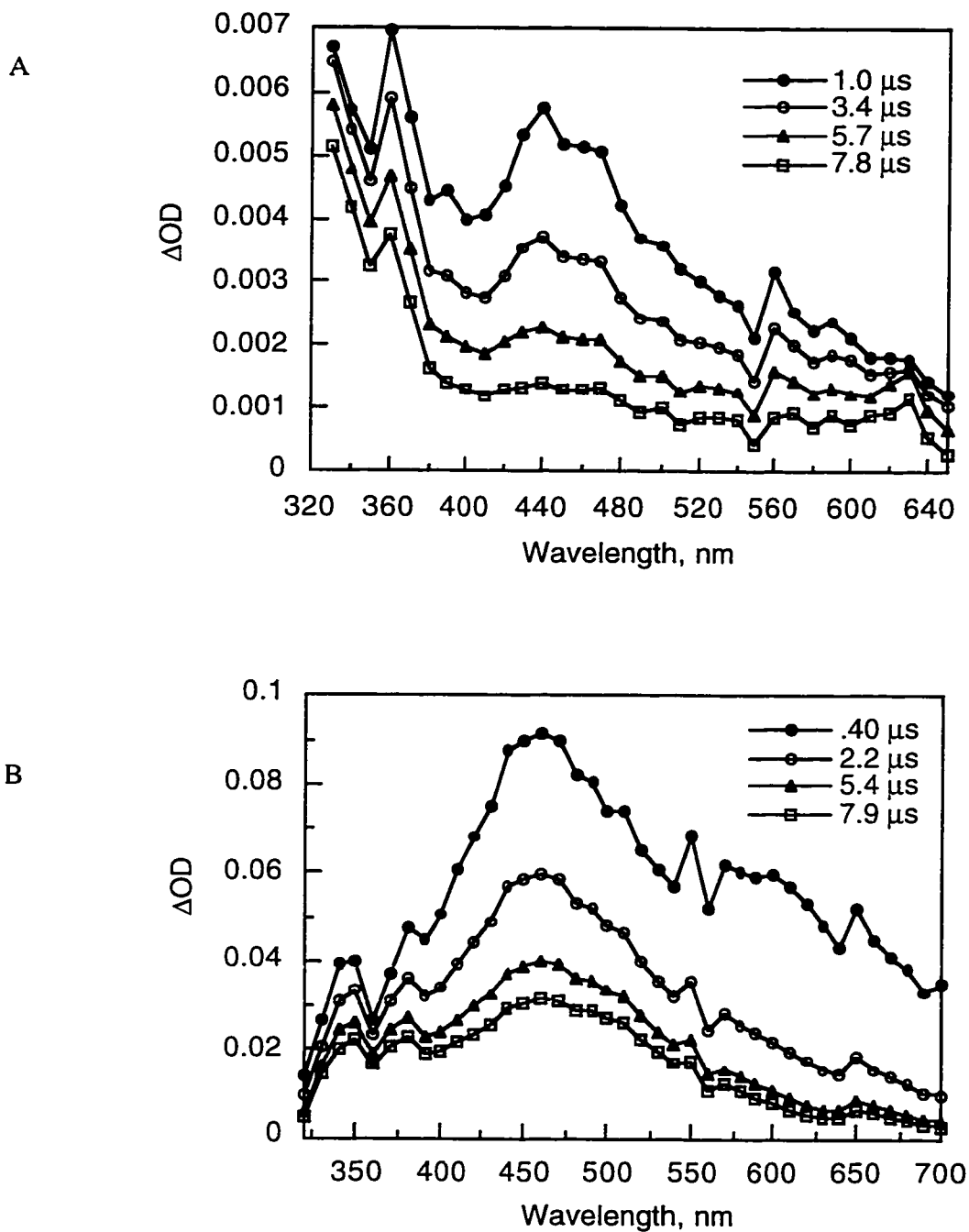


Figure 3.7: Transient spectrum (at ambient temperature) obtained by laser (308 nm) excitation of A - melatonin in acetonitrile using a static sample cell; B - melatonin in water using a static sample cell. The inset legend shows the time delays following excitation from the laser pulse.

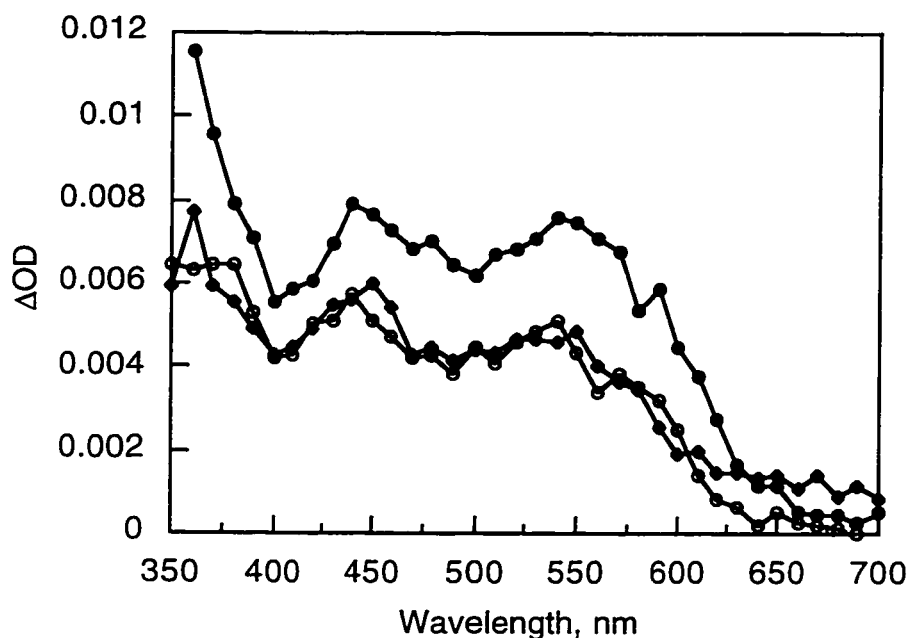


Figure 3.8: Transient spectra of melatonin in methanol (○), melatonin in acetonitrile (●), and 5-methoxyindole in methanol (◆) at ambient temperature, laser excitation at 308 nm; flow cell was used. All spectra were recorded after a $\sim 1 \mu\text{s}$ time delay following laser excitation. All samples had an optical density of 0.45 ± 0.5 prior to LFP.

A comparison of the transient spectra of 5-methoxyindole in methanol and melatonin in both methanol and acetonitrile, shows the presence of a peak at 440 nm which is shifted to 450 nm for 5-methoxyindole. A peak at 540 nm and 550 nm shows the existence of another transient in the spectra of melatonin and 5-methoxyindole, respectively.

3.3.7 Triplet State Involvement

The use of common triplet quenchers such as oxygen and 1,3-cyclohexadiene, with a triplet energy of 54 kcal/mol (226 kJ/mol), provided further insight into the identification of the triplet state in the transient spectrum. Figure 3.9 shows that in the spectrum of melatonin with added 1,3-cyclohexadiene, a transient with a maximum between 550 and 570 was apparent,

and the peaks in the wavelength range of 370 nm to 510 nm were diminished. While several of the transient peaks diminished in the presence of both oxygen and 1,3-cyclohexadiene, it is clear that this (particularly in the case of oxygen) is not unequivocal proof for the triplet state. Thus, we employed a better diagnostic method to establish the triplet state characteristics.

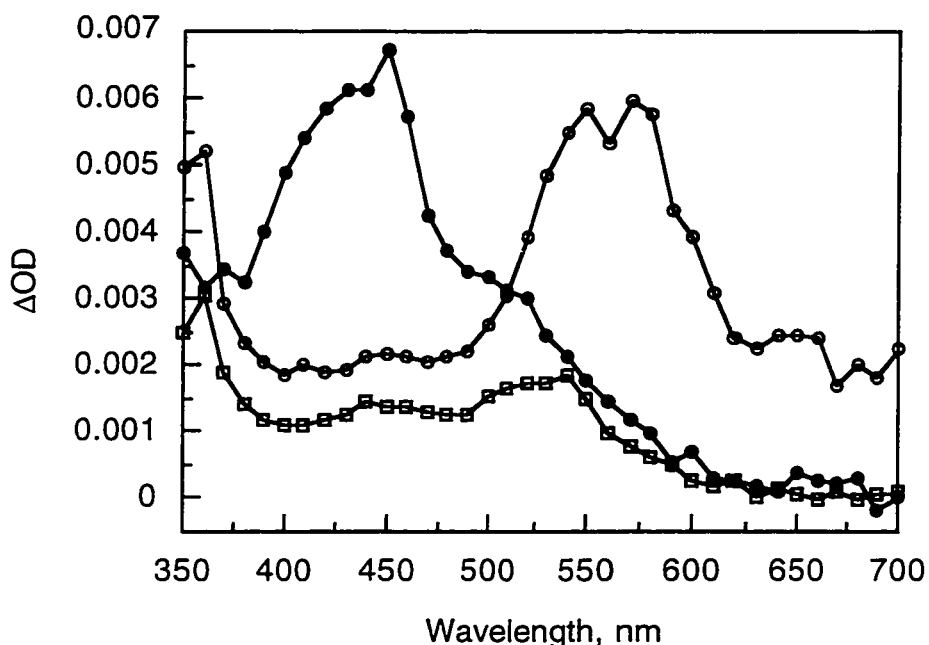


Figure 3.9: Transient spectrum of melatonin showing the effects of quenching by oxygen (\square) and diene (\circ); melatonin spectrum in the absence of quencher (\bullet) shows absorption between 370 nm and 550 nm. Excitation wavelength - 308 nm at ambient temperature using a static sample cell. The time delay following laser excitation is $\sim 1 \mu\text{s}$ for each spectrum.

In order to exploit the advantages of triplet quenching, it is desirable to employ a quencher that, through energy transfer, leads to a readily detectable triplet state for the acceptor. The quencher should be unreactive towards melatonin, be transparent at the excitation wavelength, its triplet energy must be lower than that of melatonin, and the triplet-triplet absorption of the quencher must be strong and easily resolved to allow for the time-resolved monitoring of its growth. Biphenyl, with a triplet energy of 65.8 kcal/mol (275 kJ/mol),^{23,35}

met these criteria, and was the triplet quencher of choice. Sensitization by melatonin is depicted by the simplified Jablonski diagram in Figure 3.10.

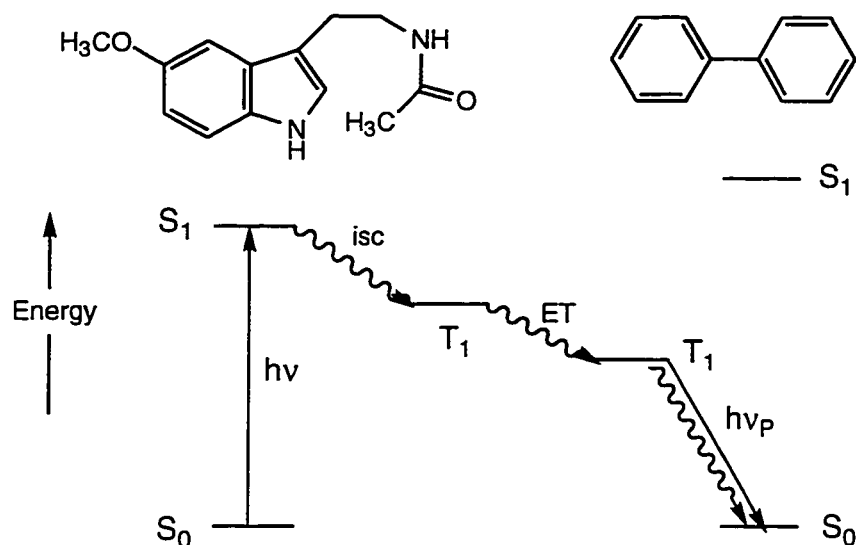


Figure 3.10: Simplified Jablonski diagram showing energy transfer from the triplet of melatonin to the triplet of biphenyl; S_0 and S_1 represent the ground state and excited state singlet energy levels, respectively, and T_1 represents the triplet state energy levels for both biphenyl and melatonin; isc is intersystem crossing and ET is energy transfer.

In order to suppress interferences and unnecessary complications arising from possible multiphoton absorption processes, a light diffuser was used to attenuate the laser beam, thus providing a lower intensity, homogeneous excitation source. Multiphoton processes could lead to electron ejection and partial recapture by biphenyl. Figure 3.11 shows a peak at ~ 400 nm in the transient spectrum that disappears with the diffuser-attenuated laser beam. Because all of the conditions and time delays are the same for spectra A and B in Figure 3.11, the impact of this adventitious transient on the growing biphenyl triplet is unmistakable.

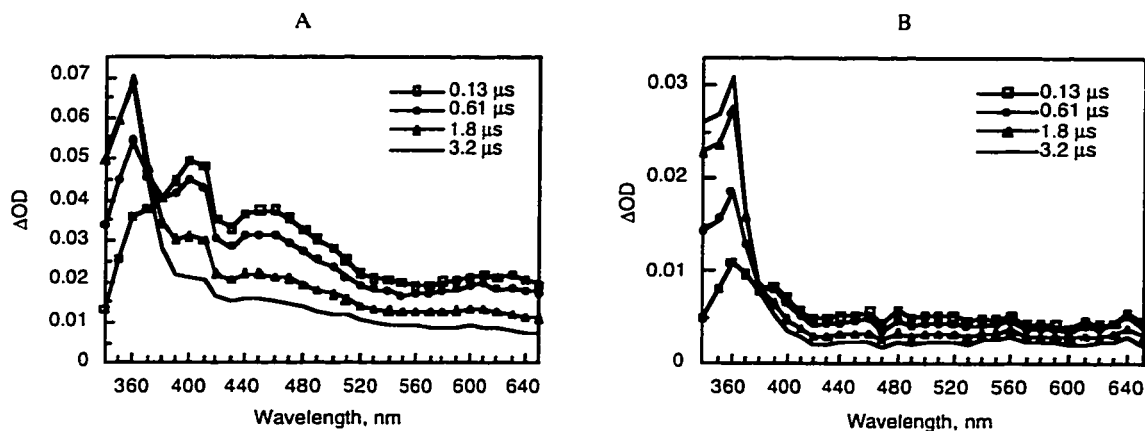


Figure 3.11: Transient spectrum of 0.1 mM melatonin and 0.34 mM biphenyl (excitation at 308 nm): A - without light diffuser; B - with light diffuser. The inset legend shows the time delay following laser excitation. N.B.: The peak at ~400 nm in A is probably due to a transient induced by a multiphoton event.

Energy transfer from the triplet of melatonin to biphenyl was monitored by measuring the growth of the quencher triplet as the concentration of biphenyl was increased while that of melatonin remained constant. The growth of the biphenyl triplet was monitored at 360 nm and was easily measured (see inset in Figure 3.12). If interaction involves energy transfer, then the rate of decay of the triplet sensitizer (melatonin) should match the rate of growth of the quencher excited state. The rate constants for energy transfer to the triplet of the quencher were obtained by fitting the growth kinetic traces for each concentration of quencher (k_{obs}) with first order kinetics, thus:

$$k_{\text{obs}} = k_0 + k_3 [\text{biphenyl}] \quad 3.8$$

where k_0 is the rate constant of melatonin triplet decay in the absence of quencher, and k_3 , the slope of the line, is the bimolecular rate constant for energy transfer to biphenyl. A plot of the triplet growth rate constant as a function of biphenyl concentration (Figure 3.12) revealed that in the absence of quencher, the melatonin triplet decays with a rate constant of about 4.8×10^5

s^{-1} , corresponding to a lifetime of 2.1 μs , and the rate constant of energy transfer from the melatonin triplet to the triplet biphenyl is $7.7 \times 10^8 M^{-1}s^{-1}$. The inset in the same figure shows a representative kinetic growth trace for triplet biphenyl.

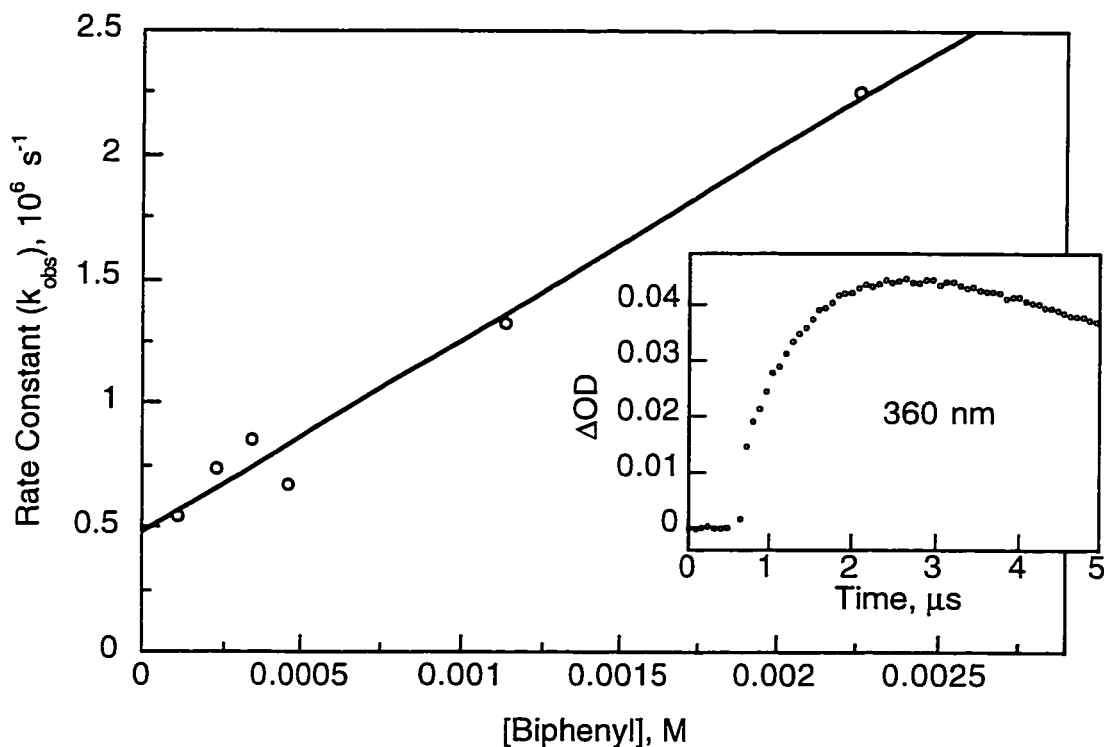


Figure 3.12: Dependence of the rate constant for the growth of biphenyl triplet as a function of quencher concentration. The slope ($7.7 \times 10^8 M^{-1}s^{-1}$) corresponds to the rate constant for energy transfer. *Inset*: Growth of the biphenyl triplet for 1.2 mM biphenyl.

The rate constant in the absence of quencher was used as a reference with which to examine the transient spectrum of melatonin (Figure 3.7). A curve fit of the kinetic decay trace of the peak at 440 nm gave a rate constant of $4.2 \times 10^5 s^{-1}$ which was similar to the triplet rate constant derived from the biphenyl studies. Thus we have assigned the absorption at 440 nm to the triplet state, which is in accordance with other published indolyl triplet absorptions; for

example, the indole and tryptophan triplets absorb at 440 nm and 450 nm respectively.³⁶ Interestingly the rate constant for the melatonin triplet decay in water was found to be $1.5 \times 10^6 \text{ s}^{-1}$ at 440 nm - which is greater than that in organic solvents by almost an order of magnitude - and a corresponding shorter triplet lifetime of 0.7 μs .

3.3.8 Intersystem Crossing Quantum Yield

The intersystem crossing yield for melatonin was determined using acetophenone as the reference and biphenyl as quencher; the triplet of acetophenone absorbs at 320 nm, its triplet energy lies at 74.1 kcal/mol (310 kJ/mol), and the quantum yield for intersystem crossing is ~ 1.0 .^{23,35} Based on the rate constants derived from quenching studies, the concentration of biphenyl (A) required to quench approximately 99% of the melatonin triplets was calculated to be 0.05 M using equation 3.9.

$$[A] = \frac{k_d}{\frac{k_q}{\Phi_{ET}} - k_q} \quad 3.9$$

The concentration of biphenyl used was $0.049 \pm 0.002 \text{ M}$ with melatonin in acetonitrile and $0.050 \pm 0.002 \text{ M}$ with acetophenone in acetonitrile. Biphenyl has a very low molar extinction coefficient at the exciting wavelength used for this measurement. While absorption at the millimolar levels used in the LFP quenching experiments was negligible, absorption of the higher concentration of biphenyl (0.05 M) used in this case was significant, i.e. ~ 0.02 . A correction for this absorption (equation 3.10) was applied to the ΔOD values prior to calculating the intersystem crossing quantum yields:

$$C = \text{TOD}_{bt} \times \frac{\text{OD}_b}{\text{OD}_{b+s}} \quad 3.10$$

where C is the correction to be subtracted from the highest ΔOD of the sensitized biphenyl triplet, TOD_{br} is highest value of ΔOD of the biphenyl triplet, OD_b is the optical density of a 0.05 M biphenyl solution and OD_{b+S} is the optical density of the biphenyl and sensitizer solution. The magnitude of the biphenyl triplet signals at 360 nm were compared for these two solutions which were optically matched solutions at the laser wavelength (308 nm). Compared to that of the acetophenone/biphenyl sample, the optical density of the biphenyl triplet in the melatonin sample was weak (Figure 3.13), and the intersystem crossing yield was found to be correspondingly low at $0.22 \pm 10\%$. This relatively low quantum yield for intersystem crossing is consistent with intersystem crossing efficiencies for other indoles³⁷ and is at least partially responsible for the poor efficiency with which melatonin generates singlet oxygen.

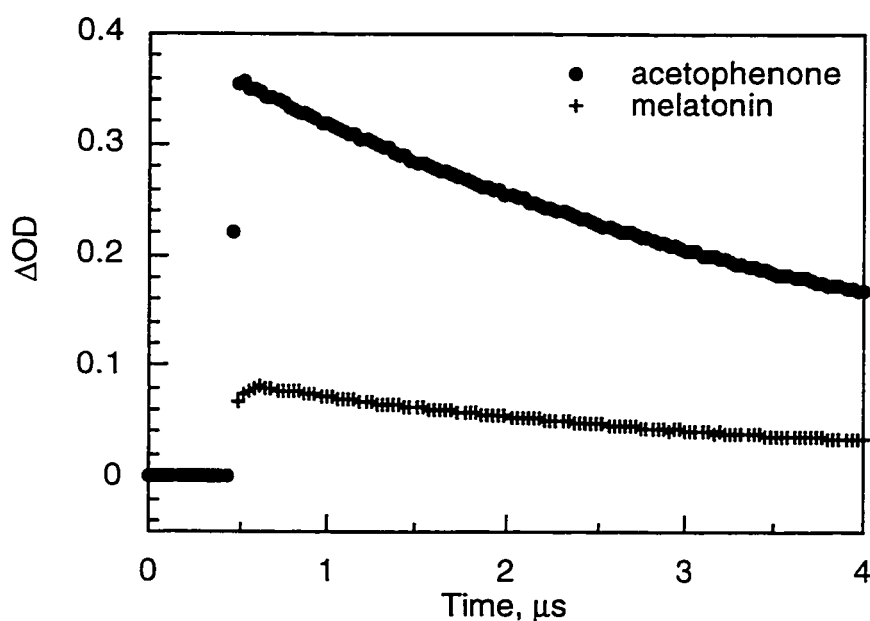


Figure 3.13: Kinetic decay traces of the biphenyl triplet sensitized by melatonin (optical density of melatonin and biphenyl solution was 0.307) and acetophenone (optical density of acetophenone and biphenyl solution was 0.298) at ambient temperature, monitored at 360 nm; excitation was at 308 nm and the time window was 200 ns.

3.4.0 Discussion

3.4.1 Absorption Characteristics and Electronic Transitions

Since the molecular structure of melatonin embodies two chromophores, the aromatic π system of the indole ring and the carbonyl of the amide side chain, two electronic transitions are possible upon absorption of a photon. Whether the transition occurs from the ring as a $\pi\pi^*$ or whether it occurs from the carbonyl as a $n\pi^*$ can sometimes be deduced from the spectra and the energy splitting between the lowest excited singlet (S_1) and the lowest excited triplet (T_1) states. Excited states arising from a $\pi\pi^*$ transition have greater S_1 — T_1 energy splittings, typically between 30 and 40 kcal/mol (126 - 167 kJ/mol), compared to $n\pi^*$ transitions which are usually between 8 and 10 kcal/mol (33 - 42 kJ/mol). The energy gap between the (0,0) band of singlet emission (obtained from the overlap area between the singlet excitation and emission spectra in Figure 3.5) and the (0,0) band of triplet emission was calculated to be ~27 kcal/mol (113 kJ/mol), indicating the likelihood of a $\pi\pi^*$ electronic transition, although it could also mean that the two states have different electronic configurations. In molecules that undergo $\pi\pi^*$ transitions of delocalized π systems, the equilibrium and ground state geometries tend to be rigid, and therefore the excitation and emission spectra do not differ significantly (a notable exception is biphenyl which is discussed further in 3.4.3). Inspection of Figure 3.5 shows the absorption and emission spectra of melatonin to be mirror images of each other, indicating similar vibrational patterns in both the ground and excited states. Since the photophysical properties of melatonin are so similar to those of tryptophan, it is quite likely that they also share a common chromophore - the indole ring. In fact, the absorption spectrum of melatonin is very similar to tryptophan which is π -isoelectronic with indole, indicating that the side chain has little bearing on the absorption properties. However, in the excited state of melatonin there is a possibility that there may be some contribution from an $n\pi^*$ transition

involving the heterocyclic nitrogen, since the vibrational pattern of the phosphorescence spectrum in Figure 3.5 shows the larger energy gaps that are typical of an $n\pi^*$ triplet.

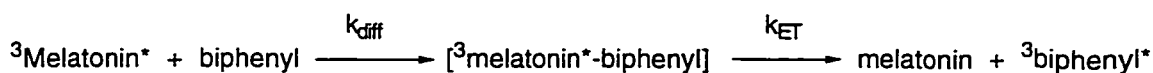
3.4.2 Fluorescence Decay Mechanisms

It appears that the side chain may influence the fluorescence properties of tryptophan and related indoles. Szabo and Rayner attributed the biexponential lifetimes of tryptophan to the presence of two stable conformations.³⁰ According to Chen *et al.*, at least two routes of radiationless deactivation contribute to the rate of fluorescence decay for indoles, and each process may be dependent upon the environment to varying extents.³⁷ Such decay pathways include photoionization, intersystem crossing, exciplex formation, quenching due to solvent interactions, hydrogen atom transfer, charge transfer, and internal conversion. In the case of melatonin, the relatively low quantum yields of fluorescence in water may be due to intramolecular quenching caused by a charge transfer mechanism between the excited electron-rich indole ring and the electrophilic carbonyl group of the amide side chain, in a conformation specifically favored by an aqueous environment. Such intramolecular processes have been proposed by Robbins *et al.* to describe similar decreases in fluorescence quantum yields of tryptophan derivatives that possess side chains including an electrophilic carbonyl group but no NH_3^+ .²⁷ Another reason for the decreased fluorescence quantum yield may be the result of an increased efficiency of intersystem crossing into the triplet manifold in water. Although the quantum yield for intersystem crossing in water was not directly measured, the relatively high ΔOD for the triplet melatonin in water - at least an order of magnitude higher than that in organic solvents (Figure 3.7 B) - indicates either a higher triplet extinction coefficient, or a much more efficient triplet yield. Although our results indicated a monoexponential melatonin fluorescence decay, it is possible that more detailed studies will unveil additional components; the characteristic multiexponential fluorescence behaviour has long since been established in the case of tryptophan and continues to be a subject of attention.²⁸

The laser flash photolysis spectra of melatonin that were obtained using a flow sample cell showed a peak at ~540 nm (Figure 3.8) which is characteristic of the radical cation of melatonin. Despite the fact that the corresponding solvated electron is not apparent in the spectra, it appears that electron ejection occurs from the singlet excited state of melatonin and may be a significant radiationless deactivation pathway. This would explain the observation that the sum of Φ_F and Φ_{ISC} does not total 1.0; in acetonitrile - the sum of these two decay processes add up to 0.82. The remaining 18% of the total quantum yield from all deactivation pathways may be partly due to the non-radiative process of electron ejection from the excited singlet state. It is possible that in the presence of molecular oxygen, this ejected electron forms superoxide, which is known to react with melatonin to produce AFMK. This would also provide an explanation for the absence of the radical cation peak at 540 nm in the transient spectrum of oxygenated melatonin (Figure 3.9). By the same reasoning, the apparent 'quenching' of all of the transients in this particular spectrum may simply be the result of chemical alteration of melatonin by superoxide.

3.4.3 Triplet Energy Transfer Efficiency

Usually, if the triplet energy of the acceptor is 3.5 kcal/mol or lower than that of the donor, then energy transfer is diffusion controlled and k_{ET} is very close to k_{diff} and follows the process depicted by Scheme 3.3.



Scheme 3.3

The triplet energy difference between melatonin and biphenyl is ~4 kcal/mol (17 kJ/mol) but the k_{ET} was determined to be $7.7 \times 10^8 \pm 10\% \text{ M}^{-1}\text{s}^{-1}$ and the k_{diff} for acetonitrile is $\sim 10^{10} \text{ M}^{-1}\text{s}^{-1}$.

Since the rate constant for energy transfer is almost two orders of magnitude below diffusion controlled, it would appear that the melatonin-biphenyl intermediate encounter complex does not always result in successful energy transfer. However, such diminished rate constants for energy transfer are typical with biphenyl because it undergoes extensive conformational reorganization in the triplet state. In ground state biphenyl, the two phenyl groups are orthogonal while in the excited state, the angle between them decreases. This conformational reorganization then becomes the rate-limiting step in the energy transfer between melatonin and biphenyl.

Chapter 4

— Antioxidant Properties of Melatonin —

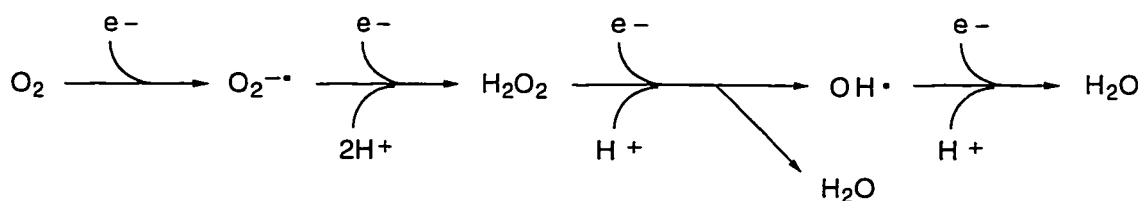
4.1.0 Introduction

Almost every recent article written about melatonin, scientific and otherwise, makes some reference to its antioxidant capabilities^{3,9-18,38-50} yet to date there is no really conclusive evidence to support this claim. The authors of many of the scientific papers in the literature have based their conclusions concerning the antioxidant activity of melatonin on scant experimental evidence. Although the belief that melatonin is a potent antioxidant is not shared by the scientific community at large,^{60,74,82} the growing popularity and increase in sales of melatonin as a nutritional supplement is indicative of the widespread acceptance of this claim by the general populace.

Indirectly, this pineal hormone does work as an antioxidant since it is able to stimulate the activity of the antioxidant enzyme, glutathione peroxidase³⁸ which reduces the free radical precursor hydroperoxides to alcohols. Melatonin has also been found to suppress the activity of cytochrome P450 which, in the process of metabolizing xenobiotics, generates free radicals.⁵¹ However, it has also been claimed that melatonin is able to trap the reactive oxygen free radicals, peroxy and hydroxyl,^{39-41,52} and thus is a potent antioxidant. The lack of scientific data and the disputable interpretations of those data which are available, has inspired us to investigate the antioxidant potential of melatonin at the molecular level using reliable and accepted methods.

4.1.1 Reactive Oxygen Species

Molecular oxygen is a biradical by virtue of its unusual electronic configuration whereby two unpaired electrons of parallel spins reside in different p orbitals. This imposes a spin restriction of opposite parallel spin on any pair of electrons accepted by oxygen during oxidation reactions by oxygen itself. Although this slows oxidative attack by molecular oxygen, which would appear to be advantageous for aerobic biological systems, one electron transfers to oxygen can occur which result in the formation of molecules or atoms having one unpaired electron, i.e., free radicals. In fact, the metabolism of oxygen involves the successive univalent one electron reduction of oxygen to water according to Scheme 4.1:

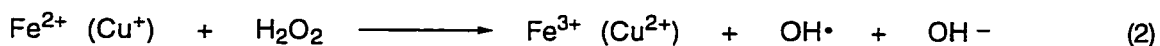


Scheme 4.1

Cellular utilization of molecular oxygen, which is essential to life, paradoxically results in the production of toxic reactive oxygen species. Many enzymatic processes generate superoxide anion, $O_2^{\bullet-}$, and/or hydrogen peroxide, H_2O_2 , which, although by themselves are not toxic, coupled with an appropriate catalyst they are generators of the very reactive, strongly oxidizing hydroxyl radical, $OH\cdot$. Since hydroxyl radicals react with most organic compounds at or near diffusion controlled rates, they can be very damaging *in vivo* close to the site of their inception. All of the four purine and pyrimidine bases in DNA are susceptible to attack and modification by $OH\cdot$. Biological cell membranes are particularly vulnerable because they contain a significant unsaturated lipid component; the allylic hydrogens are easily abstracted by the reactive hydroxyl radical. This resulting lipid radical then readily reacts with molecular

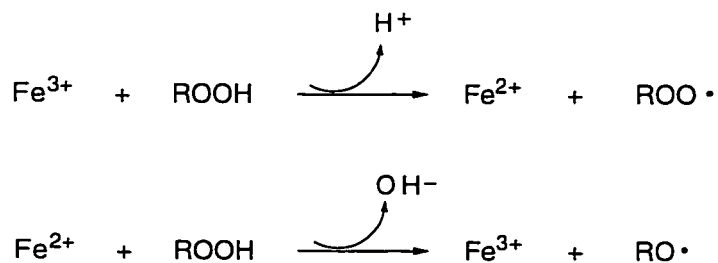
oxygen to form a peroxy radical which in turn abstracts a hydrogen from another proximal lipid or protein molecule.

Metals ions such as Fe^{2+} and Cu^+ can reduce H_2O_2 and alkyl hydroperoxides to $\text{OH}\cdot$ and alkoxy radicals respectively, via Fenton chemistry (see Scheme 4.2 below). These radicals can then initiate the peroxidation of lipids and lipoproteins.



Scheme 4.2: Hydroxyl radical generation via the Haber-Weiss reaction (1) and (2); Fenton reaction (2).

The activity of iron(II) ions is not limited to the initiation step in lipid peroxidation. They are also important contributors to the decomposition of lipid hydroperoxides to alkoxy and alkyl peroxy radicals (Scheme 4.3) which participate in the propagation of the peroxidation chain.



Scheme 4.3

Hydroxyl radicals and peroxy radicals are important initiators and propagators of such lipid peroxidation chain reactions in cell membranes. The hazards associated with radical attack induced by lipid peroxidation involve structural and functional impairment to the cellular

membranes caused by hydrogen abstraction and subsequent covalent cross-linking between membranous lipid and protein. This in turn results in a more rigid, permeable membrane which eventually leads to leakage of cytoplasm and ultimately, the demise of the cell, loss of its biological function and tissue injury.

4.1.2 Protective Defenses Against Oxidative Attack

In order to protect against oxidative attack, organisms have developed enzymatic and non-enzymatic antioxidant defenses that are in balance with the generation of reactive oxygen species.⁵³⁻⁵⁵ The enzymatic antioxidants include catalase and glutathione peroxidase which catalyze the metabolism of hydrogen peroxide and other hydroperoxides to harmless water and oxygen, and superoxide dismutase which converts the reactive superoxide anion to hydrogen peroxide. The enzymatic antioxidants provide intracellular protection while nonenzymatic antioxidants including glutathione, vitamin E, and metal chelating agents such as transferrin and ceruloplasmin provide extracellular protection and are found mainly in circulating blood plasma.

According to Ingold,⁵⁶ there are two classes of antioxidants, the chain-breaking antioxidants and the preventive antioxidants. The chain-breaking antioxidants inhibit chain propagation of oxidation by trapping free radicals via addition reactions, electron or hydrogen atom transfer. Preventive antioxidants reduce the rate of initiation of the chain reaction by peroxide decomposition, metal ion chelation, or by ultraviolet screening.

4.1.3 Melatonin vs. Vitamin E

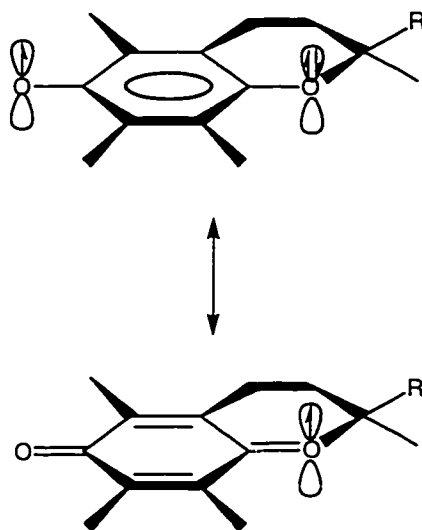
The most potent lipid-soluble, chain-breaking antioxidant *in vivo* is vitamin E.⁵⁷ Since the work of Ianas *et al.* in 1991,⁴⁵ melatonin has been alleged by many to be an antioxidant, and two years later the highly cited literature reports of Pieri and coworkers ascribed an antioxidant potency for melatonin superior to that of vitamin E.^{39,40} Based on their experiments

of inhibition of erythrocyte hemolysis⁴⁰ and inhibition of fluorescence suppression by peroxy radicals,³⁹ Pieri *et al.* concluded that while vitamin E scavenges two peroxy radicals per molecule,^{39,57} melatonin scavenges four. The implication of this claim is that melatonin could be classed as a chain-breaking antioxidant superior to vitamin E and its water-soluble hydroxychroman analogues.¹²

Moreover, in subsequent review articles it was conjectured that since melatonin is lipophilic, it could conceivably concentrate in cellular membranes where it would then scavenge initiating hydroxyl radicals and inhibit any membranous lipid autoxidation by also trapping peroxy radicals.^{12,46,58} This is contradictory to the findings of Burton, Joyce and Ingold, who published results of an earlier study, indicating that vitamin E is the major lipid-soluble chain-breaking antioxidant in human blood;⁵⁹ vitamin E was found to be the major or sole lipid-soluble chain-breaking antioxidant in normal and cancerous tissues, both human and from animals.^{59,60} Furthermore, it seems highly unlikely that melatonin could accumulate in the lipidinous membranes to a concentration high enough to really be an effective radical trap - the physiological concentration of melatonin is less than one nanomolar. Since melatonin has been shown to have relatively high solubility in aqueous medium (millimolar levels),⁶¹ equilibrium concentrations in the hydrophobic membranes would never reach the radical scavenging millimolar levels of the *in vitro* studies that have elevated melatonin to its current status as a superior antioxidant.

Since melatonin has none of the structural features of a good chain-breaking antioxidant (such as vitamin E) and since almost any organic substance can trap the highly reactive hydroxyl radical, we felt it worthwhile to investigate such opposing claims proposed in the literature. In addition to its reactivity toward hydroxyl radicals, melatonin is reported to scavenge *tert*-butoxyl and cumyloxyl radicals with rate constants of 3.4×10^7 and 6.7×10^7 M⁻¹s⁻¹, respectively, which are about seven times faster than those for indoles.²⁴ However, this ability to efficiently scavenge radicals is insufficient evidence to infer antioxidant potency. It is a requirement that the radicals formed as a result of scavenging activity be relatively unreactive

themselves. In the case of vitamin E and related tocopherols for example, the phenoxyl radical formed by reaction with peroxy radicals is stabilized by delocalization of the unpaired electron to the lone pair on the methoxyl oxygen of the heterocyclic chroman ring which is perpendicular to the plane of the ring (see Scheme 4.4). The extent of stabilization is a stereoelectronic resonance effect and depends upon the orbital overlap between the lone pairs and the aromatic π system.⁵⁷ Although the reactivity of the radical product has not yet been assessed in the case of melatonin, there are no structural features that would suggest a similar kind of stabilization.



Scheme 4.4: Resonance stabilization of the phenoxyl radical by the chroman ring.

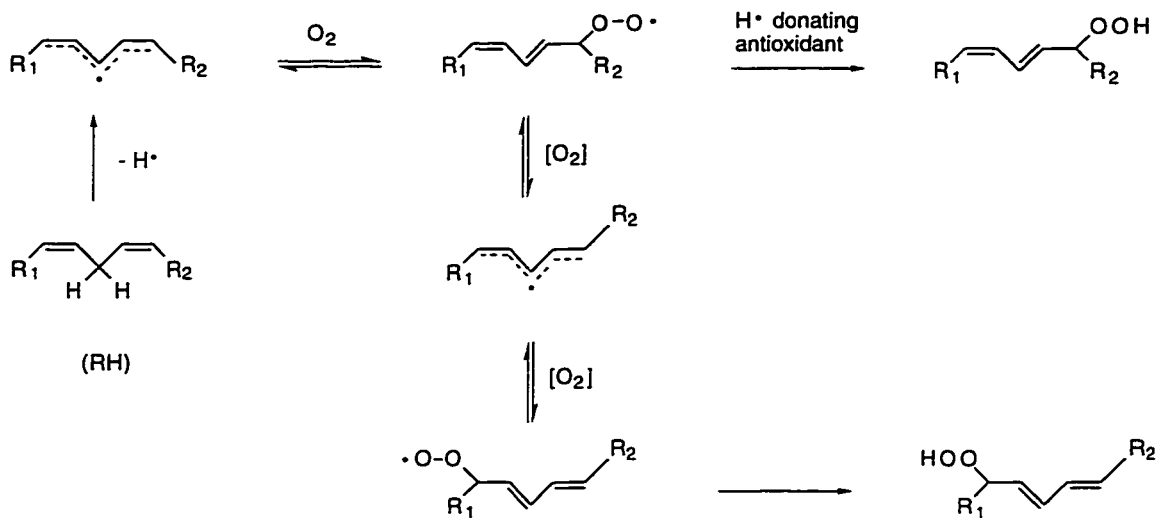
We considered it likely therefore, that if melatonin is an antioxidant, it would probably function as a preventive antioxidant as opposed to a chain-breaking antioxidant. The most likely fashion in which melatonin could exert an antioxidant effect would therefore be to suppress the catalytic effect of metal ions on lipid peroxidations. Binding agents such as transferrin and the ferroxidase, ceruloplasmin are preventive antioxidants found in human

blood serum. Hemoglobin, cytochrome-c and other heme-proteins can catalyse the decomposition of hydroperoxides in blood to generate initiating radicals for lipid peroxidations.⁶²⁻⁶⁴ Tappel⁶³ found that some nitrogenous compounds, which included histidine and tryptophan, were capable of inhibiting lipid peroxidation by the catalytically active iron in hemoglobin and cytochrome *c*. Since melatonin is derived from tryptophan in the body and is structurally quite similar, it is not implausible that it would be capable of the same type of preventive antioxidant activity.

The research comprised in this chapter was conducted in collaboration with Ross Barclay's research group at Mount Allison University in New Brunswick and Keith Ingold at the Steacie Institute of Molecular Sciences, National Research Council, Ottawa. Using a pressure transducer to measure oxygen uptake during the autoxidation of linoleic acid in a micellar, microheterogeneous environment, and styrene in both homogeneous and micellar environments, we hoped to clarify the role and mechanism of melatonin as a preventive antioxidant. Since metal ions are known to catalyze lipid and lipoprotein peroxidations *in vivo*, autoxidations of linoleic acid were also conducted in the presence of copper and iron metal ions, and the activity of melatonin as a preventive antioxidant in these systems was explored. Because melatonin has such a high fluorescence quantum yield,⁵¹ we also conducted fluorescence quenching studies; fluorescence makes a useful probe to examine the interaction between melatonin and iron ions.

4.1.4 Antioxidant Measurement - Methods and Techniques

The mechanism for peroxidation of linoleic acid, which is representative of membrane lipid peroxidation reactions, is depicted in Scheme 4.5:



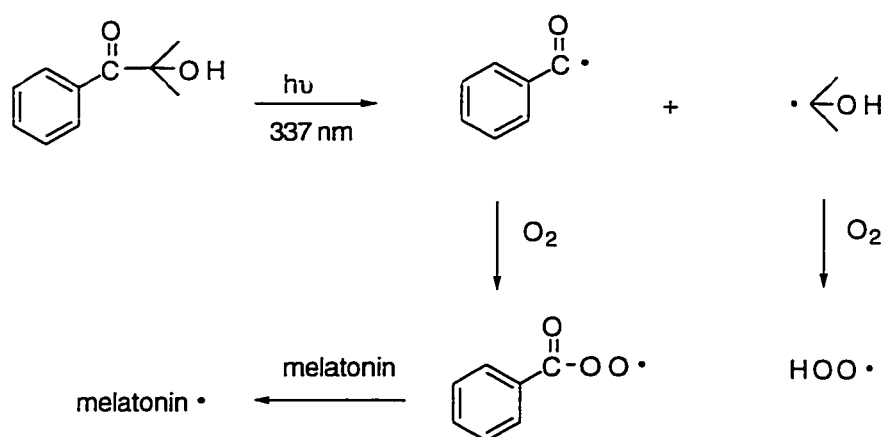
Scheme 4.5: Mechanism of peroxidation of a typical unsaturated lipid.

With the oxygen uptake method, the progress of such peroxidation reactions can be monitored, and the extent to which an added substance provides inhibition can be quantified. There are other methods and techniques that are worthy of brief discussion at this point to provide justification for this choice.

The method used by Pieri *et al.* by which it was concluded that melatonin traps peroxy radicals more efficiently than vitamin E is called the ORAC method developed by R. G. Cutler's research group.⁶⁵ ORAC is an acronym for oxygen-radical absorbing capacity. This assay measures the loss of fluorescence of β -phycoerythrin, an indicator protein possessing a fluorescence quantum yield of greater than 0.9, induced by peroxy radical attack. Peroxy radicals are generated by 2,2'-azobis(2-amidinopropane)dihydrochloride (ABAP) and the ability of a substance to trap these peroxy radicals is purportedly reflected by the persistent fluorescence of the indicator protein until the trapping substance is depleted. The β -phycoerythrin fluorescence is plotted as a function of time, and the area under the curve is integrated to give an ORAC value which, according to Cutler *et al.*, is a measure of the antioxidant activity of the substance. Since the destruction of the peroxy radicals is not

directly measured, and since fluorescence quenching can be caused by factors other than decomposition of a molecule, this method is not deemed a good predictor for true peroxy radical scavenging capability.

Before using the oxygen uptake method, which can be relatively time-consuming, we tried a simple experiment utilizing a laser flash photolysis technique. In this experiment, 2-hydroxy-2-methyl-1-phenyl-1-propan-1-one was irradiated at 337 nm to form geminate radicals which, after separation, react with oxygen at the diffusion-controlled rate to generate a mixture of peroxy and hydroperoxy radicals according to Scheme 4.6. In principle, these peroxy radicals could readily abstract a hydrogen atom from melatonin to form the transient neutral radical of melatonin whose growth at 490 nm could be easily measured.²⁴ The growth of the neutral radical of melatonin formed through hydrogen abstraction by *tert*-butoxy radicals has previously been measured by Scaiano.²⁴ The efficiency by which melatonin reacts with the peroxy radicals, thus defining its possible antioxidant potency, can be measured by the rate constant of transient growth which should be proportional to the rate of oxygen consumption by the initial radicals formed via photolysis.



Scheme 4.6: Reaction of melatonin with peroxy radicals generated in situ by LFP.

Although the laser flash photolysis spectrum revealed a growing transient over time at the wavelength of interest, i.e., 490 nm, a kinetic trace monitored at 490 nm showed a growth that was suspiciously fast and atypically curved. It was later discovered by a coworker, also working with 2-hydroxy-2-methyl-1-phenyl-1-propan-1-one, that the long-lived phenyl peroxy radical transient generated by laser flash photolysis in the presence of oxygen via Scheme 4.6 has a characteristic growth at 480 nm.⁶⁶ Thus, our experiment was rendered unsuccessful due to the interference caused by this transient. A detailed account of the experimental apparatus used to conduct the laser flash experiments is explained in the Chapter 2 of this thesis.

The thiobarbituric acid assay is another method that has been used extensively to measure lipid peroxidation. It is a colorimetric method involving reaction between thiobarbituric acid and malonaldehyde and other degradation products of unsaturated lipid peroxidation, such as 2,4-dienals or 2-enals. The thiobarbituric method was not considered an option for our purposes because it is reputed to yield unreliable results under certain conditions, especially with linoleic acid⁶⁷ which was our most biologically relevant substrate of choice.

In order to simulate the behaviour of peroxy radicals in membranes to some extent, linoleic acid provides a suitable substrate since it is structurally similar to the lipid moiety of the phospholipid bilayer in biological membranes, while micelles provide a heterogeneous, biphasic, i.e., hydrophobic and hydrophilic, biologically relevant micro-environment within which to conduct the peroxidation of linoleic acid. Micelles are molecular agglomerates formed in surfactant solutions, which, above a certain concentration - called the critical micelle concentration - have the ability to undergo self-organization. The cationic or anionic 'head' groups of the surfactant molecules orient themselves toward the polar aqueous phase while the hydrocarbon chain 'tails' of the molecules form the core of the spherical micelle; the micelles can be spherical or rod-shaped depending on surfactant concentration and temperature. Micelles are often used as simplified models for biological membranes^{68,69} for several reasons:

they are biphasic, have charged surfaces (in the case ionic surfactants), and are thermodynamically stable and structurally reproducible. Moreover, time-resolved studies using fluorescent probes have shown that molecular oxygen readily diffuses across the micellar boundaries⁷⁰ thereby making micelles an appropriate media within which to study the effect of melatonin on autoxidation reactions.

Recently, Pryor and coworkers devised a simple analytical method to study the activity of antioxidants on the autoxidation of linoleic acid in micelles.⁷¹ Their method involves monitoring the formation of conjugated diene hydroperoxide products at 234 nm during the course of the autoxidation process. The antioxidant efficiency obtained from this test is expressed relative to vitamin E and is equal to the ratio of rate constant of inhibition, k_{inh} , of the antioxidant under investigation to that of vitamin E. However, this method has one shortcoming in that the conjugated dienic hydroperoxide products are more susceptible to radical attack than the non-conjugated linoleic acid. This could result in their destruction prior to being measured giving rise to a falsely low concentration of product and hence, inaccurate antioxidant efficiencies.

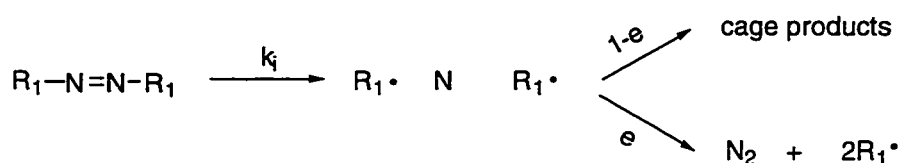
Based on a review of the available methods by which to measure the antioxidant properties of melatonin, the method of oxygen uptake using linoleic acid in micelles appeared to be a relatively good, chemically sound, *in vitro* assay. The method of oxygen uptake is a direct measurement of the consumption of oxygen by a reaction, and the suppression of oxygen uptake vis a vis the presence of an induction period directly reflects the ability of a substance to 'break' the propagation of the chain reaction by trapping peroxy radicals.

4.1.5 Oxygen Uptake Kinetic Measurements

Although the inhibition activity of phenolic antioxidants such as vitamin E is reduced in micelles compared to that in homogeneous solutions,⁶⁹ Barclay *et al.* have found that the susceptibility of an organic substrate to autoxidize, i.e. the oxidizability, is not affected by the

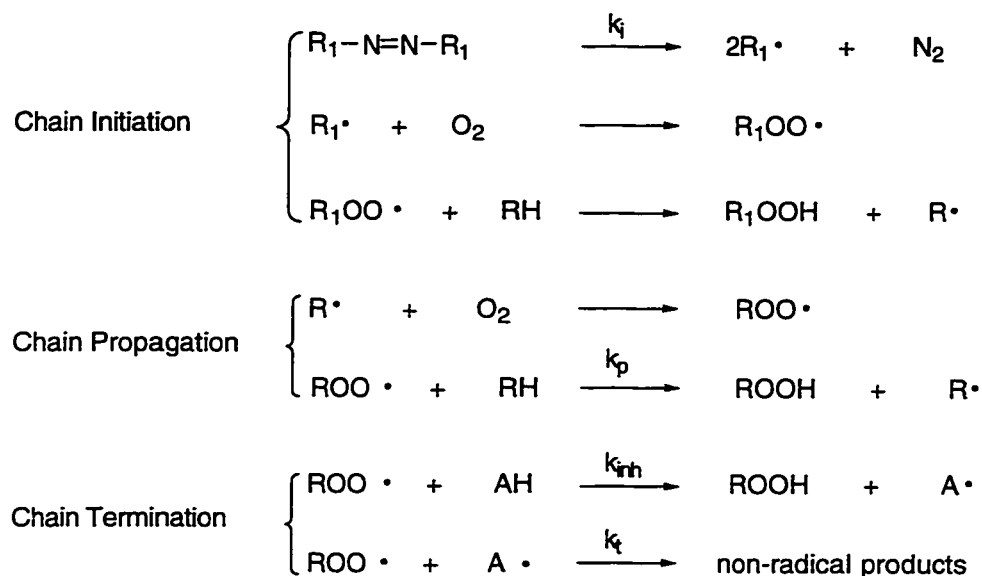
method of initiation or inhibition, nor is it significantly affected by the surrounding media. Thus the oxidizability of linoleic acid does not change from a homogeneous to a micellar environment.⁶⁹ To test the effect of melatonin in the presence of different substrates in a homogenous micro-environment, the oxygen uptake experiments were also conducted in chlorobenzene using styrene and tetralin as substrates.

In order to measure the kinetics of oxygen uptake quantitatively during the autoxidation of a substrate, azo compounds are commonly used to initiate the radical chain because they do so at reproducible rates that have already been previously determined. Thermal decomposition of the azo compounds gives rise to two radicals which, depending on the efficiency with which they escape the reaction cage, may or may not survive to initiate the chain; but their initiating activity is consistent and occurs with a constant rate. Scheme 4.7 describes the thermal decomposition process of a typical azo-initiator.



Scheme 4.7: Thermal decomposition of azo-initiator, where 'e' represents the fraction of escape from the reaction cage.

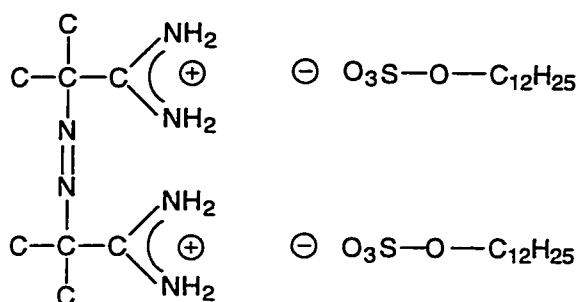
The hydrophobic core forms an area of increased microviscosity within the media whereby the diffusion and escape of radicals from their reaction 'cage' is impeded somewhat, that is, escape is controlled by the micro-environment. The step-wise, free radical propagation of the autoxidation chain is represented in Scheme 4.8 below:



Scheme 4.8: Typical azo-initiated autoxidation showing free radical initiation and propagation resulting in a chain reaction, where $R_1-N=N-R_1$ is the azo initiator and k_i is the rate constant for initiation, RH is the substrate, AH is the inhibitor and k_{inh} is the rate constant for inhibition, and k_p and k_t are the rate constants for propagation and termination, respectively. In order for chain termination to occur, the radical of the inhibitor $A\cdot$ that is formed in the Chain Termination step must be relatively unreactive towards O_2 and C-H bonds.

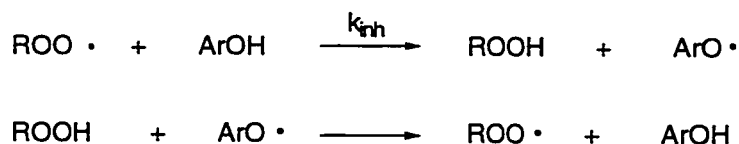
The water soluble initiator, azobis(2-amidinopropane•HCl) or ABAP, was used to initiate and provide a constant radical production rate for peroxidation reactions conducted in SDS micelles. The problem with most water-soluble initiators in micellar systems is that they tend to reside and generate their initiating radicals in the aqueous phase; the radicals must then diffuse into the micelle to initiate the attack on the lipid substrate. In the process of diffusion, these radicals are themselves vulnerable to being scavenged by any added water-soluble inhibitor before they reach their target. Although the fluorescence spectrum of melatonin in buffered 0.5 M SDS (*vide infra*) shows that it resides predominantly in the organic core of the micelles, melatonin has appreciable solubility in aqueous solution,⁶¹ a property which presents

potential complications for kinetic measurements. Despite its solubility in water, ABAP partitions efficiently into the micelles by about 91%⁷¹ in 0.1 M SDS. Barclay⁷² suggests that this may be due to a Coulombic attraction between the negatively charged surface of the micelle and the positively charged amidino groups on this azo initiator as shown below:



The substrates styrene and linoleic acid partition almost entirely into the hydrophobic core of the micelle (e.g., 95% for linoleic acid). Thus, it was assumed that with ABAP, the initiating radicals are generated within the micelle or close to the micellar boundary, proximal to their target substrate.

In addition to the fact that the kinetics of the autoxidation of styrene and subsequent inhibition by chain-breaking antioxidants have been thoroughly studied and are well understood, styrene was selected as a substrate to test the antioxidant impact of melatonin for three major reasons: 1) styrene forms a polyperoxide instead of a hydroperoxide in the chain terminating process; as a polyperoxide, there are no easily abstractable hydrogens available to enable the occurrence of the reverse of the inhibition reaction (exemplified by Scheme 4.9) which would complicate the kinetics of the system;



Scheme 4.9

2) the chain transfer involving hydrogen abstraction from the substrate by the phenoxy radical of the inhibitor does not occur with styrene; and 3) styrene has a high rate constant for chain propagation, i.e. $41 \text{ M}^{-1}\text{s}^{-1}$ at 30°C , which means that the rate of oxidation is measurable and oxidation remains a chain reaction even after inhibition.

The kinetics of the uninhibited autoxidation of organic substrates in both homogeneous and heterogeneous micellar solutions are described in the literature by the rate law expressed in equation 4.1, below.⁷³

$$-\frac{d[\text{O}_2]}{dt} = \frac{k_p[\text{RH}]R_i^{\frac{1}{2}}}{2k_t^{\frac{1}{2}}} \quad 4.1$$

However, in micelles, this equation can be considered only a close approximation to the true rate law because it does not reflect the microheterogeneous nature of the system and the fact that the rate in micelles changes with surfactant concentration.

In the case of inhibited autoxidations, the rate at which peroxy radicals are formed during initiation is equal to the rate at which peroxy radicals are scavenged, so that:

$$R_i = 2k_t e [R_i - N = N - R_i] = k_{inh} \times n[\text{AH}] \times [\text{ROO} \bullet] \quad 4.2$$

where R_i is the rate of chain initiation and n , a stoichiometric factor, is the number of peroxy radicals trapped per molecule of inhibitor; n can be calculated using the measured values of R_i and the induction period, τ , by equation 4.3 below. In the case of phenolic antioxidants such as vitamin E and its analogues, n has been found to be 2,^{57,69} which means that each tocopherol molecule reacts with two radicals (see 'Chain Termination' in Scheme 4.8).

$$n = \frac{R_i \tau}{[ArOH]} \quad 4.3$$

Rearranging and substituting for ROO• in (2) gives rise to the rate law for the inhibited autoxidation expressed in equation 4.4:

$$-\frac{d[O_2]}{dt} = \frac{k_p[RH]R_i^{\frac{1}{2}}}{k_{inh} \times n[AH]^{\frac{1}{2}}} \quad 4.4$$

4.2.0 Materials and Methods

The experimental conditions employed were followed as per the method established by Barclay *et al.*⁶⁸ Using a pressure transducer instrument similar to the one we used, they measured rates of initiation, R_i , by measuring the induction period during which oxidation is suppressed by an efficient phenolic antioxidant, and the efficiencies of chain initiation, e , which they obtained by measuring the azo initiator decomposition rate. By duplicating their experimental conditions, we were able to use their e and R_i values in order to correct for nitrogen evolution from azo initiator decomposition and oxygen consumption from the initiating free radicals formed. The corrections were applied as follows:

1) For N_2 evolution from initiator decomposition:



2) For O_2 consumption by free radicals released by initiator decomposition:



3) For O₂ evolution at termination of peroxy radicals formed in 2):



4) The net correction for the measured rate is therefore:

$$\frac{-d[O_2]}{dt(\text{corr})} = \frac{-d[O_2]}{dt(\text{measured})} + (1 - e)k_t [R_1 - N = N - R_1] \quad 4.5$$

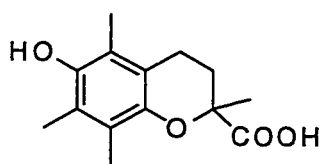
where k_t for azobis(2-amidinopropane•HCl) (ABAP) in SDS is $3.8 \times 10^{-7} \text{ s}^{-1}$ and the average e is 0.43; k_t for 2,2'-(bis(isobutyronitrile) (AIBN) in styrene is $9.3 \times 10^{-8} \text{ s}^{-1}$ and the average e is 0.64.^{57,68}

4.2.1 Autoxidation of Styrene and Tetralin

Both styrene (Aldrich) and 1,2,3,4-hydronaphthalene (tetralin, Aldrich) substrates were percolated through alumina (to remove the catechol polymerization inhibitor) and silica gel respectively, and then distilled prior to use. Substrate aliquots of $2.0 \pm 0.05 \text{ mL}$ were added to the reaction cell and the impact of different concentrations of melatonin on the rate of oxygen uptake was determined by injecting small aliquots (μL volumes) into the reaction cell. Oxygen uptake experiments were performed in duplicate for styrene and once for tetralin. The initiator used for these homogeneous studies was 2,2'-bis(isobutyronitrile) (AIBN, Eastman, used as received); $\sim 2.5 \times 10^{-2} \text{ M}$ concentration of AIBN was directly prepared in the $2.0 \pm 0.05 \text{ mL}$ of styrene or tetralin. Melatonin stock solutions, $3.4 \times 10^{-4} \text{ M}$, were prepared in Omnisolv grade chlorobenzene solvent which was used without further purification.

4.2.2 Autoxidation of Styrene and Linoleic Acid in Micelles

Oxygen uptake experiments were conducted using 4.8×10^{-4} moles of styrene (Aldrich) (see 4.2.1 for purification details) as a substrate in 2.0 ± 0.05 mL of buffered (pH 7.0) sodium dodecyl sulfate (SDS) (used as received from Bio-Rad) solution. 0.5 M SDS solutions were prepared with 0.1 M phosphate buffer pH 7.0, which was prepared with 0.05 M each of NaH_2PO_4 and Na_2HPO_4 (Fisher, used as received). The 0.05 M NaH_2PO_4 and Na_2HPO_4 solutions were prepared analytically and consistently such that the concentrations were always within 2% of each other. All styrene peroxidations were initiated with 2.2×10^{-5} moles of azobis(2-amidinopropane•HCl) (ABAP) which was purchased from Polysciences Inc. and stored at $\sim -10^\circ\text{C}$. The effects of adding 2.8×10^{-8} moles each of melatonin and a water-soluble vitamin E analogue, 2,5,7,8-tetramethyl-6-hydroxychroman-2-carboxylate, commonly known as trolox, on the rate of oxygen uptake by styrene were observed. Both melatonin and trolox solutions were prepared analytically, and the uncertainties associated with the concentrations reported did not exceed 1%. The combined effect of both melatonin and trolox on oxygen consumption by styrene was also measured. The structure of trolox is depicted below:



Trolox

Autoxidations of linoleic acid (Aldrich 99% purity, used as received then flushed with N_2 and stored at $\sim -10^\circ\text{C}$) were conducted in the presence and absence of ABAP. Solutions of ABAP (1.2×10^{-2} M) were prepared for each initiated run by sonicating and vortex mixing the

For the experiments performed to determine the antioxidant efficacy of melatonin in the presence of a known quantity of added Fe^{2+} ions, the phosphate buffer solutions were prepared as stated above, and used after purification by treatment with a chelating resin (Sigma) to remove traces of metal ions. A series of additional experiments involving Cu^{2+} and Fe^{3+} and a known chelant were conducted in buffer that was used as prepared without further treatment so that the effect of melatonin could be observed in an environment containing a catalytic amount of metal ions (trace) as well as a stoichiometric amount. An aliquot of $40 \pm 0.1 \mu\text{L}$ of linoleic acid (1.2×10^{-4} moles) was added to $2.0 \pm 0.05 \text{ mL}$ of ABAP-SDS solution containing 2.3×10^{-5} moles of ABAP, and the kinetics of the peroxidation process were determined using a pressure transducer (described in Chapter 2) to monitor oxygen consumption. In each run, the rate of oxygen uptake by the autoxidation of linoleic acid as a function of time was measured in the presence of trace amounts of metal ions and $\sim 10^{-7}$ moles of added metal ions. 1.0×10^{-7} moles of melatonin was added to the reaction cell either before or after the addition of metal ions. These runs were repeated using 4.0×10^{-7} moles of Fe^{2+} as catalyst and 8.1×10^{-8} moles of a common metal ion chelator instead of melatonin added to the reaction cell. Linoleic acid autoxidation was also conducted with trace metal ions removed and melatonin introduced to the system *after* the addition of Fe^{2+} .

Metals: Metal ion solutions were prepared in demineralized water using $\text{CuSO}_4 \cdot 5\text{H}_2\text{O}$, $\text{FeSO}_4 \cdot 7\text{H}_2\text{O}$, and FeCl_3 (Fisher, used as received). Stock solution concentrations were $2.6 \times 10^{-2} \text{ M}$ in Cu^{2+} and $5.0 \times 10^{-2} \text{ M}$ in Fe^{2+} and Fe^{3+} ions. All $\text{FeSO}_4 \cdot 7\text{H}_2\text{O}$ solutions were prepared immediately prior to injection into the reaction cell while the iron(III) and Cu(II) solutions were prepared within 1-2 hours before using. All metal ion solutions were prepared analytically; the uncertainty in the concentrations reported did not exceed 1%. An aliquot of $10 \pm 0.1 \mu\text{L}$ of each metal solution was added to a linoleic acid autoxidation run after a steady rate of oxygen uptake was established.

Melatonin: 1.00×10^{-2} M melatonin (ACROS, used as received) was prepared in buffered SDS solution; $10 \pm 0.1 \mu\text{L}$ was added to the reaction cell at varying times before or after the addition of the metal ion solution. All melatonin solutions were prepared analytically; the uncertainty of the concentrations reported did not exceed 1%. The actual time of melatonin addition varied according to the effect of the metal ion on the rate of oxygen uptake by linoleic acid.

Diethylenetriaminepentaacetic acid: N,N-bis[2-(bis[Carboxymethyl]amino)ethyl]-glycine (DTPA), a common metal ion chelator, used as received from Aldrich, was prepared in buffer solution to a concentration of 8.00×10^{-3} M. DTPA solutions were prepared analytically; the uncertainty of the concentrations reported did not exceed 1%. The solubility of DTPA is not as high as melatonin in aqueous solution, therefore the concentration of Fe^{2+} was lowered accordingly. An aliquot of $10 \pm 0.1 \mu\text{L}$ of the DTPA solution was added to the reaction cell at varying times before or after the addition of the metal ion solution.

The uncertainties associated with the reported rates of oxygen uptake using the pressure transducer were $\sim 2\%$.

4.2.3 Fluorescence Studies

Phosphate buffer solution (1×10^{-3} M) pH 7.0, was prepared using 5×10^{-4} M each of NaH_2PO_4 and Na_2HPO_4 and was treated with Chelex chelating prior to use. A 0.5 M SDS solution was prepared using the phosphate buffer. A lower concentration of buffer (0.001 M as opposed to 0.1 M) was used in the fluorescence studies compared to that of the oxygen uptake experiments in order to minimize absorption by the solvent medium during the fluorescence measurements. Various concentrations of $\text{FeSO}_4 \cdot 7\text{H}_2\text{O}$ solutions were prepared in buffered SDS to which were added 1.15×10^{-4} M melatonin. Concentrations of Fe^{2+} in

these solutions ranged from one half order of magnitude below the concentration of melatonin to one and a half orders of magnitude above it. As in the oxygen uptake studies, all solutions were prepared analytically and the uncertainties associated with the concentrations reported did not exceed 1%. Absorption and fluorescence spectra of each solution were measured using a Varian Cary-1 spectrophotometer and a Perkin Elmer LS-50 spectrofluorimeter, respectively. A 0.2 cm path length quartz cuvette, suitable for conducting fluorescence measurements, was used to obtain absorption and fluorescence spectra in order to minimize the possibility of a filtering effect from the iron in solution. The fluorescence spectra were measured with front-face arrangement using an excitation wavelength of 280 nm.

4.3.0 Results

4.3.1 Oxygen Uptake: Tetralin and Styrene Substrates

No induction period was noted for melatonin upon addition to styrene and tetralin in homogeneous solution. However, addition of melatonin induced a reproducible reduction in the rate of oxygen uptake by styrene that increased as a function of increasing melatonin concentration. A reciprocal plot offers a convenient way of extrapolating the effect to high melatonin concentrations; extrapolation to the y-intercept of the reciprocal plot (Figure 4.1), which includes data from both collaborating laboratories, shows that the maximum reduction obtainable by melatonin is 72%.

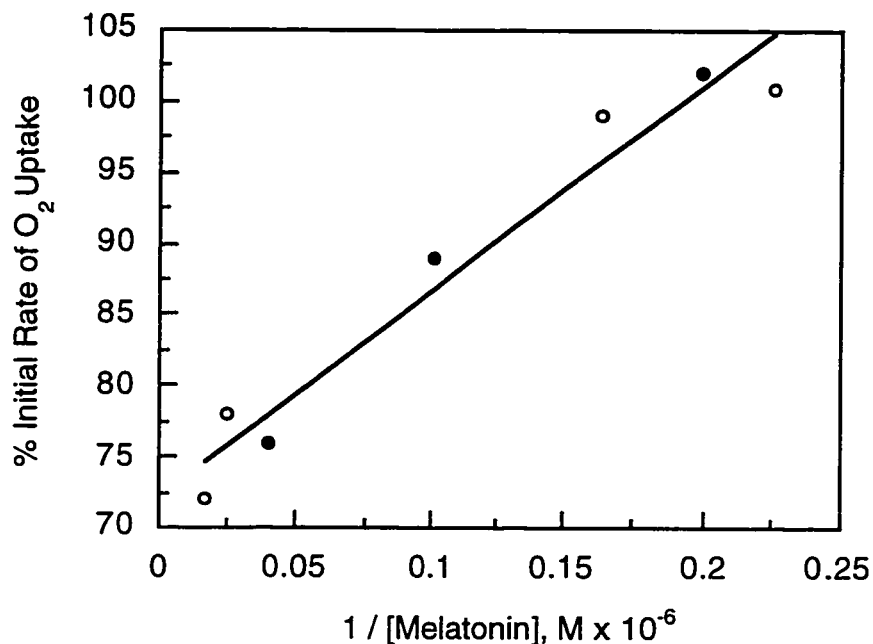


Figure 4.1: Reciprocal plot showing the effect of melatonin concentration on the rate of oxygen uptake by styrene at $30 \pm 0.5^\circ\text{C}$. The filled circles and hollow circles represent data obtained by the author, using 0.028 M AIBN and 8.73 M styrene, and Ross Barclay's group,⁷⁴ using 0.021 M AIBN and 1.98 M of styrene in chlorobenzene, respectively.

4.3.2 Oxygen Uptake: Styrene in SDS

As expected, an induction period, typical of the chain-breaking antioxidants, was observed upon addition of trolox to a styrene peroxidation system in buffered SDS micelles. No induction period was observed when an equivalent amount of melatonin was added (comparable to trolox in the previous runs) under identical conditions, however a reproducible reduction of about 15% in the rate of oxygen uptake by styrene was evident. According to observations by Barclay's research group,⁷⁴ this reduction in rate increased as a function of increasing melatonin concentration until it reached a plateau at around 40%. Figure 4.2 shows

the relative impact of melatonin and trolox on the concentration of oxygen consumed over time by styrene in a heterogeneous environment.

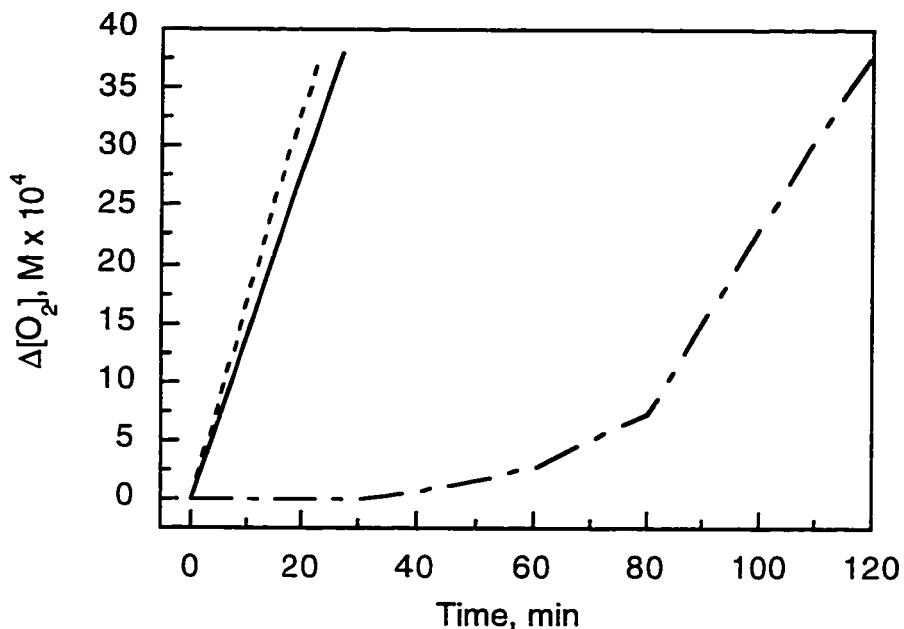


Figure 4.2: Effect of melatonin, 2.8×10^{-8} moles, and trolox, 2.8×10^{-8} moles, on the uninhibited rate of oxygen uptake by styrene, 4.8×10^{-4} moles, in 2.0 ml of buffered 0.5 M SDS. The peroxidation of styrene in SDS was thermally initiated by 2.2×10^{-5} moles of ABAP at $30 \pm 0.5^\circ\text{C}$. The dashed line represents the uninhibited rate, the solid line represents the rate after addition of melatonin and the dotted-dashed line represents the rate after addition of trolox. The concentration of oxygen consumed (plotted as the ordinate) was easily calculated from the raw data (see 2.2.1) since the reaction cell was calibrated to be $9.52 \times 10^{-7} \pm 2\%$ mol O_2/Volt and the volume in the reaction cell was known.

To check for synergism between melatonin and trolox, another experiment was conducted whereby a 1:1 mixture of melatonin and trolox was added to a thermally initiated styrene peroxidation in buffered SDS. An induction period of 74 minutes was observed which

is similar, within experimental error, to the 82 minute induction period observed with trolox alone, indicating that there was no synergism or combined effect observed between the two additives (not shown). This lack of synergism between melatonin and a known chain-breaking antioxidant was confirmed by Barclay's group⁷⁴ in a similar experiment.

4.3.3 Oxygen Uptake: Linoleic Acid in SDS - Effect of Metal Ions

All three metal ions, Cu^{2+} , Fe^{2+} , and Fe^{3+} , induced a catalytic effect upon the rate of oxygen uptake by linoleic acid. In the case of Fe^{2+} , a significant increase in the rate was observed; the rate immediately escalated and then steadily decreased. Figure 4.3 and 4.4 show that shortly after adding the iron(II), addition of melatonin caused an immediate decline in the rate to slightly below the former rate just prior to adding iron(II). A similar effect was observed when the chelant DTPA was added to the reaction cell following Fe^{2+} addition (Figure 4.5).

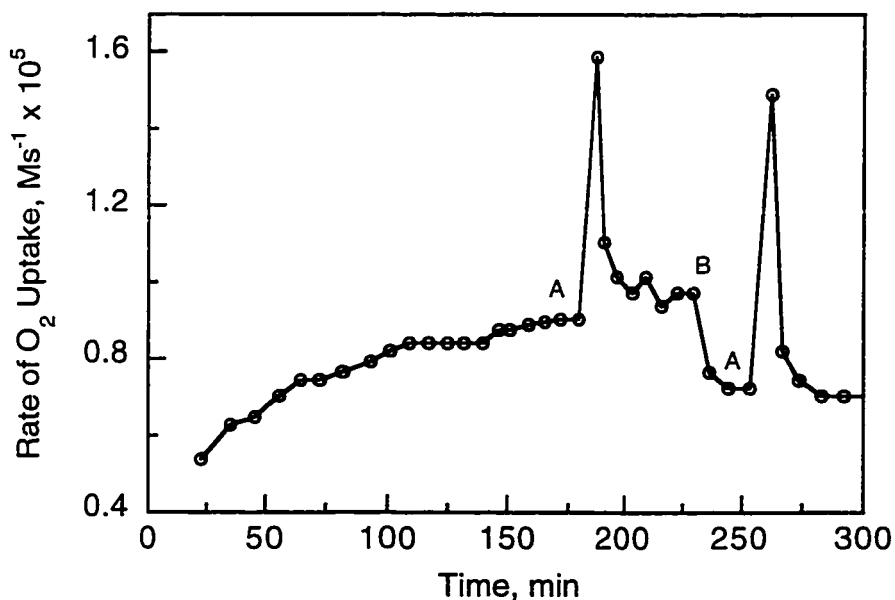


Figure 4.3: Effect of melatonin on the Fe^{2+} catalysed rate of O_2 uptake by linoleic acid in buffered 0.5 M SDS (pH 7.0), thermally initiated by 2.3×10^{-5} moles of ABAP at $30 \pm 0.5^\circ\text{C}$,

as a function of time. A - indicates injection of 5.0×10^{-7} moles of Fe^{2+} into the reaction cell; B - indicates injection of 1.0×10^{-7} moles of melatonin into the reaction cell. The buffer solution was treated with Chelex resin to eliminate trace metal ions. N.B. It is interesting to note here that even though the buffer solution was treated with Chelex resin to remove trace metal ions, residual minute contaminants are present in sufficient amounts to catalyse the autoxidation process. This is evident by the slight, but steady rise in the rate of oxygen uptake over time prior to addition of metal ions.

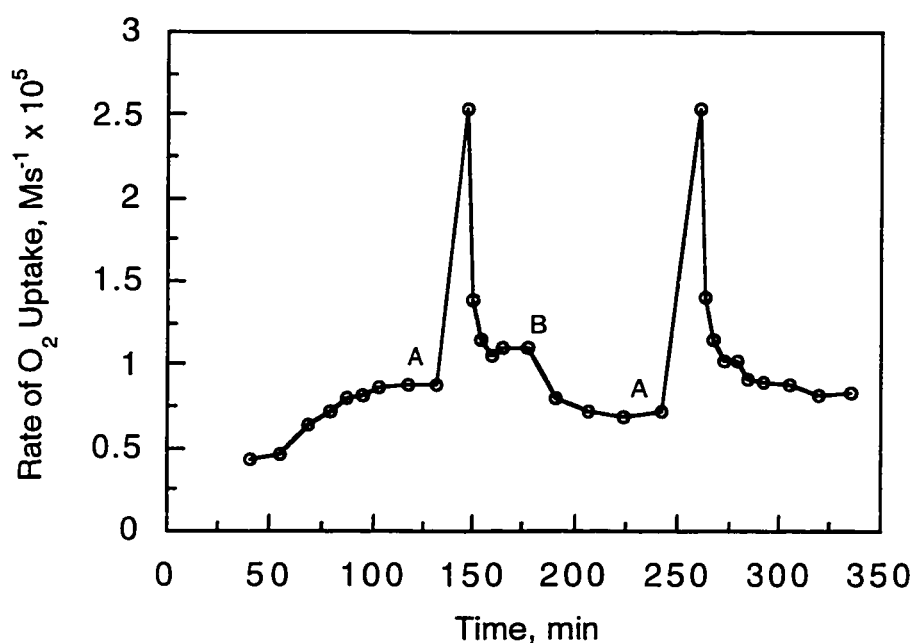


Figure 4.4: Effect of melatonin on the Fe^{2+} catalysed rate of O_2 uptake by linoleic acid in buffered 0.5 M SDS, thermally initiated by 2.3×10^{-5} moles of ABAP at $30 \pm 0.5^\circ\text{C}$, as a function of time. A - indicates injection of 5.0×10^{-7} moles of Fe^{2+} into the reaction cell. B - indicates injection of 1.0×10^{-7} moles of melatonin into the reaction cell. N.B. Background trace metal ions present, see note in Figure 4.3.

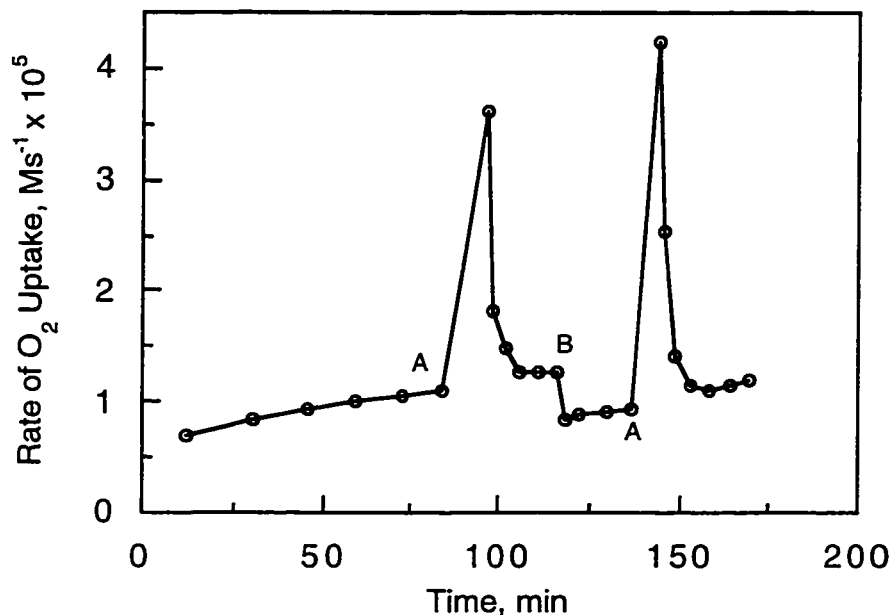


Figure 4.5: Effect of DTPA on the Fe^{2+} catalysed rate of O_2 uptake by linoleic acid in buffered 0.5 M SDS, thermally initiated by 2.3×10^{-5} moles of ABAP at $30 \pm 0.5^\circ\text{C}$, as a function of time. A - indicates injection of 4.0×10^{-7} moles of Fe^{2+} into the reaction cell; B - indicates injection of 8.1×10^{-8} moles of DTPA into the reaction cell.

When melatonin was added to the reaction cell prior to the addition of Fe^{2+} , a 19% reduction in the rate of oxygen uptake was noted (see Figure 4.6). Upon addition of Fe^{2+} , the rate increased as before, however the 'lifetime' of the effect induced by iron was much shorter than that in the absence of melatonin, that is, the rate of decrease of the rate of oxygen uptake was much faster with melatonin present initially. Once the rate of oxygen uptake had re-established, it remained stable and did not rise within the allotted time period. It is remarkable that in the presence of melatonin, the rate of oxygen uptake of linoleic acid consistently returned to a steady 'baseline' rate after successive injections of iron(II) (Figure 4.6).

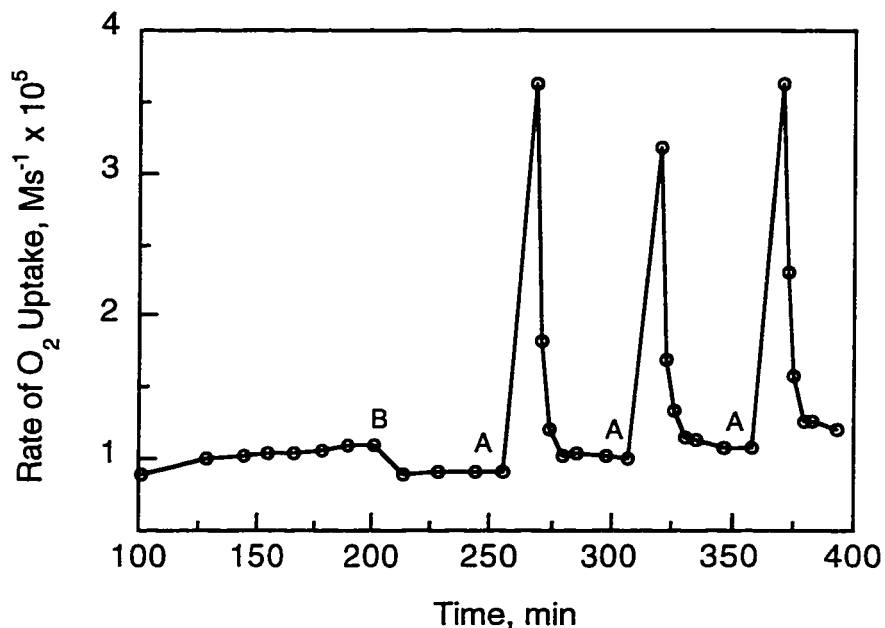


Figure 4.6: Effect of melatonin on the rate of O₂ uptake by linoleic acid in buffered 0.5 M SDS, thermally initiated by 2.3×10^{-5} moles of ABAP at $30 \pm 0.5^\circ\text{C}$, as a function of time (prior to adding Fe²⁺). A - indicates injection of 5.0×10^{-7} moles of Fe²⁺ into the reaction cell. B - indicates injection of 1.0×10^{-7} moles of melatonin into the reaction cell. N.B. Background trace metal ions present, see note in Figure 4.3.

When the chelant DTPA was added to the reaction cell prior to addition of Fe²⁺, the rate dropped to 55% lower than the initial rate of oxygen uptake, indicating efficient binding of trace catalytic quantities of metal ions. Figure 4.7 shows that upon addition of a stoichiometric amount of Fe²⁺, the rate increased as expected in the presence of DTPA, but did not reach the usual level and immediately returned to its former rate. However, the rate of oxygen uptake following the addition of iron did not stabilize and, unlike the similar melatonin experiment, the rate rose again within the allotted time period. This rising 'baseline' was also observed after the addition of Fe²⁺ to the system in which DTPA was added to the reaction cell prior to adding Fe²⁺ as shown in Figure 4.4.

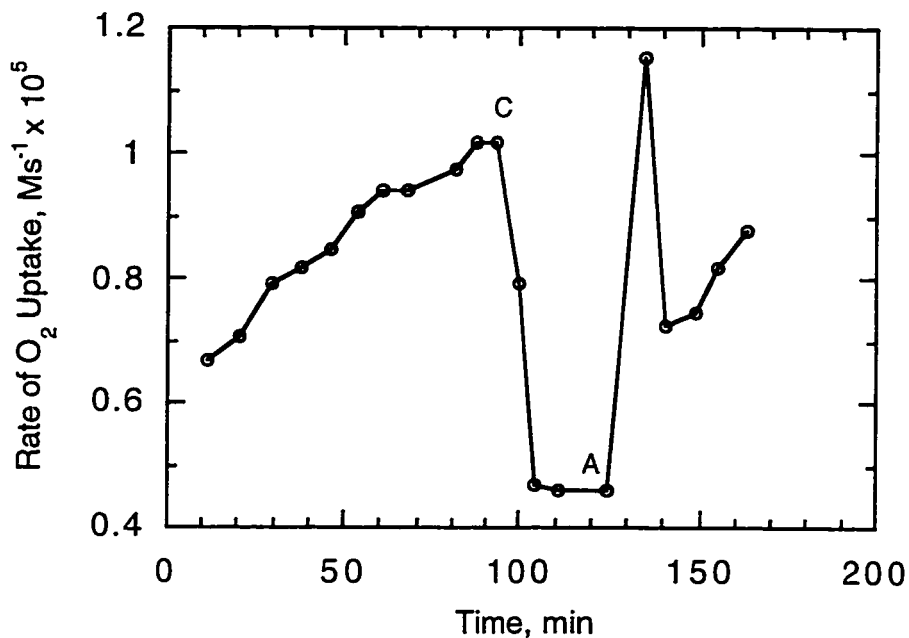


Figure 4.7: Effect of DTPA on the rate of O₂ uptake of linoleic acid in buffered 0.5 M SDS, thermally initiated by 2.3×10^{-5} moles of ABAP at $30 \pm 0.5^\circ\text{C}$, as a function of time (prior to adding Fe²⁺). A - indicates injection of 4.0×10^{-7} moles of Fe²⁺ into the reaction cell. C - indicates injection of 8.1×10^{-8} moles of DTPA into the reaction cell.

Both Cu²⁺ and Fe³⁺ had a similar impact on the linoleic autoxidation reaction. Unlike Fe²⁺, these metal cations caused a relatively slow, steady enhancement of the rate of oxygen uptake over time. After 70 minutes of exposure to the metal ions, the increase in rate of O₂ uptake by linoleic acid was reduced in the presence of melatonin by $2.8 \times 10^{-6} \text{ Ms}^{-1}$ and $2.9 \times 10^{-7} \text{ Ms}^{-1}$ in the case of Cu²⁺ and Fe³⁺, respectively. Figures 4.4 and 4.8 show that although Cu²⁺ and Fe³⁺ exert less of an impact on the peroxidations, the quenching effect of adding melatonin to the catalytic system was the same for all three metals ions. Not only does melatonin deactivate the metal ion catalysts, it also holds the rate of oxygen uptake constant for significantly long periods of time.

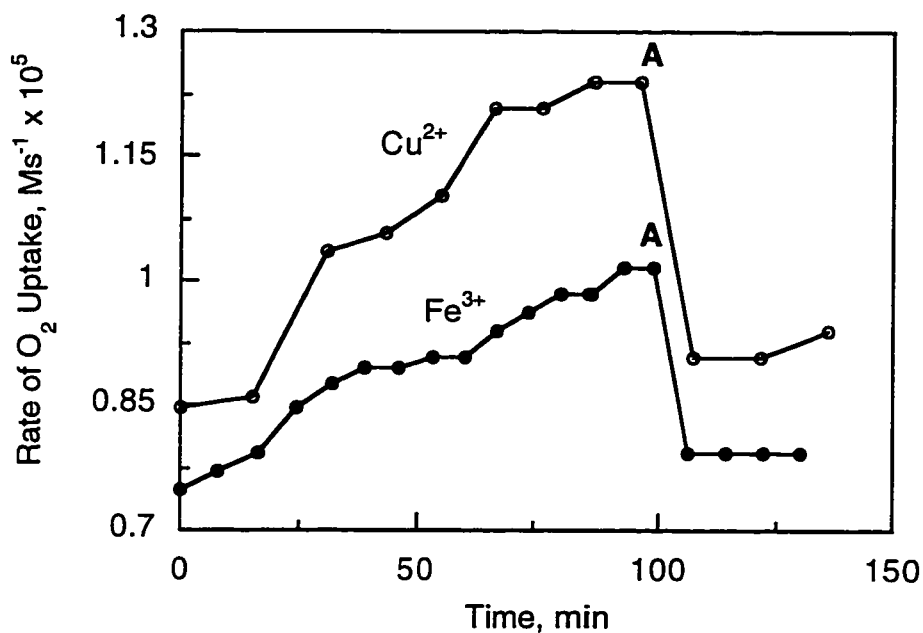
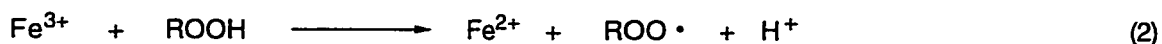


Figure 4.8: Effect of melatonin on the Cu²⁺ and Fe³⁺-induced rate enhancements of O₂ uptake by linoleic acid in buffered 0.5 M SDS, thermally initiated by 2.3 × 10⁻⁵ moles of ABAP at 30 ± 0.5°C, as a function of time. Amount of Fe³⁺ added to the reaction cell was 5.0 × 10⁻⁷ moles; amount of Cu²⁺ added was 2.6 × 10⁻⁷ moles. A - indicates injection of 1.0 × 10⁻⁷ moles of melatonin into the reaction cell. The data has been plotted from the point at which the metal ions were injected into the peroxidation system: time = 0 min.

Iron(III) is not a particularly good catalyst for peroxidation reactions⁶⁰; the slow increase in O₂ uptake rate that was observed in the presence of Fe³⁺ is probably due to the formation of relatively low amounts of the catalytically active Fe²⁺ resulting from an equilibrium that establishes between the two iron species in solution. It is also feasible that, as hydroperoxides accumulate from the autoxidation process, a back reaction with Fe³⁺ occurs to regenerate the catalytic form of Fe²⁺ (Scheme 4.10) in a much less efficient way. The overall effect is a slow net increase in the rate of O₂ uptake.



Scheme 4.10

The rate of oxygen uptake by linoleic acid was also measured in the absence of initiator to ensure that the catalytic impact of the metal ions and the subsequent quenching of that effect by melatonin were not influenced by the presence of the initiator. Although the kinetic traces were predictably inconsistent in that they were not linear over the voltage range measured, the overall trend observed in the uninitiated reactions was similar to that of the initiated reactions (results not shown). The relative impact on the rate of oxygen uptake by the peroxidation of linoleic acid in micelles for each of the metal ions was similar, as was the effect induced by added melatonin.

4.3.4 Fluorescence Studies

The absorption spectra in Figure 4.9 A show no change in the shape or shift in the wavelength of the absorption maxima with respect to increasing iron(II) concentration. However, the fluorescence spectra show a steady decrease in peak intensity with increasing Fe^{2+} concentration (see Figure 4.9 B).

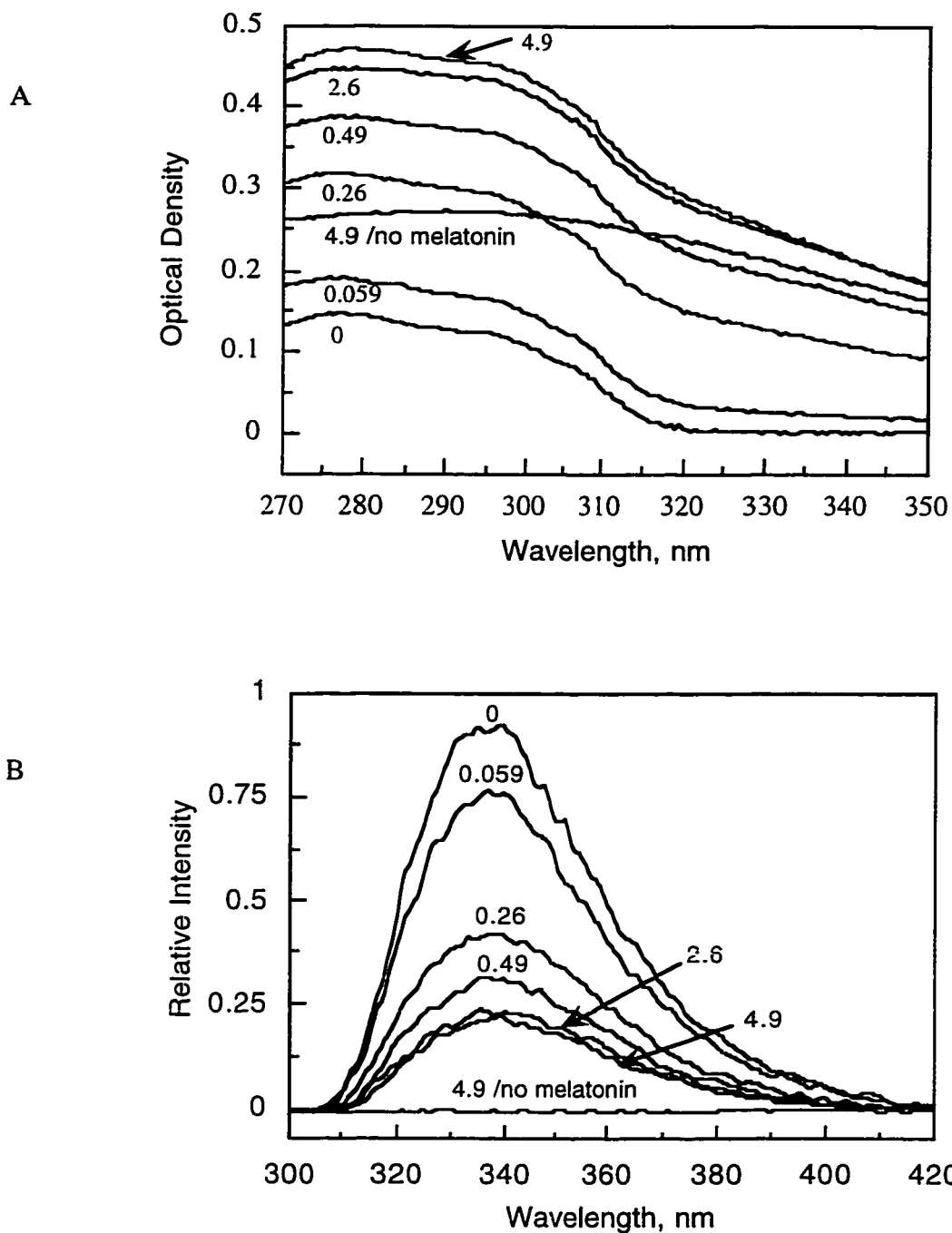


Figure 4.9: A - Absorption spectra of 0.115 mM melatonin solutions in buffered 0.5 M SDS, pH 7.0, with increasing Fe^{2+} concentration added using a 2 mm optical path; B - fluorescence spectrum of 0.115 mM melatonin in buffered 0.5 M SDS, pH 7.0 (excitation wavelength used was 280 nm). Concentrations of Fe^{2+} added, expressed as millimolar units, are shown next to their corresponding melatonin spectra in both A and B.

The fluorescence maximum of ~340 nm in Figure 4.9 B is characteristic of melatonin in organic media; in water, the maximum is slightly red-shifted to ~350 nm (*vide supra*). This indicates that melatonin is located predominantly in the core of the micelle.

A Stern-Volmer plot of the ratio of melatonin fluorescence maximum intensity to melatonin + Fe²⁺ fluorescence maximum intensity vs. Fe²⁺ concentration shows a linear trend up to a concentration of ~0.6 x 10⁻³ M Fe²⁺ where it begins to plateau (See Figure 4.10).

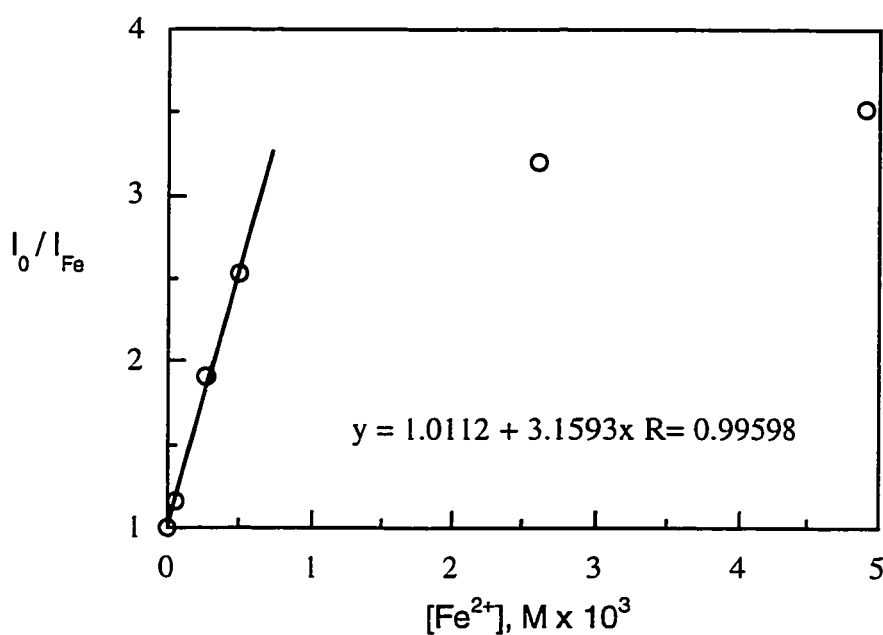


Figure 4.10: Stern-Volmer plot of the ratio of corrected fluorescence intensity of melatonin to that of melatonin in micelles with added Fe²⁺.

Neglecting any interference by absorption, the linear portion of the Stern-Volmer plot can be expressed as:

$$\frac{I_0}{I} = 1 + k_q \tau [\text{Fe}^{2+}] \quad 4.6$$

where I_0 and I are the intensities of melatonin fluorescence in the absence and presence of iron respectively, k_q is the rate constant for Fe^{2+} quenching, t is the fluorescence lifetime of melatonin, and $[\text{Fe}^{2+}]$ is the concentration of Fe^{2+} added. Intensities were calculated as the integrated area under each fluorescence spectrum in Figure 4.9 B from 300 nm to 420 nm, and each calculated fluorescence ratio on the Stern-Volmer plot was corrected for the competitive absorption by iron of the excitation wavelength used - calculated from the absorption spectra in Figure 4.9 A.

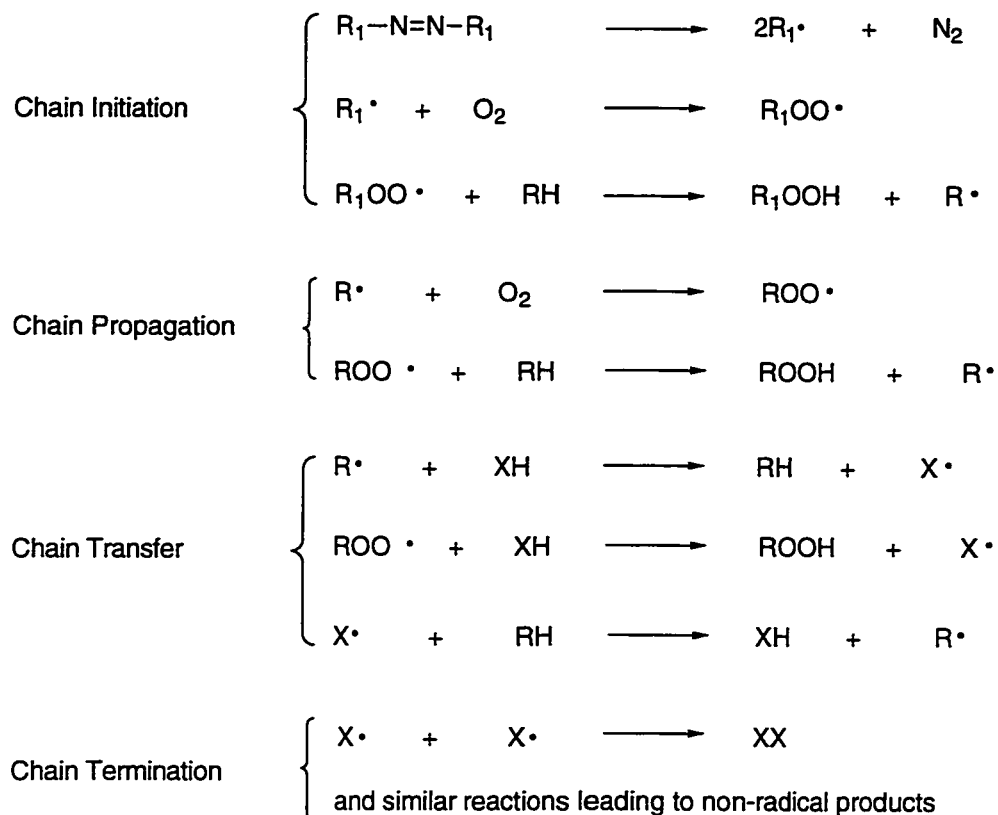
Since the slope of the line is $k_q \tau$, and the lifetime of melatonin fluorescence in organic solvents was previously determined to be ~ 6 ns,⁵¹ the rate constant for quenching by Fe^{2+} , k_q was readily calculated to be $5 \times 10^{11} \text{ s}^{-1}$. This faster-than-diffusion-controlled rate (k_{diff} in aqueous solution is $\sim 6 \times 10^9$) indicates that binding may indeed be occurring between melatonin and iron. Furthermore, the ~ 5 mM micellar concentration (which is calculated by dividing the surfactant concentration by 97 - the aggregation number for 0.5 M SDS) is much higher than the ~ 0.7 mM concentration of iron required to quench the melatonin fluorescence, which provides statistical evidence that the micellar medium does not contribute to the quenching, i.e. the number of micelles present in solution far exceeds the number of quenching iron ions that are electrostatically attracted to the anionic surface of the micelles. Although the plateau in Figure 4.10 may be indicative of saturation of the binding sites on melatonin, the efficiency of binding, or binding constant, cannot be easily determined from these experiments.

4.4.0 Discussion

It is evident from the results of the oxygen uptake experiments using different substrates in different environments, that melatonin does not act as a typical chain-breaking

antioxidant. At best, melatonin may be considered a mild retarder of lipid peroxidations. Inhibitors of autoxidation reactions, such as vitamin E and its analogues, are slowly consumed over a long period of time - the 'induction' period - as they suppress substrate oxidation. During the induction period, the rate at which peroxy radicals are trapped by the inhibitor is approximately equal to the rate at which they are generated until the inhibitor is completely depleted; then the velocity of autoxidation resumes unhindered. Retarders, on the other hand, act in a different way; no induction period is observed, the substrate oxidation proceeds at a slower but steady rate, and retarders persist in solution much longer than inhibitors before they are consumed.

The behaviour of melatonin as a retarder in the autoxidation experiments reported in this work is similar to that of *p*-cresol in the autoxidation of benzaldehyde initiated by benzoyl peroxide reported by Waters and Wickham-Jones.⁷⁵ They suggested that retardation involves a chain transfer step to account for the reduction as well as a chain-propagating radical generation step induced by the regeneration of the retarder itself as in Scheme 4.11 to account for the absence of an induction period.



Scheme 4.11: Mechanism for retarded autoxidation involving chain transfer where $R_1-N=N-R_1$ represents the azo initiator (ABAP or AIBN), RH denotes the substrate (linoleic acid or styrene), and X denotes the retarder (melatonin).

The oxygen uptake rate reductions induced by the addition of melatonin that were observed in both collaborating laboratories under heterogeneous and homogeneous environments indicate that melatonin acts as a retarder via a similar mechanism by which it first traps radicals as a chain transfer agent and is then subsequently regenerated by creating more chain-propagating radicals. The rate at which melatonin trapped radicals exceeded the rate at which chain-propagating radicals were formed during its regeneration so that the net overall effect was a slower, steady rate of oxygen uptake over a long period of time (see Figures 4.2 and 4.6). Retardation by melatonin is also evident in the metal ion catalysed linoleic acid

peroxidations experiments whereby the addition of melatonin after the first injection of Fe^{2+} ions not only causes a reduction in the enhanced rate of oxygen uptake induced by the metal ion, but also prevented the 'baseline' rate from escalating with subsequent injections of Fe^{2+} (see Figure 4.6). Even after the oxidizing linoleic acid had consumed several micromoles of oxygen, the rate of oxygen uptake remained constant. This is further proof that melatonin operates by a different mechanism compared to inhibitors such as trolox; this difference is clearly evident in Figure 4.2. Waters and Wickham suggested that retarders operate by trapping active radicals as chain transfer agents, but in a regeneration step, they substitute a series of slow reactions for a series of fast ones so that the rate of peroxy radical generation always exceeds the rate of scavenging.⁷⁵

4.4.1 Product Studies in Mimetic Bilayer Systems

Further evidence in support of our findings that melatonin does not function as a chain-breaking antioxidant came from the results of product studies that Barclay's group conducted following peroxidation of a mimetic bilayer membrane system. They analysed the hydroperoxide products from the peroxidation of 1-palmitoyl-2-linoleoylphosphatidylcholine to determine the ratio of kinetic to thermodynamic products. This ratio is a measure of the hydrogen atom donating ability of an antioxidant: a high proportion of kinetic products indicates efficient hydrogen atom transfer before isomerisation of the initial peroxy radical to a more thermodynamically favoured configuration has a chance to occur. Through HPLC analysis of the hydroperoxide products, which were reduced and converted to the corresponding hydroxymethyl esters shown in Figure 4.14, Barclay's group⁷⁴ found that the ratio of cis,trans (kinetic products) to trans,trans (thermodynamic products) for the uninhibited peroxidation was 0.59 ± 0.1 . The addition of 3.6×10^{-8} moles of vitamin E raised this cis,trans to trans,trans ratio to 2.21 ± 0.12 , while the ratio obtained upon addition of a similar amount of melatonin was 0.62 ± 0.12 . Since melatonin induced little change in the uninhibited

ratio compared to vitamin E, a known peroxy radical trapping, chain-breaking antioxidant, further proves that melatonin does not behave as an efficient peroxy radical scavenger *in vitro*.

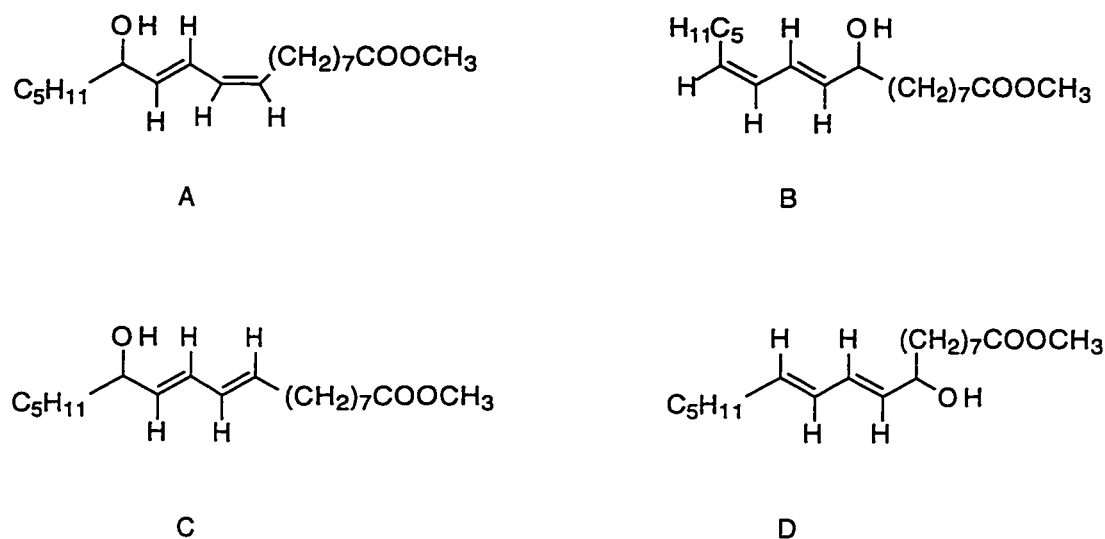
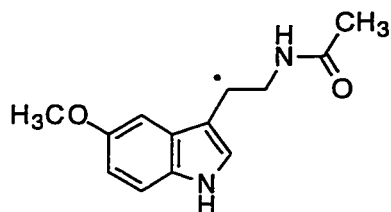


Figure 4.13: Peroxidation products of PLPC. Kinetic products: A - methyl 13-hydroxy-*cis*-9, *trans*-11-octadecadienoate, and B - methyl 9-hydroxy-*trans*-10, *cis*-12-octadecadienoate. Thermodynamic products: C - methyl 13-hydroxy-*trans*-9, *trans*-11-octadecadienoate and D - methyl 9-hydroxy-*trans*-10, *trans*-12-octadecadienoate.

4.4.2 A Proposed Radical Trapping Mechanism

We attempted determine the site of reaction and propose a mechanism for the radical trapping/chain transfer activity of melatonin to account for the experimental evidence, using a computational approach. Burton and Ingold suggested that the superior chain breaking antioxidant properties of vitamin E and analogues could be directly related to the formation of a stereoelectronically stabilized neutral phenoxy radical (*vide supra*) upon reaction with a peroxy radical.³⁸ We conducted a computational exercise to determine the most stable neutral radical conformation of melatonin based on relative heats of formation of geometry optimized

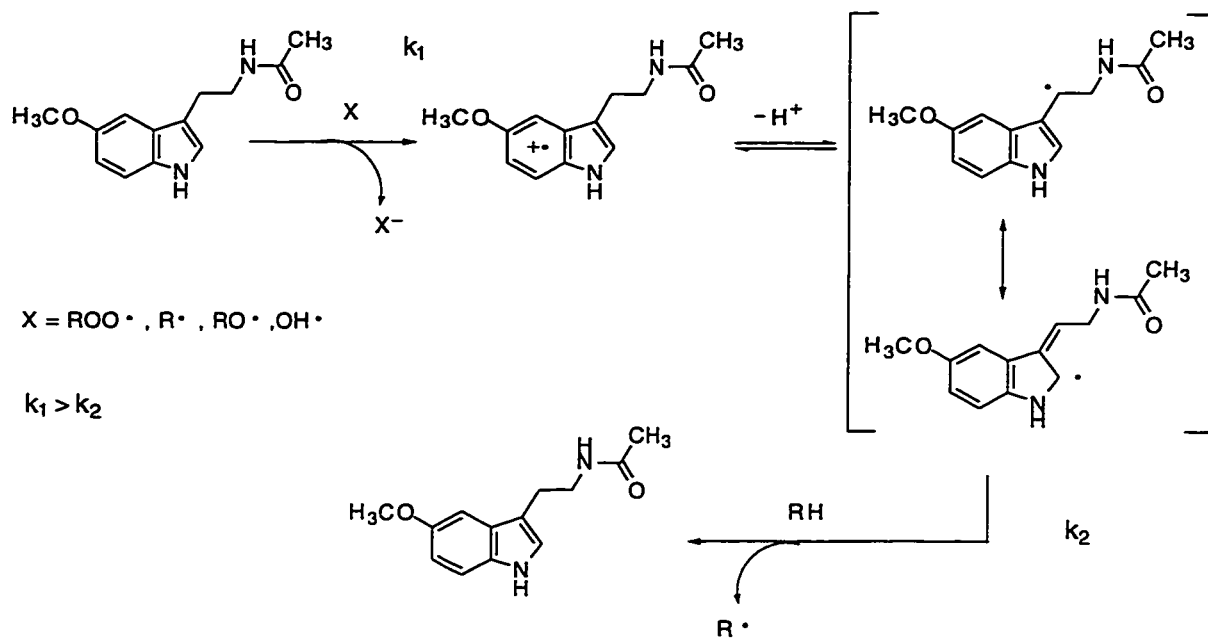
conformations using PM3 (see Appendix 1). Our results indicated that the site of hydrogen donation is most likely the carbon adjacent to the indole ring shown in the structure below:



This neutral radical structure is also intuitively relatively stable since it is resonance stabilized by conjugation with the pyrrole ring. However, this structure lacks the greater stability afforded by resonance with the entire indole ring π system which might then be somewhat comparable to the stabilized phenoxy radical of vitamin E. Notwithstanding, the resonance provided by conjugation with the pyrrole ring is probably sufficient to stabilize the neutral melatonin radical to the extent that a noticeable reduction in the rate of oxygen uptake is incurred. The total lack of an induction period with the addition of melatonin indicates that the neutral radical must participate in chain propagation.

In a recent review article,¹⁰ Reiter reported that the radical scavenging mechanism to describe the antioxidant activity of melatonin involves electron transfer from melatonin to form the radical cation (interestingly, Reiter refers to a figure of the neutral radical of melatonin as the radical cation!). Scaiano showed that melatonin reacts with free radicals by donating a hydrogen atom to the free radical²⁴ in much the same way that vitamin E does and, contrary to Reiter's report, both melatonin and vitamin E end up as neutral radicals. While the rate constants for abstraction of hydrogen from melatonin by *tert*-butoxyl and cumyloxyl radicals were readily detectable by the spectroscopic method he used, neither the site of hydrogen abstraction, nor the fate of the neutral melatonin radical could be elucidated. The mechanism that is expounded in the literature and generally accepted as that by which melatonin traps radicals (and thus acts as an antioxidant) is one that involves electron transfer rather than

hydrogen atom transfer from melatonin. A comparison of the differences between the heats of formation of the neutral radical and melatonin molecule in the gas phase, and the radical cation and melatonin molecule in the aqueous phase (in Table A.1) shows that the stability of the neutral melatonin radical resulting from hydrogen abstraction far exceeds that of the radical cation, the product of electron transfer from the neutral melatonin molecule. If melatonin transfers an electron to a highly reactive oxidizing species, the computational results indicate that the radical cation intermediate would probably lose a hydrogen forming the neutral radical to achieve stability. This is in agreement with experimental data generated by Al-Kazwini *et al.*³⁴ who studied the reaction of several substituted indoles with the strong oxidant N_3^\bullet , which reacts mainly by electron transfer with high rate constants to form N_3^- . They showed that with methoxyindoles (substituted at the 3 position as with melatonin), formation of neutral indolyl radicals was favoured over the corresponding radical cation in aqueous solutions when the pH exceeds the pK_A of the neutral radical. The pK_A of the neutral tryptophan radical is 4.3³⁴ and other related indolyl radicals have pK_A values of between 4.5-6.5.³³ It is likely, therefore, that at the physiological pH of 7.4, melatonin will react with oxidizing species such as hydroxyl and peroxy radicals to ultimately form the neutral radical of melatonin as opposed to the radical cation, as suggested by Reiter. Whether as a chain transfer agent melatonin gives up an electron or donates a hydrogen is unknown. Based on our experimental and computational results, there is evidence to suggest that hydrogen atom donation by melatonin is the most favourable pathway. Thus, a proposed mechanism for reactivity of melatonin with highly oxidizing free radicals at physiological pH is represented by Scheme 4.12.



Scheme 4.12: Proposed mechanism for reaction of melatonin with oxidizing free radicals.

4.4.3 Melatonin is a Preventive Antioxidant

Under our experimental conditions, in the presence of catalytic metal ions, melatonin induced a reduction in the rate of linoleic acid oxygen uptake, similar to that of the chelant DTPA; a comparison of Figures 4.4 and 4.5 shows that the system's response induced by the addition of melatonin matched that which occurred upon addition of DTPA. DTPA is a very efficient chelant of metal ions, superior to EDTA. Although EDTA is most commonly used to chelate metal ions in autoxidation studies, DTPA was selected as a chelant because it wraps itself around iron binding five of the six coordination sites on the metal, thus occluding the peroxide pathway to iron and the Fenton reaction somewhat.

Since EDTA binds only four sites at a pH of 7.0, with the lone pairs from its two nitrogens and its two anionic oxygens, the geometry of the complex it forms with iron is fairly open and is still able to catalyze the formation of hydroxyl and alkoxy radicals from hydroperoxide and alkyl peroxides, respectively.^{76,77} However, the disadvantage associated

with using DTPA is that, over time, under the conditions of radical chain propagation, the hydrogens on the carbon adjacent to the middle nitrogen are easily abstracted thereby facilitating the decomposition of the chelant. The observed increase in the rate after the initial surge and subsequent decline in the rate upon addition of Fe^{2+} seen in both Figures 4.3 and 4.4 can be explained by the fact that unlike melatonin, DTPA is not a retarder, therefore does not undergo regeneration. Another possibility is that since DTPA is susceptible to decomposition by radical attack, the consequent formation of a carbon-centred radical would consume oxygen, thus driving the rate of oxygen uptake up again. Therefore, although it is a superior binding agent compared to EDTA for our purposes, its usefulness as a practical chelant to deactivate metal ions in solutions would appear to be limited to non-radical applications. It was necessary to use DTPA in this work because it functions as a chelant without catalyzing the Fenton reaction to the extent that EDTA does,^{76,77} and the use of DTPA yielded reliable, representative results before undergoing decomposition.

Since DTPA is not an antioxidant nor a retarder of peroxidation reactions, it can be assumed that DTPA suppresses the metal ion catalytic effect through binding and that melatonin interacts with the metal ions in a manner similar to that of the chelant. Further proof of this mechanism was seen in the results of the fluorescence studies with Fe^{2+} as quencher which strongly indicated binding between melatonin and Fe^{2+} . The metal ion catalysed oxygen uptake experiments and the fluorescence quenching experiment provide strong evidence that melatonin is a preventive antioxidant in that it is capable of deactivating the catalytic effect of metal ions on lipid peroxidations through binding.

4.4.4 Melatonin as a Ligand and Fenton Chemistry

Although melatonin was inferior to DTPA at 'mopping' up the background metal ions, it clearly impaired the catalytic effect of added metal ions to a similar extent. Molecular modelling using MM2 indicated that an iron complex with melatonin as a bidentate ligand with binding occurring between iron and the two melatonin nitrogens is very strained and

energetically unfavourable. Although bidentate binding between iron and melatonin at the indole nitrogen and carbonyl oxygen was computationally more energetically feasible, it appears more likely that binding occurs at only one of the six coordination sites of iron. Such unidentate binding would leave available active sites on the iron but there are other factors that can affect the ability of a ligand to impede or favour the formation of hydroxyl or alkoxy radicals due to Fenton chemistry.

In addition to the effect that the geometry of the complex has on the Fenton reaction and perhaps more importantly, the ligand can have a significant impact on the redox potential of the M^n/M^{n+1} half cell. It is possible that the interaction with melatonin reduces the redox potential of the metal ions to such an extent that their catalytic power is severely weakened. Oxidation of Fe^{2+} by the hydroperoxides of linoleic acid in micelles during peroxidation in our oxygen uptake experiments may be greatly altered by the bound melatonin, regardless of its orientation or strength of binding in the complex. Moreover, since melatonin scavenges hydroxyl radicals efficiently, it is feasible that any peroxy radicals formed would be intercepted by the melatonin ligand such that the peroxidation would be slowed via the retardation mechanism proposed in Scheme 4.12. It has been found that even though EDTA as a ligand is also able to scavenge OH^\bullet radicals produced by the Fenton degradation of hydrogen peroxide, it has a favourable effect on the redox potential such that the net effect makes the iron-EDTA complex a good Fenton catalyst.^{55,76,77} Alteration of the redox potential of a metal ion by a ligand is a common consequence of binding; even though 'free' iron ions are not available *in vivo*, many bound forms can act as Fenton catalysts for this reason.^{53,55,77}

In an experiment involving the reduction of ferricytochrome *c* by various indoles, Perez-Reyes and Mason found that while serotonin reduced ferricytochrome *c* at physiological pH, neither melatonin, tryptophan, nor 5-methoxyserotonin facilitated the reduction.⁷⁸ Most notably, they also found that serotonin acted synergistically with NADH to reduce ferricytochrome *c*, a result which they attributed to the binding of serotonin with ferricytochrome *c* thereby causing an increase in the ease of ferricytochrome *c* reduction.

Since DTPA is not an antioxidant nor a retarder of peroxidation reactions, it can be assumed that DTPA suppresses the metal ion catalytic effect through binding and that melatonin interacts with the metal ions in a manner similar to that of the chelant. Further proof of this mechanism was seen in the results of the fluorescence studies with Fe^{2+} as quencher which strongly indicated binding between melatonin and Fe^{2+} . The metal ion catalysed oxygen uptake experiments and the fluorescence quenching experiment provide strong evidence that melatonin is a preventive antioxidant in that it is capable of deactivating the catalytic impact of metal ions on lipid peroxidations.

In vivo there is a steady background level of intracellular and extracellular metal ions, virtually all of which are sequestered by enzymes, proteins (e.g. hemoglobin, transferrin, lactoferrin, ferritin), membranes, nucleic acids, or chelating agents. However, through tissue injury and the destruction of heme by enzymatic processes and peroxy radical attack, a sudden surge of released free iron in the plasma presents a significant hazard by inducing the initiation of cascades of peroxidation chain reactions *in vivo*. Our results indicate that melatonin may be capable of inhibiting such initiation since it is able to deactivate catalytic metal ions *in vitro*. The deactivation mechanism may be analogous to that of some nitrogenous compounds which, upon binding, are known to exert an inhibitory effect on catalytically active heme proteins. Tappel reported that the weakly bound complexes, formed by the combination of the nitrogen atoms of tryptophan and histidine with the iron-porphyrin, are able to thwart any catalytic activity by heme proteins.⁶³ He suggested that the steric bulk of the bound nitrogen-bearing molecule blocks the path to the iron nucleus thus protecting the lipid peroxide from degradation. Heme compounds themselves are susceptible to destruction by the radicals formed during lipid peroxidation and peroxide decomposition which results in release of the bound iron, which in turn causes further catalysis of the lipid peroxidation.⁶²⁻⁶⁴ Since tryptophan and melatonin share structural similarities, both being indole derivatives, melatonin may also share the capability of binding to the iron-porphyrin of heme in a similar fashion to provide comparable antioxidant protection.

A combination of altered redox potential of the metal, steric hindrance by the bulk of the complex itself, and scavenging by the ligand melatonin may indeed explain the observed decrease in metal ion-catalysed rate of oxygen uptake by linoleic acid in micelles upon addition of melatonin.

4.4.5 Interpretations in the Literature Revisited

From a review of the literature, it appears that melatonin's reputation as an extremely potent hydroxyl radical scavenger arose largely from a widely cited spin trapping study by Tan *et al.*⁴¹ Since tryptophan and other related indoles are known to trap hydroxyls with rate constants of between 1.2 and $1.7 \times 10^{10} \text{ M}^{-1}\text{s}^{-1}$,⁵² the likelihood of melatonin efficiently scavenging hydroxyl radicals is undisputed. However, Tan *et al.* measured the *relative* scavenging efficiencies of mannitol, glutathione and melatonin analogues⁴¹ using a procedure that was clearly flawed. They generated hydroxyl radicals by photolysing H_2O_2 with ultraviolet radiation of 254 nm in the presence of a spin trapping agent, 5,5-dimethylpyrroline-N-oxide (DMPO), which reacts to form a spin adduct with hydroxyl radicals with a rate constant of $3.2 \times 10^9 \text{ M}^{-1}\text{s}^{-1}$, along with the competing substrate. They then measured the amount of adduct generated using HPLC and electron spin resonance (ESR). However, since melatonin absorbs at the wavelength used to photolyse the hydrogen peroxide, the competition for irradiating photons between melatonin and H_2O_2 would decrease the actual yield of hydroxyl radicals generated that could further react to form adducts with DMPO. Tan *et al.* did not correct for the absorption of photons at 254 nm from melatonin. Therefore the adduct concentration would be lowered by a factor related to the fraction of the irradiating photons absorbed by melatonin. There is no doubt that melatonin is a good hydroxyl radical trap, but the comparison to glutathione and mannitol is invalid because the absorption of irradiating photons by melatonin was not accounted for.

More recently, Matuszak *et al.* conducted an ESR study using the same spin-trapping agent, DMPO, in order to determine the rate constants of hydroxyl radical scavenging by

melatonin and its major metabolites.⁵² These researchers used Fenton chemistry to decompose hydrogen peroxide and then observed the competition between DMPO and the melatonin substrates for the ensuing hydroxyl radicals. They observed a concentration dependent reduction in the ESR signal amplitude with melatonin. Although they interpreted their results as proof of efficient hydroxyl radical scavenging, these results may have arisen from the deactivation of Fenton type hydroxyl radical generation via Fe^{2+} through binding with melatonin. Interestingly, they also observed hydroxyl radical production with Fe^{3+} and 6-hydroxymelatonin, a major melatonin metabolite in the liver, *without* any externally added H_2O_2 .

Metal ion deactivation may provide an explanation for most, if not all, of the observations and reports that ascribe peroxy radical scavenging, antioxidant activity to melatonin *in vitro*. Since many of these antioxidant studies were conducted using tissue homogenates or erythrocytes^{17,39,45,46} liberated metal ions were likely available in catalytic amounts for peroxidation reactions. The experiments of Ianas *et al.*⁴⁵, which culminated in the first report to accredit melatonin with antioxidant properties, were conducted on hypothalamic homogenates using luminol and H_2O_2 - an unintended recipe for Fenton chemistry! The suppression of the Fenton-driven hydroxyl and alkoxy radical generation by melatonin through binding with the catalytic amounts of iron ions in the tissue homogenate could well be mistaken for peroxy trapping behavior.

Many *in vitro* peroxidation systems have been initiated by the intentional addition of Fe^{2+} to study the antioxidant role of melatonin. For example, Sewernyk and coworkers recently measured the relative efficacy of melatonin and glutathione to protect spleenocytes from lipid peroxidation initiated by Fenton reagents.⁴⁴ The superior electron-donating properties of melatonin, they concluded, was the reason that melatonin was found to offer better spleenocyte antioxidant protection under their experimental conditions. However, it is possible that these researchers were simply observing the inhibitory effects of iron deactivation by chelation with melatonin, thus blocking or retarding the Fenton reaction.

In another *in vitro* study, Poeggeler *et al.* reported that melatonin acts synergistically with trolox, ascorbate and glutathione to scavenge radicals formed by the presence of the Fenton reagents, FeSO_4 and H_2O_2 .⁴³ This claim is contradictory to the results obtained in our oxygen uptake measurements, where no synergism between melatonin and trolox was observed. The apparent synergism that Poeggeler *et al.* observed, which again was attributed to electron transfer mediation by melatonin, was most likely due to the complexation of Fe^{2+} rendering it unavailable to participate in the Fenton reaction. Their observation of antioxidant synergism with the combination of melatonin and known chain-breaking antioxidants is actually further proof that melatonin is a preventive antioxidant. If melatonin behaved as a chain-breaking antioxidant, it would induce an overall combined *additive* effect. Synergism can only be achieved if the combination of antioxidants work by different mechanisms.

Poeggeler *et al.* exploited the fluorescence properties of melatonin in much the same way we did.¹¹ In the presence of iron(II) sulfate and hydrogen peroxide, they observed a decrease in melatonin fluorescence which they interpreted to be the result of oxidation of melatonin by *in situ* hydroxyl radicals. In the same publication, they described the results of another experiment in which it appears as though they repeated Tan's procedure⁴¹ to generate hydroxyl radicals by irradiating H_2O_2 with UV in the presence of melatonin, although they did not provide details of their experimental procedure. Once again, they detected a decrease in the fluorescence of melatonin, however this experiment suffers from the same design flaws as that of Tan and coworkers⁴¹ which renders the results meaningless. The decrease in melatonin fluorescence observed in the presence of Fenton reagents may simply be caused by chelation of iron by melatonin, as demonstrated in our experiments.

On the subject of melatonin's antioxidant activity, the literature abounds with misinformation and confused interpretations of data. For example, in a review article by Pierrefiche and Laborit,¹⁷ antioxidant properties of melatonin were attributed to its indolic structure. In an effort to substantiate their theory, these authors cited an antioxidant study by Christen *et al.* in 1990 which involved tryptophan and some of its indolic metabolites.⁷⁹

However, antioxidant activity was only detected by Christen and coworkers in those tryptophan derivatives containing a hydroxyl group bound to a phenyl ring. The antioxidant activity Christen *et al.* observed was therefore likely due to the facile hydrogen-donating and subsequent stabilizing properties associated with this structural component, much like that of the tocopherols. In the same review article, Pierrefiche and Laborit included some experimental results from a comparison of the antioxidant activities of melatonin with 6-hydroxymelatonin, 5-hydroxytryptamine and butylated hydroxytoluene in mouse brain homogenates, using the thiobarbituric acid assay. Although all compounds tested indeed demonstrated antioxidant behaviour, the mechanism of inhibition by melatonin differed from that of the other antioxidants, all of which possess structural features typical of chain-breaking antioxidants. Since mouse brain homogenate contains significant levels of iron, it is more likely that melatonin functions as a preventive antioxidant to chelate the iron rather than to trap peroxy radicals as Pierrefiche and Laborit suggest. Trapping peroxy radicals to inhibit peroxidation implies that melatonin functions as a chain-breaking antioxidant which is contrary to our findings reported here.

Chapter 5

— Conclusions —

5.1.0 Conclusions

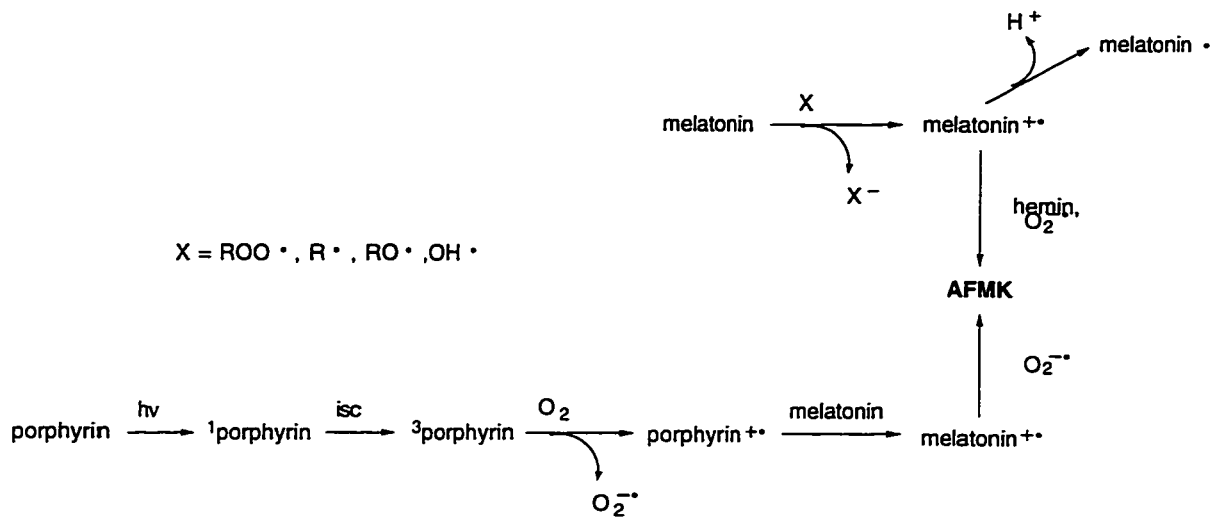
The physiological functions of melatonin have been scrutinized extensively in the literature.^{2,3,9,12,13,15,38,42,48-50,58} While its role as a neurohormone that governs the circadian rhythm via the mediation of photoperiodic information is well established, melatonin's ubiquitous presence in the body and in nature suggest that it may have other protective functions. It has recently been established that melatonin efficiently quenches benzophenone triplets in acetonitrile with a rate constant of $7.6 \times 10^9 \text{ M}^{-1}\text{s}^{-1}$ and traps photoinduced alkoxy radicals at rates greater than $10^7 \text{ M}^{-1}\text{s}^{-1}$.²⁴ Through such *in vitro* experimentation under a variety of conditions and in different media, elucidation of molecular mechanisms leading to feasible detoxification roles for melatonin is possible. The results of relevant investigations in this thesis have culminated in proposed mechanisms to explain the *potential* for detoxification activity by melatonin *in vivo*. Examination of the photophysical and photochemical properties of melatonin have shed some light on its retinal role while oxygen uptake experiments have exposed some of the misconceptions regarding its antioxidant activity.

5.1.1 Spectroscopy and The Role of Retinal Melatonin

The human lens filters light below 400 nm, and children have the added capability of transmitting a narrow band of light at 320 nm with about 20% efficiency.^{21,22} Since melatonin is transparent to light above this wavelength, it is unlikely that retinally synthesized melatonin participates as an ocular photosensitizer. Using time-resolved state-of-the-art spectroscopic techniques, we have characterized the photochemical and photophysical properties of

melatonin. In doing so, we have established that the excited states of melatonin are much like its precursor tryptophan, such that any photochemical involvement of melatonin *in vivo* would arise directly from sensitization of its triplet state, or indirectly by ground state reaction with proximal excited species. Our spectroscopic investigation indicates that melatonin fluoresces strongly at ~340 nm with a quantum yield of between 0.5 and 0.6 and a lifetime of 5-6 ns in organic media. In water, melatonin has slightly different fluorescence properties with a fluorescent maximum at 350 nm, a decreased quantum yield of 0.2 and a lifetime of 3.6 ns. Intersystem crossing into the triplet manifold is inefficient in organic solvents with a quantum yield of only 0.22. Characterization of the triplet showed a T—T absorption wavelength of 440 nm, a triplet energy of 70 kcal/mol, and lifetimes of 2.1 μs in acetonitrile and 0.7 μs in water. In sensitizing the triplet state of biphenyl, energy transfer from triplet melatonin proved to be quite efficient with a rate constant of $7.7 \times 10^8 \text{ M}^{-1}\text{s}^{-1}$.

Our studies have also shown that melatonin is a poor sensitizer of singlet oxygen (~3%) and Reszka *et al.* have found that melatonin efficiently scavenges photosensitized singlet oxygen with a rate constant of about $6 \times 10^7 \text{ M}^{-1}\text{s}^{-1}$, without sustaining chemical alteration.²⁵ The efficiency with which melatonin quenches singlet oxygen is comparable to that of 1,4-diazabicyclooctane (DABCO), a commonly used singlet oxygen quencher with a rate constant of $3 \times 10^7 \text{ M}^{-1}\text{s}^{-1}$. Protoporphyrin, which is present in the blood that directly feeds the retina, absorbs light at wavelengths greater than 400 nm and can efficiently sensitize singlet oxygen, which in turn can cause ocular tissue damage. Biologically damaging superoxide anion, which is produced in the presence of visible and UV radiation, is also generated by electron transfer to molecular oxygen by excited protoporphyrin.^{3,9} The radical cation of melatonin, an intermediate species formed either by reaction with free radicals or through electron abstraction by the photochemically produced porphyrin radical cation, reacts readily with superoxide anion. With a rich supply of porphyrins and superoxide anion available in the eye, it is likely that retinal melatonin undergoes rapid photosensitized oxidation to the kynuramine AFMK at physiological pH as depicted in Scheme 5.1.

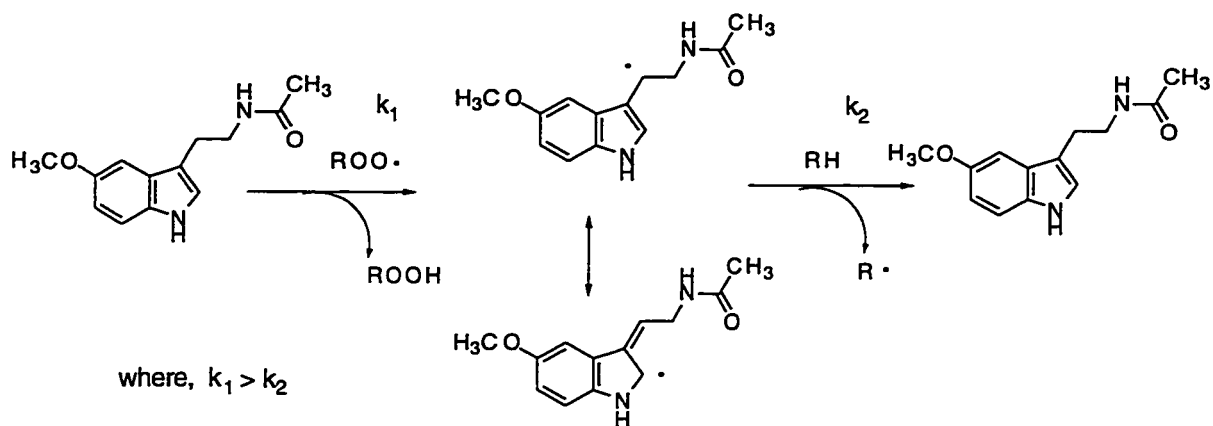


Scheme 5.1: Addition of oxygen and cleavage of the pyrrole ring by reaction of superoxide anion with melatonin in the retina.

This suggests that the detoxification role of retinal melatonin may include, to some degree, that of protective radical trap and quencher for both singlet oxygen and any harmful photochemistry arising from the triplet excited state of other ocular chromophores. It is interesting to note however, that the analogous metabolite of tryptophan, N-formyl-kynuramine can sensitize the photooxidation of some amino acids and nucleotides at wavelengths greater than 320 nm. Walrant and Santus reported a significant contribution from singlet oxygen generated by N-formyl-kynuramine in photooxidative damage to susceptible amino acids such as tryptophan and histidine.⁸⁰ It is quite likely that the structurally related melatonin metabolite, N-acetyl-N-formyl-5-methoxykynuramine, is also capable of sensitizing singlet oxygen. Although this would be inconsequential to adults, it may be of some importance to children since their lenses are capable of transmitting a window of light at precisely the absorption maximum of this metabolite.

5.1.2 The Antioxidant Role of Melatonin

The experimental evidence presented by Burton and Ingold strongly indicates that vitamin E is a superior chain-breaking radical scavenger.⁵⁷ Using similar techniques, i.e., oxygen uptake, under comparable conditions, the results presented in this thesis indicate that melatonin is a mild retarder of lipid peroxidation reactions, *not* a chain-breaking antioxidant as is currently believed, and may act as a preventive antioxidant by interfering with metal ion catalysts. Similarly, Evans *et al.* reported rate constants for scavenging photochemically generated radicals by vitamin E⁸¹ that were at least an order of magnitude greater than those reported by Scaiano for melatonin under comparable conditions. These *in vitro* experiments strongly suggest that melatonin is not only an inferior radical trap compared to vitamin E, but its participation in lipid peroxidation reactions follows a different mechanism than that reported for vitamin E. The retardation mechanism for melatonin proposed in this thesis is consistent with the mechanism for radical trapping proposed by Scaiano.²⁴ Unlike the mechanism for antioxidant activity suggested in the literature, we propose that melatonin gives up a hydrogen atom to peroxy radicals as opposed to an electron. However, without the superior stabilizing stereoelectronic resonance system (*vide supra*), the neutral radical rapidly recaptures a hydrogen atom from the lipid substrate to propagate the chain. Melatonin functions as a retarder by virtue of the fact that the rate constant for hydrogen abstraction from melatonin by peroxy radicals exceeds that of hydrogen abstraction from the lipid substrate, thereby resulting in an overall net decrease in the chain reaction rate.



Scheme 5.2: Proposed mechanism for peroxy radical trapping and lipid peroxidation retardation, where $\text{ROO}\cdot$ represents a peroxy radical and RH represents the lipid substrate.

The results obtained from peroxidation studies conducted by Barclay *et al.*⁷⁴ provide further evidence in support of this retardation mechanism. The fact that they saw only a slight increase in the ratio of kinetic to thermodynamic peroxidation products indicates that melatonin traps radicals at a slower rate compared to vitamin E thereby allowing for the formation of the thermodynamically favourable radical conformation prior to hydrogen abstraction to form the hydroperoxide.

Our results and those of Barclay's group definitively show that melatonin is not a chain breaking antioxidant. However, under the conditions used in our experiments, it appears that melatonin interacts with metal ions to curtail catalytic action on lipid peroxidations such that it may be classed as a preventive antioxidant. We speculate that a possible mechanism for this interaction may be through weak binding with the metal ions to alter the redox potential, thereby interfering with the catalytic potential. As a metal ion chelator, melatonin can provide on-site protection for hydroxyl radicals that are formed through the Fenton mechanism. From this perspective, the results of many experiments - most of which involved metal ions to varying extents - reported in the literature, which lead to the popular belief that melatonin is a 'peroxy radical trap superior to vitamin E', can be reinterpreted as metal ion deactivation by melatonin.

5.2.1 Final Comments

Neither the research in this thesis nor a critical examination of the literature support the claims that melatonin's role *in vivo* includes that of a detoxification agent. The physiological picomolar levels do not bring melatonin into a concentration range for sufficient molecular encounters with toxic free radicals, even taking into account the possibility of accumulation and concentration in tissue.⁸² The spectroscopy and free radical chemistry do indicate that melatonin may have some benefit at pharmacological doses, but it is unlikely that this indoleamine is as potent a detoxifier as is claimed by some, and in fact may even be harmful if administered to prepubescent children.

Claims to Original Research

We have characterized the photophysical and spectroscopic properties of N-acetyl-5-methoxytryptamine (melatonin) for the first time, and in doing so, have contributed to the knowledge of the physiological roles and limitations for retinal melatonin. We have shown that:

1. Melatonin fluoresces strongly at ~340 nm with a quantum yield of between 0.5 and 0.6 and a lifetime of 5-6 ns in organic media. In water, melatonin has slightly different fluorescence properties with the fluorescent maximum red-shifted to 350 nm, a decreased quantum yield of 0.2 and a lifetime of 3.6 ns.
2. Intersystem crossing into the triplet manifold is inefficient in organic solvents with a quantum yield of only 0.22. Characterization of the triplet showed a T—T absorption wavelength of 440 nm, a triplet energy of 70 kcal/mol, and lifetimes of 2.1 μ s in acetonitrile and 0.7 μ s in water. Energy transfer from triplet melatonin to biphenyl proved to be efficient with a rate constant of $7.7 \times 10^8 \text{ M}^{-1}\text{s}^{-1}$.
3. The photophysical and spectral characteristics of melatonin are very similar to tryptophan.

We have measured the impact of melatonin on the rate of oxygen uptake in peroxidation chain reactions and have observed melatonin fluorescence quenching by iron(II) and in doing so, have contributed to the knowledge concerning the antioxidant activity of melatonin by showing that:

4. Melatonin is not a chain-breaking antioxidant like vitamin E and related tocopherols since it does not efficiently trap peroxy radicals as is currently believed. Melatonin is a weak retarder of free radical peroxidation.
5. In the presence of metal ion catalysts, melatonin can act as a preventive antioxidant by chelating the metal ions.

Appendix 1

A.1.0 A Computational Approach

In order to determine the site of hydrogen abstraction the relative heats of formation for each of six possible radical configurations of melatonin were calculated and compared. Another computational exercise was conducted to determine the relative stability of the radical cation versus the neutral radical of melatonin. To perform calculations on the neutral free radicals, six likely candidates for stable melatonin radical structures were constructed (Figure A.1), and then the lowest energy conformation for each was determined and geometry optimized using the semi-empirical method PM3. All of these calculations, using Silicon Graphics workstation with Spartan Version 4.0 software, were conducted *in vacuo* because this software does not support open-shell solvation. The heats of formation generated by the geometry optimization were compared to determine which of the radical sites was most stable, with the assumption that the lower the heat of formation, the more stable the radical.

A.2.1 Locating the Lowest Energy Conformation

In this exercise, a Monte Carlo conformer search was chosen on the basis that it is well-suited to molecules such as melatonin, that contain several single bonds. For this particular computational application, the Monte Carlo algorithm in Spartan, was set up to invoke random displacements via a 60° rotation about one of any of the seven freely rotatable bonds on a randomly generated starting structure of melatonin. The default settings for population size and number of generations (cycles) involved in the search were thirty-five and one hundred respectively. In the Monte Carlo method, a bond is selected at random and rotated. Then the potential energy of the population, or ensemble of conformers is calculated by a formula which involves the total potential energy contribution from the bonds, angles, torsions, electron repulsion, and electron exchange. If the perturbation results in a decrease in the potential

energy of the system, then it is accepted. If there is an increase in energy, the rotation is subjected to the following test:

if $e^{\Delta V/kT} > a$, the rotation is discarded

if $e^{\Delta V/kT} < a$, the rotation is accepted,

where ΔV is the change in potential energy of the population arising from the rotation, k is the Boltzman distribution constant, T is the temperature, and a is a random number between 0 and 1, generated by the method. The population remains constant throughout the entire procedure which is repeated 100 times.

Melatonin structures were submitted for a conformer search, but all failed prior to reaching 55 cycles due to insufficient 'Swap space' memory. This proved to be most unfortunate because the Monte Carlo method provides an excellent means of transcending the ubiquitous potential energy barrier to explore new, and possibly deeper minima. The fact that higher energy conformers have a chance of being accepted allows this to occur. An alternative, albeit highly inferior, trial-and-error geometry search was then performed to locate the lowest energy geometry. The angles between the two side branches and the indole ring, as well as the angle between the carbon and amide linkage, were manually perturbed in a random fashion to create a variety of conformations of melatonin. Geometry optimizations were performed on each of these conformations - the lowest energy structure calculated was found to be about -71 kcal/mol. This conformation was then used as a template to generate the six radical structures for geometry optimization and subsequent comparison.

A.2.2 Methods for Geometry Optimization

The size of the melatonin molecule precludes the use of *ab initio* Hartree Fock methods for geometry optimization. Semi-empirical methods such as AM1 and PM3, which incorporate adjustable parameters that are calibrated against experimental data, are fast and accurate enough

for the purposes of this computational exercise. The average errors associated with calculations of heats of formation for 194 molecules containing H, C, N, and O that were tested using PM3, was 4.4 kcal/mol as opposed to AM1 which gave an average error of 7.2 kcal/mol.⁸³ Stewart has reported average differences in the heats of formation calculated for 276 such compounds to be 5.7 kcal/mol and 7.5 kcal/mol using PM3 and AM1, respectively.⁸⁴ Similarly, the average error for ΔH_f for neutral radicals was 7.4 kcal/mol for PM3 as compared with 8.0 kcal/mol for AM1.⁸³ Since the heats of formation were the basis of comparison for the relative free radical stabilities, the obvious choice for this computational exercise appeared to be PM3.

All geometry optimizations included a molecular mechanical correction to compensate for the height of the rotational barrier about the amide linkage that is found to be low with NDDO methods (Neglect of Diatomic Differential Overlap) such as PM3. All open-shell molecules were calculated using the Unrestricted Hartree Fock (UHF) which places spin up and spin down electrons in their own molecular orbitals unlike Restricted Hartree Fock in which the molecular orbitals are doubly occupied by each type of spin. The advantage of using UHF for radicals is that more realistic spin densities are generated due to the fact that spin polarization is allowed for.

A.3.1 Computational Results

The radical structures of melatonin are shown in Figure A.1 and the calculated heats of formation for the radical structures and the radical cation are tabulated below in Table A.1.

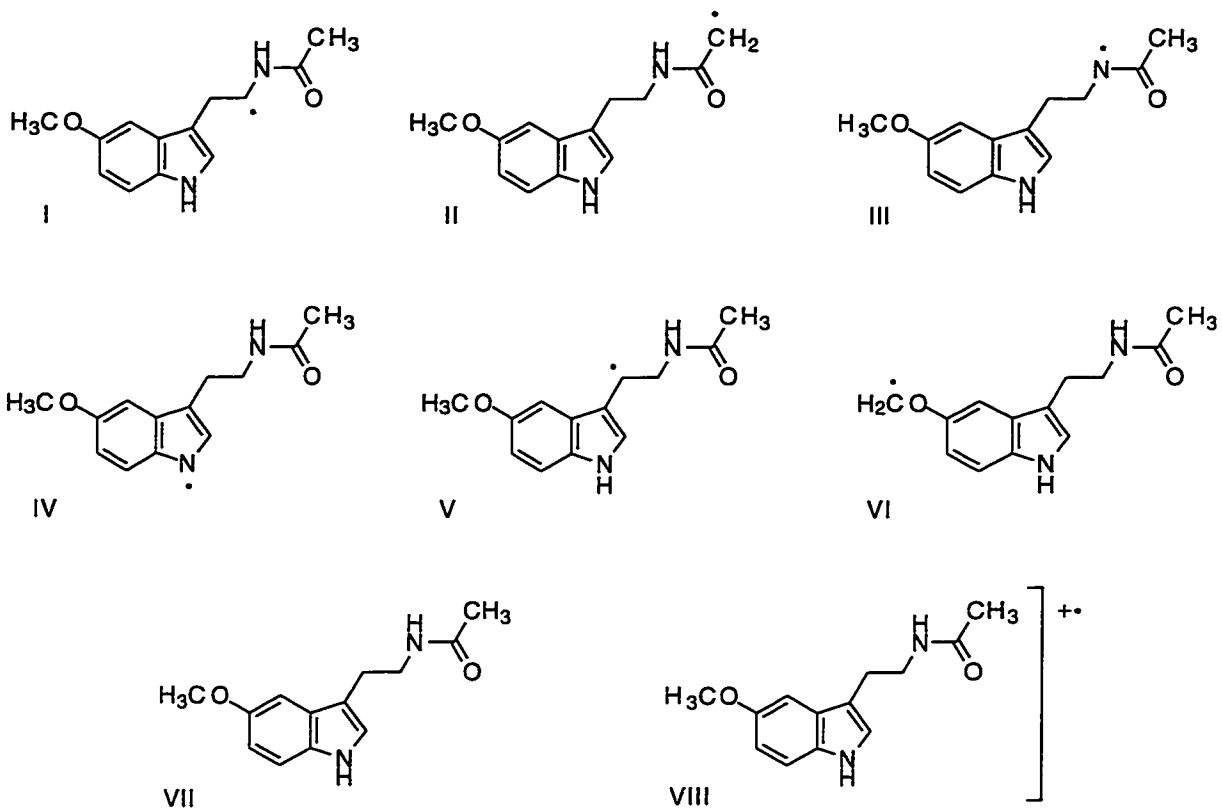


Figure A.1: Proposed radical structures (I-VI) following hydrogen atom abstraction from melatonin molecule (VII); radical cation of melatonin (VIII) following electron transfer.

Indole Derivative	ΔH_f (kcal/mol)	μ (Debye)
I	-25.647	3.068
II	-13.167	4.524
III	-18.691	4.332
IV	-18.864	5.055
V	-30.332	2.389
VI	-20.647	5.233
VII(g)	-47.822	4.503
VII(s)	-70.537	4.598
VIII(s)	125.587	n/a

Table A.1: PM3 calculation results, using Silicon Graphics workstation with Spartan Version 4.0 software, where ΔH_f is the heat of formation, and μ is the dipole moment; (g) - gas phase; (s) - solvated (water)

Atomic charges for the heavy atoms of all of the melatonin radicals, solvated and *in vacuo* molecules, tabulated in Table A.2, show that nothing unusual or unexpected happens with respect to the assignment of the net charge, as a result of hydrogen abstraction. The most stable radical, determined to be V, shows the lowest net negative charge at the 3 position of the indole ring, the greatest change in negative charge of all of the carbon centred-radicals indicating an apparent charge neutralization within the pyrrole part of the ring on this structure. This could be due to spin delocalization onto the benzene moiety of the ring which may stabilize the radical to some extent. The effects of solvation are most pronounced at the acetyl carbon and the carbon furthest from the nitrogen in the indole ring (C14) at the benzene/pyrrole ring junction; both carbon centres become more positive with solvation under aqueous

conditions. The numbering scheme for the heavy atoms of melatonin for Table A.2 is given in Figure A.2.

ATOM	I	II	III	IV	V	VI	VII(s)	VII(g)
N1	-0.103	-0.351	-0.615	-0.297	-0.334	-0.324	-0.284	-0.292
C2	-0.286	0.179	0.505	0.244	0.236	0.090	0.159	0.195
C3	0.513	0.612	0.756	0.492	0.516	0.520	0.479	0.475
O4	-0.547	-0.572	-0.526	-0.589	-0.570	-0.558	-0.596	-0.570
C6	-0.088	-0.275	-0.236	-0.009	-0.009	0.031	0.236	0.034
C9	0.161	0.022	0.068	-0.110	-0.263	-0.014	0.042	0.048
C10	-0.342	-0.201	-0.345	-0.153	-0.096	-0.153	-0.273	-0.202
C13	0.112	0.044	0.132	0.296	-0.002	0.001	0.085	0.051
C14	0.052	-0.108	-0.130	-0.086	-0.0032	-0.055	-0.061	-0.144
N16	-0.307	-0.310	-0.301	-0.542	-0.299	-0.220	-0.343	-0.301
C17	0.146	0.218	0.228	0.374	0.149	0.131	0.218	0.211
C19	-0.335	-0.231	-0.155	-0.221	-0.209	-0.184	-0.268	-0.178
C20	-0.154	-0.201	-0.196	-0.184	-0.135	-0.176	-0.214	-0.186
C22	-0.236	-0.173	-0.175	-0.170	-0.211	-0.176	-0.169	-0.169
C24	0.340	0.266	0.231	0.251	0.259	0.216	0.265	0.230
O26	-0.403	-0.386	-0.370	-0.354	-0.357	-0.213	-0.385	-0.370
C27	0.329	0.267	0.290	0.219	0.224	-0.128	0.242	0.267

Table A.2: Table of atomic charges - melatonin and neutral radicals (heavy atoms only). The radical centres are bolded.

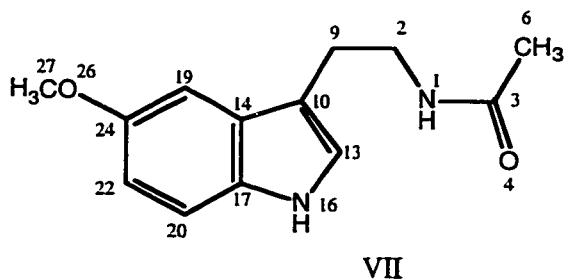


Figure A.2: Numbering scheme for heavy atoms of melatonin for Table A.2.

The effects of solvation on the melatonin molecule are quite pronounced. The heat of formation drops from -47.822 kcal/mol to -70.537 kcal/mol (Table A.2), probably due to the stabilizing effects of hydrogen bonding with the water solvent. It is also interesting to note that the lowest dipole moment belongs to the most stable melatonin radical. This may be related to the apparent charge delocalization in the indole ring, mentioned above, which creates less polarization of charge in the radical.

References

- 1) Lerner, A. B., Case, J. B. and Heinzelman, R. V. (1959) Structure of Melatonin., *J. Am Chem. Soc.*, **81**, 6084-6085.
- 2) Hardeland, R., Balzer, I., Poeggeler, B., Fuhrberg, B., Uria, H., Behrmann, G., Wolf, R., Meyer, T. J. and Reiter, R. J. (1995) On the Primary Functions of Melatonin in Evolution: Mediation of Photoperiodic Signals in a Unicell, Photooxidation, and Scavenging of Free Radicals., *J. Pineal Res.*, **18**, 104-111.
- 3) Reiter, R. J. (1991) Pineal Melatonin: Cell Biology of Its Synthesis and of Its Physiological Interactions., *Endocrine Rev.*, **12**, No. 2, 151-180.
- 4) Hollyfield, J. G. and Basinger, S. F. (1978) Photoreceptor Shedding can be Initiated Within the Eye., *Nature*, **274**, 794-796.
- 5) Besharse, J. C. and Dunis, D. A. (1983) Methoxyindoles and Photoreceptor Metabolism: Activation of Rod Shedding., *Science*, **219**, 1341-1343.
- 6) Menaker, M. (1985) Eyes - the Second (and Third) Pineal Glands? In *Photoperiodism, Melatonin and the Pineal.*, Pitman, London.
- 7) Menaker, M. (1985) General Discussion. I. In *Photoperiodism, Melatonin and the Pineal*, Pitman, London.
- 8) Gern, W. A. and Ralph, C. L. (1979) Melatonin Synthesis in the Retina., *Science*, **204**, 183-184.
- 9) Hardeland, R., Reiter, R. J., Poeggeler, B. and Tan, D-X. (1993) The Significance of the Metabolism of the Neurohormone Melatonin: Antioxidative Protection and Formation of Bioactive Substances., *Neurosci. Biobehav. Rev.*, **17**, 347-357.
- 10) Reiter, R. J. (1997) Antioxidant Actions of Melatonin. *Adv. Pharmacol.*, **38**, 103-117.
- 11) Poeggeler, B., Saarela, S., Reiter, R. J., Tan, D-X., Chen, L-D., Manchester, L. C. and Barlow-Walden, L. R. (1994) Melatonin - A Highly Potent Endogenous Radical

- Scavenger and Electron Donor: New Aspects of the Oxidation Chemistry of the Oxidation Chemistry of this Indole Accessed In Vitro., *Ann. N. Y. Acad. Sci.*, **738**, 419-420.
- 12) Reiter, R.J., Melchiorri, D., Sewerynek, E., Poeggeler, B., Barlow-Walden, L., Chuang, J., Ortiz, G. G., and Acuna-Castroviejo, D. (1995) A Review Of The Evidence Supporting Melatonin's Role as an Antioxidant., *J. Pineal Res.*, **18**, 1-11.
 - 13) Reiter, R. J. (1995) Oxidative Processes and Oxidative Defense Mechanisms in the Aging Brain., *FASEB J.*, **9**, 526-533.
 - 14) Poeggeler, B. Reiter, R. J., Tan, D-X., Chen, L-D. and Manchester, L. C. (1993) Melatonin, Hydroxyl Radical- Mediated Oxidative Damage, and Aging: a Hypothesis., *J. Pineal Res.*, **14**, 151-168.
 - 15) Reiter, R. J., Poeggeler, B., Tan, D-X, Chen, L-D., Manchester, L. C. and Guerrero, J. M. (1993) Antioxidant Capacity of Melatonin: A Novel Action Not Requiring a Receptor., *Neuroendocrinol. Lett.*, **15**, 103-116.
 - 16) Reiter, R. J. and Robinson, J. (1995) *Melatonin: Your Body's Natural Wonder Drug*. Bantam Books, New York.
 - 17) Pierrefiche, G. and Laborit, H. (1995) Oxygen Free Radicals, Melatonin, and Aging., *Exp. Gerontol.*, **30**, Nos. 3/4, 213-227.
 - 18) Nichols, M. (1997) Forever Young: Can Hormones Really Stave Off Old Age? *Maclean's*, (July), 44-48.
 - 19) Reiter, R. J. (1995) The Role of the Neurohormone Melatonin as a Buffer Against Macromolecular Oxidative Damage., *Neurochem. Int.*, **27**, 453-460.
 - 20) Cagnoli, C. M., Atabay, C., Kharlamova, E. and Manev, H. (1995) Melatonin Protects Neurons from Singlet Oxygen-Induced Apoptosis., *J. Pineal Res.*, **18**, 222-226.
 - 21) Dillon, J. (1991) The Photophysics and Photobiology of the Eye., *J. Photochem. Photobiol. B Biol.*, **10**, 23-40.

- 22) Roberts, J. E. (1995) Visible Light Induced Changes in the Immune Response Through an Eye-Brain Mechanism (Photoneuroimmunology), *J. Photochem. Photobiol. B Biol.*, **29**, 3-15.
- 23) Carmichael, I. and Hug, G. L. (1989) Spectroscopy and Intramolecular Photophysics of Triplet States., In *Handbook of Organic Photochemistry*, J. C. Scaiano, Ed., CRC Press, Boca Raton, FL.
- 24) Scaiano, J. C. (1995) Exploratory Laser Flash Photolysis Study of Free Radical Reactions and Magnetic Field Effects in Melatonin Chemistry., *J. Pineal Res.*, **19**, 189-195.
- 25) Reszka, K. J., Matuszak, Z., Bilski, P., Martinez, L. J. and Chignell, C. F. (1996) Antioxidant Properties of Melatonin., 18th Annual Meeting of the Bioelectromagnetics Society, p. 176.
- 26) Girotti, A. W. (1990) Photodynamic Lipid Peroxidation in Biological Systems., *Photochem. Photobiol.*, **51**(4), 497-509.
- 27) Robbins, R. J., Fleming, G. R., Beddard, G. S., Robinson, G. W., Thistlewaite, P. J. and Woolfe, G. J. (1980) Photophysics of Aqueous Tryptophan: pH and Temperature Effects., *J. Am. Chem. Soc.*, **102**, 6271-6279.
- 28) Chen, Y., Gai, F. and Petrich, J. (1994) Single-Exponential Fluorescence Decay of the Nonnatural Amino Acid 7-Azatriptophan and the Nonexponential Decay of Tryptophan in Water., *J. Phys. Chem.*, **98**, 2203-2209.
- 29) Birks, J. B. (1970) *Photophysics of Aromatic Molecules.*, Wiley-Interscience, New York.
- 30) Szabo, A. G. and Rayner, D. M. (1980) Fluorescence Decay of Tryptophan Conformers in Aqueous Solution., *J. Am. Chem. Soc.*, **102**, 554-563.
- 31) Vanderkooi, J. M. (1991) Tryptophan Phosphorescence from Proteins at Room Temperature., In *Topics in Fluorescence Spectroscopy*, Vol. 3, *Biochemical Applications.*, J. R. Lackowicz, Ed., Plenum Press.

- 32) Nau, W., M. and Scaiano, J. C. (1996) Oxygen Quenching of Ketones and Diketones., *J. Phys. Chem.*, **100**, 11360-11367.
- 33) Jovanovic, S. V. and Steenken, S. (1992) Substituent Effects on the Spectral, Acid-Base, and Redox Properties of Indolyl Radicals: A Pulse Radiolysis Study., *J. Phys. Chem.*, **96**, 6674-6679.
- 34) Al-Kazwini, A. T., O'Neill, P., Adams, G. E. and Cundall, R. B. (1990) One-Electron Oxidation of Methoxylated and Hydroxylated Indoles by $N_3\bullet$. 1. Characterization of the Primary Indolic Radicals., *J. Phys. Chem.*, **94**, 6666-6670.
- 35) Murov, S. L. (1973) *Handbook of Photochemistry.*, Marcel Dekker, New York.
- 36) Carmichael, I. and Hug, G. L. (1986) Triplet-Triplet Absorption Spectra of Organic Molecules in Condensed Phases., *J. Phys. Chem. Ref. Data*, **15**, 1-250.
- 37) Chen, Y., Liu, B., Yu, H.-T. and Barkley, M. D. (1996) The Peptide Bond Quenches Indole Fluorescence., *J. Am. Chem. Soc.*, **118**, 9271-9278.
- 38) Reiter, R. J. (1995) The Pineal Gland and Melatonin in Relation to Aging: A Summary of the Theories and of the Data., *Exp. Gerontol.*, **30**, Nos. 3/4, 199-212.
- 39) Pieri, C., Moroni, F., Marra, M., Marcheselli, F. and Recchioni, R. (1995) Melatonin is an Efficient Antioxidant., *Arch. Gerontol. and Ger.*, **20**, 159-165.
- 40) Pieri, C., Marra, M., Moroni, F., Recchioni, R. and Marcheselli, F. (1994) Melatonin: A Peroxyl Radical Scavenger More Effective Than Vitamin E., *Life Sci. Pharm. Lett.*, **55**, 271-276.
- 41) Tan, D.-X., Chen, L.-D., Poeggeler, B., Manchester, L. C. and Reiter, R. R. Melatonin: A Potent, Endogenous Hydroxyl Radical Scavenger., (1993) *Endocrine J.*, **1**, 57-60.
- 42) Pieri, C., Marra, M., Gaspar, R. and Damjanovich, S. (1996) Melatonin Protects from Oxidation but Does Not Prevent the Alipoprotein Derivatization., *Biochem. Biophys. Res. Com.*, **222**, 256-260.

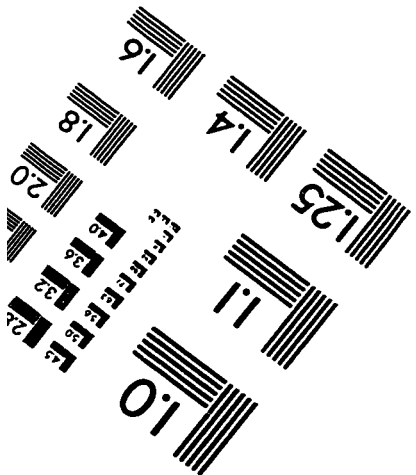
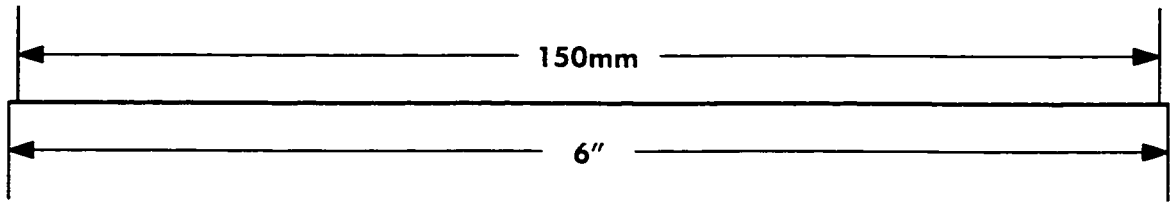
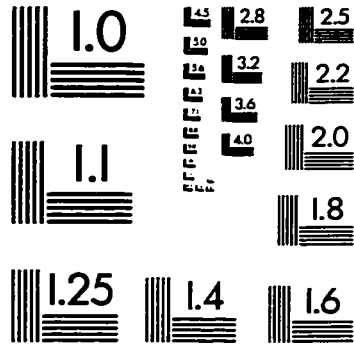
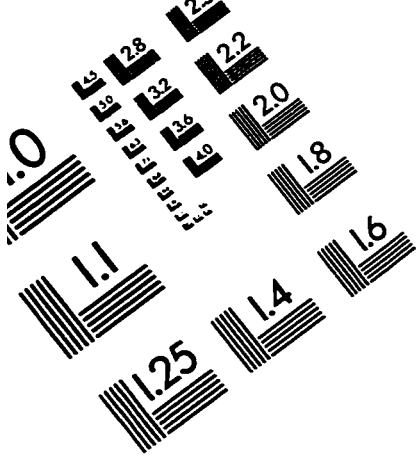
- 43) Poeggeler, B., Reiter, R.J., Hardeland, R., Sewerynek, E., Melchiorri, D. and Barlow-Walden, L. (1995) Melatonin, A Mediator of Electron Transfer and Repair Reactions, Acts Synergistically with the Chain-Breaking Antioxidants Ascorbate, Trolox and Glutathione. *Neuroendocrin. Lett.*, **17**, No. 2, 87-92.
- 44) Sewerynek, E., Melchiorri, D., Reiter, R. J. and Lewinski, A. (1996) Melatonin and Glutathione Reduce Lipid Peroxidation Products in Lymphocytes Cultured with H₂O₂ and Iron., *J. Thymol.*, **4**, Suppl. No. 1, 88-92.
- 45) Ianas, O., Olinescu, R. and Badescu, I. (1991) Melatonin in Oxidative Processes., *Rom. J. Endocrinol.*, **29**, No. 3;4, 147-153.
- 46) Chan, T-Y., Tang, P-L. (1996) Characterization of the Antioxidant Effects of Melatonin and Related Indoles In Vitro., *J Pineal Res.*, **20**, 187-191.
- 47) Kiester, E., Jr. and Kiester, S. V. (1996) Melatonin. Should We Be Taking It? *Reader's Digest*, (July), 104-108.
- 48) Reiter, R. J., Tan, D-X., Poeggeler, B., Chen, L-D. and Menedez-Pelaez, A. (1994) Melatonin, Free Radicals and Cancer Initiation., *Adv. Pineal Res.*, **7**, 211-228.
- 49) Abe, M., Reiter, R. J., Orhii, P. B., Hara, M. and Poeggeler, B. (1994) Inhibitory Effect of Melatonin on Cataract Formation in Newborn Rats: Evidence for an Antioxidative Role for Melatonin., *J. Pineal Res.*, **17**, 94-100.
- 50) Reiter, R. J., Tan, D-X., Poeggeler, B., Menendez-Pelaez, A., Chen, L-D. and Saarela, S. (1994) Melatonin As a Free Radical Scavenger: Implications for Aging and Age-Related Diseases., *Ann. N. Y. Acad. Sci.*, **719**, 1-12.
- 51) King, M. and Scaiano, J. C. (1997) The Excited States of Melatonin., *Photochem. Photobiol.*, **65**(3), 538-542.
- 52) Matuszak, Z., Reszka, K. J. and Chignell, C. F. (1997) Reaction of Melatonin and Related Indoles with Hydroxyl Radicals: EPR and Spin Trapping Investigations., *Free Radic. Biol. Med.*, **23**, No. 3, 367-372.

- 53) Halliwell, B. and Gutteridge, J. M. C. (1992) Biologically Relevant Metal Ion-Dependant Hydroxyl Radical Generation. An Update., *FEBS Lett.*, **307**, 108-112.
- 54) Yu, B. P. (1994) Cellular Defenses Against Damage From Reactive Oxygen Species. *Physiol. Rev.*, **74**, No. 1, 139-157.
- 55) Youngman, R. J. (1984) Oxygen Activation: Is the Hydroxyl Radical Always Biologically Relevant? *Trends Biochem. Sci.*, 280-283.
- 56) Ingold, K.U. (1968) Inhibition of Autoxidation., *Adv. Chem. Ser.*, **75**, 296-305.
- 57) Burton, G. W. and Ingold, K. U. (1981) Autoxidation of Biological Molecules. 1. The Antioxidant Activity of Vitamin E and Related Chain-Breaking Phenolic Antioxidants in Vitro., *J. Am. Chem. Soc.*, **103**, 6472-6477.
- 58) Menendez-Pelaez, A. and Reiter, R. J. (1993) Distribution of Melatonin in Mammalian Tissues: The Relative Importance of Nuclear Versus Cytosolic Localization., *J. Pineal Res.*, **15**, 59-69.
- 59) Burton, G. W., Joyce, A. and Ingold, K. U. (1983) Is Vitamin E the Only Lipid-Soluble Chain-Breaking Antioxidant in Human Blood Plasma and Erythrocyte Membranes? *Arch. Biochem. and Biophys.*, **221**, No.1, 281-290.
- 60) Ingold, K. U., personal communication.
- 61) Shida, C. S., Castrucci, A. M. L. and Lamy-Freund, M. T. (1994) High Melatonin Solubility in Aqueous Medium., *J. Pineal Res.*, **16**, 198-201.
- 62) Tappel, A. L. (1954) Studies of the Mechanism of Vitamin E Action. II. Inhibition of Unsaturated Fatty Acid Oxidation Catalyzed by Hematin Compounds., *Arch. Biochem. and Biophys.*, **50**, 473-485.
- 63) Tappel, A. L. (1955) Unsaturated Lipide Oxidation Catalyzed by Hematin Compounds. *J. Biol. Chem.*, **217**, 721-733.
- 64) Gutteridge, J. M. C. (1986) Iron Promoters of the Fenton Reaction and Lipid Peroxidation Can Be Released From Haemoglobin by Peroxides., *FEBS Lett.*, **201**, No. 2, 291-295.

- 65) Cao, G., Alessio, H. M. and Cutler, R. G. (1993) Oxygen-Radical Absorbance Capacity Assay for Antioxidants., *Free Radic. Biol. Med.*, **14**, 303-311.
- 66) Hancock-Chen, T. and Scaiano, J. C. (1997) Non-Linear Effects and a Cascade of Radical Events Leading to Laser-Specific Generation of Active Oxygen Species., submitted for publication.
- 67) Wills, E. D. (1966) Mechanism of Lipid Peroxide Formation in Animal Tissues., *Biochem. J.*, **99**, 667-676.
- 68) Barclay, L. R. C., Locke, S. J., MacNeil, J. M. and Vankessel, J. (1984) Autoxidation of Micelles and Model Membranes. Quantitative Kinetic Measurements Can be Made by Using Either Water-Soluble or Lipid-Soluble Chain-breaking Antioxidants., *J. Am. Chem. Soc.*, **106**, 2479-2481
- 69) Barclay, L. R. C. (1992) Model Biomembranes: Quantitative Studies of Peroxidation, Antioxidant Action, Partitioning, and Oxidative Stress., *Can. J. Chem.*, **71**, 1-16.
- 70) Turro, N. J., Gratzel, M. and Braun, A. M. (1980) Photophysical and Photochemical Processes in Micellar Systems., *Angew. Chem. Int. Ed. Engl.*, **19**, 675-696.
- 71) Pryor, W. A., Cornicelli, J. A., Devall, L. J., Tait, B., Trivedi, B. K., Witiak, D. T. and Wu, M. (1993) A Rapid Screening Test to Determine the Antioxidant Potencies of Natural and Synthetic Antioxidants., *J. Org. Chem.*, **58**, 3521-3532.
- 72) Barclay, L. R. C., Baskin, K. A., Locke, S. J. and Schaefer, T. D. (1987) Benzophenone-Sensitized Autoxidation of Linoleate in Solution and Sodium Dodecyl Sulfate Micelles., *Can. J. Chem.* **65**, 2529-2540.
- 73) Barclay, L. R. C., Locke, S. J. and MacNeil, J. M. (1983) The Autoxidation of Unsaturated Lipids in Micelles. Synergism of Inhibitors Vitamins C and E., *Can. J. Chem.*, **61**, 1288-1290.
- 74) Barclay, L. R. C., Antunes, F., Norris, J. Q. and Xi, F. (1997) personal communication.

- 75) Waters, W. A. and Wickham-Jones, C. (1951) The Retardation of Benzaldehyde Autoxidation by *p*-Cresol., *J. Chem. Soc.*, 812-823.
- 76) McCord, J. M. and Day, E. D., Jr. (1978) Superoxide Dependent Production of Hydroxyl Radical Catalyzed by Iron-EDTA Complex., *FEBS Lett.*, **86**, 139-142.
- 77) Halliwell, B. and Gutteridge, J. M. (1986) Oxygen Free Radicals and Iron in Relation to Biology and Medicine: Some Problems and Concepts., *Arch. Biochem. and Biophys.*, **246**, No. 2, 501-514.
- 78) Perez-Reyes, E. and Mason, R. P. (1981) Characterization of the Structure and Reactions of Free Radicals from Serotonin and Related Indoles., *J. Biol. Chem.*, **256**, No. 5, 2427-2432.
- 79) Christen, S., Peterhans, E. and Stocker, R. (1990) Antioxidant Activities of Some Tryptophan Metabolites: Possible Implication for Inflammatory Diseases., *Proc. Natl. Acad. Sci. USA*, **87**, 2506-2510.
- 80) Walrant, P. and Santus, R. (1974) N-Formyl-Kynurenine, A Tryptophan Photooxidation Product, As a Photodynamic Sensitizer., *Photochem. Photobiol.*, **19**, 411-417.
- 81) Evans, C., Scaiano, J. C. and Ingold, K. U. (1992) Absolute Kinetics of Hydrogen Abstraction From α -Tocopherol by Several Reactive Species Including an Alkyl Radical., *J. Am Chem. Soc.*, **114**, 4589-4593.
- 82) Reppert, S. M. and Weaver, D. R. (1995) Melatonin Madness., *Cell*, **83**, 1059-1062.
- 83) St. Amant, A. (1996) personal communication.
- 84) Stewart, J. P. (1989) Optimization of Parameters for Semiempirical Methods II. Applications., *J. Comp. Chem.*, **10**, No.2, 221-264.
- 85) Carlberg, C. and Irmgard, W. (1995) The Orphan Receptor Family RZR/ROR, Melatonin and 5-Lipoxygenase: An Unexpected Relationship., *J. Pineal Res.*, **18**, 171-178.

TEST TARGET (QA-3)



APPLIED IMAGE, Inc
1653 East Main Street
Rochester, NY 14609 USA
Phone: 716/482-0300
Fax: 716/288-5989

© 1993, Applied Image, Inc., All Rights Reserved